UNIVERSITY OF HAWAII
LIBRARY

Nov 2 '50

The
PHILOSOPHICAL MAGAZINE

FIRST PUBLISHED IN 1798

. 41 SEVENTH SERIES No. 321 October, 1950

A Journal of Theoretical Experimental and Applied Physics

EDITOR
PROFESSOR N. F. MOTT, M.A., D.Sc., F.R.S.

EDITORIAL BOARD
SIR LAWRENCE BRAGG, O.B.E., M.C., M.A., D.Sc., F.R.S.
ALLAN FERGUSON, M.A., D.Sc.
SIR GEORGE THOMSON, M.A., D.Sc., F.R.S.
PROFESSOR A. M. TYNDALL, C.B.E., D.Sc., F.R.S.

PRICE 10s.
Annual Subscription £5 2s. 6d. payable in advance.

ED AND PUBLISHED BY TAYLOR & FRANCIS LTD., RED LION COURT, FLEET ST., LONDON, E.C.4.

Annals of Science

A QUARTERLY REVIEW OF
THE HISTORY OF SCIENCE
SINCE THE RENAISSANCE

EDITORS

D. McKIE, D.Sc., Ph.D.,
University College, London.

HARCOURT BROWN, M.A., Ph.D.,
Brown University, Providence, R.I., U.S.A.

H. W. ROBINSON,
Former Librarian,
Royal Society of London.

ANNUAL SUBSCRIPTION
£2 0s. 0d.
OR
10s. 6d.
PER PART
POST FREE

TAYLOR & FRANCIS, LTD., Red Lion Court, Fleet Street, LONDON, E.C.4

ALERE FLAMMAM

THE MATHEMATICAL WORKS
OF JOHN WALLIS, D.D., F.R.S.

by

J. F. SCOTT, Ph.D., B.A.

"His work will be indispensable to those interested in the early history of The Royal Society. I commend to all students of the Seventeenth Century, whether scientific or humane, this learned and lucid book."—Extract from foreword by Prof. E. N. da C. Andrade, D.Sc., Ph.D., F.R.S.

Recommended for publication by University of London

12/6 net

Printed and Published by:

TAYLOR & FRANCIS, LTD.
RED LION COURT, FLEET STREET, LONDON, E.C.4.

CONTENTS OF No. 321.

Page

LXXXIX. The Statistics of Correlated Events.—I. By C. Domb, Clarendon Laboratory, Oxford 969

XC. The Di-Iso-Electronic Row and the Effective Charge in the L Isorows. By Anthony Felix Richter, Caroline University, Prague .. 983

XCI. The Laminar Boundary Layer on Solids of Revolution. By L. G. Whitehead, Ph.D., and G. S. Canetti, Ph.D., Aeronautical Department, Queen Mary College, University of London 988

XCII. A Theory of Radar Information. By P. M. Woodward, B.A., and I. L. Davies, M.A., T.R.E., Ministry of Supply 1001

XCIII. Some Optical Properties of Evaporated Layers of Silver, Copper and Tin. By D. G. Avery, Ph.D., Royal Holloway College, London University. (Plates XXXII. & XXXIII.) 1018

XCIV. The Magnetic Deflection of Fast Charged Particles in the Photographic Emulsion. By C. C. Dilworth, S. J. Goldsack, Y. Goldschmidt-Clermont and F. Levy. (Plate XXXIV.) 1032

XCV. The Momentum and Sign of Fast Cosmic Ray Particles. By J. E. Moyal, Department of Mathematics, The University, Manchester.. 1058

XCVI. Correspondence :—

- The Velocity of Second Sound Below 1° K. By K. R. Atkins and D. V. Osborne, Royal Society Mond Lab., Cambridge 1078
- The Velocity of Flow of Helium II in the Creeping Film. By L. C. Jackson and D. G. Henshaw, H.H. Wills Physical Laboratory, University of Bristol 1081

⁂All communications for the Philosophical Magazine should be addressed, post-paid, to the Editors, c/o Messrs. Taylor and Francis, Ltd., Red Lion Court, Fleet Street, London, England.

LXXXIX. *The Statistics of Correlated Events.*—I.

By C. Domb,
Clarendon Laboratory, Oxford*.

[Received, June 20, 1950].

Summary.

The present paper is an attempt to formulate the mathematical properties of events occurring in time with a correlation between them. One effect of the correlation is a change in the mean square deviation of the number of events occurring in an interval of time t. By analogy with the shot effect in the presence of space change, this is denoted by a factor Γ^2 for large t, and Γ^2 is evaluated in terms of the interval distributions between events. For finite intervals t a corresponding factor $\gamma^2(t)$ is introduced, which usually tends to 1 as $t \to 0$. A correlation function between events occurring at times separated by an interval τ is defined, and its relation to $\gamma^2(t)$ is discussed. A generalization of Campbell's Theorem applying to correlated events is derived. Finally the problem of the random partitioning of correlated events is discussed.

§1. Introduction.

Suppose that events occur randomly and independently in time, the probability of an event occurring in the interval $(t, t+dt)$ being λdt; such events will be referred to briefly as " random events ". There are a number of problems in which the concept of random events can be regarded as a valid physical approximation, and as a typical example we may take the emission of electrons from a cathode in a valve. The properties of random events have been studied extensively, particularly in connection with the shot effect and the properties of random noise. Little attention, however, seems to have been paid to the properties of " correlated events ", that is, events in which the probability of an occurrence at a certain time is dependent on the distribution of events which have occurred previously.

The most common physical problem in which there is a correlation between events is the shot effect in the presence of space charge, and here the correlating mechanism is enormously complicated. However, the essential physical results of the correlation can be expressed quite simply. For random events it can readily be shown (*e. g.* Bateman 1910) that, if n is the number of events occurring in a finite interval of length t,

$$\mathrm{E}(n)=\lambda t, \quad . \quad . \quad . \quad . \quad . \quad . \quad . \quad . \quad . \quad (1)$$

$$\mathrm{E}(n^2)-[\mathrm{E}(n)]^2=\lambda t, \quad . \quad . \quad . \quad . \quad . \quad . \quad . \quad . \quad . \quad (2)$$

---

* Communicated by Prof. M. H. L. Pryce.

where E(u) denotes the expectation, or mean value of u. In the presence of space charge there are two changes in the above formulæ. Firstly, the mean number of events is reduced, so that we now have

$$E(n)=\alpha\lambda t, \quad . \quad . \quad . \quad . \quad . \quad . \quad . \quad . \quad . \quad . \quad (3)$$

where α lies between 0 and 1. Secondly, the fluctuations are smoothed, so that

$$E(n^2)-[E(n)]^2 \sim \Gamma^2\alpha\lambda t, \quad . \quad . \quad . \quad . \quad . \quad . \quad . \quad . \quad (4)$$

where Γ^2 lies between 0 and 1, and is usually referred to as the space charge reduction factor. It should be noted that although (2) is valid for an interval of any length, t, the definition of Γ^2 in (4) usually refers to the asymptotic value for large t; this point will be considered in more detail later in § 5.

A good deal of work has been done on the evaluation of Γ^2 in particular cases of physical interest (see North (1940) for references). In point of fact, however, the relations (3) and (4) arise immediately a correlation is introduced between events, and a fundamental analysis in terms of the theory of probability should be possible, giving α and Γ^2 in terms of the correlations between events. As far as the writer is aware, the only attempt along these lines is that of Whittaker (1938).

In the present paper it is proposed to consider classes of correlated events in which the probability of an event occurring at a given time depends on the time of occurrence of the previous r events. This means that any r intervals between successive occurrences are correlated, and such events will be referred to as events of class r. For many types of non-random events this is not a particularly simple definition. For example, if we consider a purely random primary series in which each primary event is followed by a secondary event at a fixed time τ after it, one can easily see that the complete set of primary and secondary events are of class ∞, even though the properties of the set are easy to discuss by elementary means. Nevertheless, given any set of events, the property immediately accessible to observation is the length of successive intervals, and one of our purposes is to relate the interval distributions to α and Γ^2 defined in (3) and (4).

§ 2. EVENTS OF CLASS 1.

We first consider in detail the properties of events in which the probability of an occurrence depends only on the time which has elapsed from the previous occurrence. This type of problem arises in the theory of particle counters, and has been discussed by a number of authors (see *e. g.* Feller 1948); it has also arisen recently in connection with genetics (Owen 1949). The advantageous feature of events of class 1 is that an exact solution is available in terms of Laplace transforms (Domb 1948, Owen 1949), and the physical properties of the solution can readily be determined. We now proceed to deduce this solution; much of the development will parallel previous discussions, but the results are required in a somewhat different form.

Suppose that if no event has occurred in an interval ξ after a given event, the probability of an occurrence in the interval $(\xi, \xi+d\xi)$ is $\lambda f(\xi)d\xi$. In cases of practical interest, we should expect $f(\xi)$ to tend to unity for large ξ. Let $\phi(\xi)$ be the probability that no event occurs in an interval ξ after a given event. Then

$$\phi(\xi+d\xi)=\phi(\xi)[1-\lambda f(\xi)d\xi]$$

or

$$\phi(\xi)=e^{-\lambda \mathrm{F}(\xi)}\left(\mathrm{F}(\xi)=\int_0^\xi f(u)\,du\right). \quad . \quad . \quad . \quad . \quad (5)$$

The probability that the interval between two successive events has length between ξ and $\xi+d\xi$ is thus

$$\lambda f(\xi)e^{-\lambda \mathrm{F}(\xi)}d\xi=g(\xi)\,d\xi. \quad . \quad . \quad . \quad . \quad . \quad . \quad . \quad . \quad (6)$$

Now let $u_n(t)$ be the probability that n events occur in the interval $(0, t)$. We can divide $u_n(t)$ into mutually exclusive classes in which the last event occurs in $(t-\eta, t-\eta+d\eta)$, the probability being $u_n(t, \eta)\,d\eta$. It is easy to see that

$$u_n(t, \eta)=e^{-\lambda \mathrm{F}(\eta)}u_n(t-\eta, 0)=e^{-\lambda \mathrm{F}(\eta)}w_n(t-\eta), \quad . \quad . \quad . \quad (7)$$

so that

$$u_n(t)=\int_0^t u_n(t, \eta)\,d\eta=\int_0^t e^{-\lambda \mathrm{F}(\eta)}w_n(t-\eta)\,d\eta. \quad . \quad . \quad . \quad (8)$$

We may rewrite (8) symbolically in the form

$$u_n(t)=\mathrm{P}w_n(t), \quad . \quad . \quad . \quad . \quad . \quad . \quad . \quad . \quad . \quad (9)$$

where P is the linear operator defined by (8).

$w_n(t)$ can similarly be divided into mutually exclusive classes in which the last event but one occurs in $(t-\zeta, t-\zeta+d\zeta)$, and as above, we deduce that

$$w_n(t)=\int_0^t w_{n-1}(t-\zeta)g(\zeta)\,d\zeta, \quad . \quad . \quad . \quad . \quad . \quad . \quad . \quad (10)$$

or symbolically

$$w_n(t)=\mathrm{Q}w_{n-1}(t)=\mathrm{Q}^{n-1}w_1(t), \quad . \quad . \quad . \quad . \quad . \quad . \quad . \quad (11)$$

where Q is the linear operator defined by (10).

In discussing the probability distribution of numbers of events it is usually convenient to introduce the moment generating function, for example,

$$w(\theta, t)=\sum_1^\infty w_n(t)e^{n\theta}=\sum_1^\infty e^{n\theta}\mathrm{Q}^{n-1}w_1(t). \quad . \quad . \quad . \quad . \quad (12)$$

Now for any finite t we can reasonably assume that the probability of n events occurring tends to zero as n tends to infinity. Thus we may write symbolically

$$w(\theta, t)=\frac{w_1(t)e^\theta}{1-\mathrm{Q}e^\theta}, \quad . \quad . \quad . \quad . \quad . \quad . \quad . \quad . \quad (13)$$

so that $w(\theta, t)$ satisfies an integral equation. We have discussed the solution in terms of linear operators, since the whole development can be formally generalized to events of class r, provided the operators P and Q are re-defined appropriately.

We now particularize to events of class 1, and take Laplace transforms* in t. The Laplace transform of any function will be denoted by a capital letter; for example $G(p)$ will be used for the Laplace transform of $g(t)$ defined in (6). The operators P, Q now have a very simple interpretation, Q corresponding to a multiplication by $G(p)$, and P to a multiplication by $[1-G(p)]/p$. Equation (13) becomes

$$w(\theta, p)=\frac{w_1(p)e^{\theta}}{1-G(p)e^{\theta}}=\frac{w_1(p)}{e^{-\theta}-G(p)} \quad . \; . \; . \; . \; . \; . \quad (14)$$

and correspondingly,

$$U(\theta, p)=\frac{w_1(p)[1-G(p)]}{p[e^{-\theta}-G(p)]}. \quad . \; . \; . \; . \; . \; . \; . \; . \quad (15)$$

To specify the solution completely we should now consider the initial conditions at $t=0$, and hence determine $w_1(t)$. But in fact, as we should expect, the asymptotic solution for sufficiently large t is independent of $w_1(t)$ and depends only on the form of $g(t)$. This asymptotic solution can be derived by expanding (15) as a series of residues (Domb 1948),

$$u(\theta, t)=\sum_s A_s(\theta, t)e^{m_s t}, \quad . \; . \; . \; . \; . \; . \; . \quad (16)$$

where the m_s are the roots of

$$e^{-\theta}-G(p)=0. \quad . \; . \; . \; . \; . \; . \; . \; . \; . \quad (17)$$

The dominant term is given by the real root m_1 of (17), and one can readily obtain an expansion of this root in powers of θ, the coefficients of which are the asymptotic values of the cumulants of the $u_n(t)$ distribution. We find that

$$\left.\begin{aligned} E(n)&\sim t/g_1, \\ E(n^2)-[E(n)]^2&\sim (g_2/g_1^3-1/g_1)t, \end{aligned}\right\} \quad . \; . \; . \; . \; . \; . \quad (18)$$

where

$$g_r=\int_0^{\infty} t^r g(t)\,dt,$$

and is the rth moment of the $g(t)$ distribution. Hence in the notation of §1,

$$\left.\begin{aligned} \alpha&=1/\lambda g_1, \\ \Gamma^2&=g_2/g_1^2-1. \end{aligned}\right\} \quad . \; . \; . \; . \; . \; . \; . \; . \; . \quad (19)$$

---

* We depart here from the notation of Domb (1948) and define the Laplace transform of a function $y(t)$ as $\int_0^{\infty} y(t)e^{-pt}\,dt$. This is now adopted by many writers, and leads to some simplication of formulæ,

It is important to observe that Γ^2 depends only on the first two moments of the $g(t)$ distribution. Thus $g(t)$ could be replaced by any other distribution having the same first two moments without altering Γ^2; as a particular example $g(t)$ could be formally replaced by an error distribution whose first two moments are g_1 and g_2, although this is not feasible physically, since t cannot be negative. Similar considerations apply to higher moments of the $u_n(t)$ and $g(t)$ distributions, but these are not usually of physical interest.

We shall now give a few practical examples to illustrate the evaluation of (19).

(i) An α-particle counter of constant recovery time β. $g(t)$ is the sum of two distributions, a fixed length β and a distribution $\lambda e^{-\lambda u}du$.

$$\left.\begin{aligned} g_1&=\beta+1/\lambda, & \alpha&=1/(1+\lambda\beta), \\ g_2-g_1^2&=1/\lambda^2, & \Gamma^2&=1/(1+\lambda\beta)^2, \end{aligned}\right\} \quad . \quad . \quad . \quad (20)$$

so that Γ^2 is always less than 1, as we should expect.

(ii) Consider $g(t)=\dfrac{\lambda^\nu t^{\nu-1}}{\Gamma(\nu)}e^{-\lambda t}$; $\nu=1$ corresponds to the uncorrelated case, $0<\nu<1$ corresponds to an attractive correlation, and $\nu>1$ to a repulsive correlation. In this case $\mathrm{G}(p)=(\lambda/p+\lambda)^\nu$, and equation (17) can be solved exactly giving

$$m_1=-\lambda+\lambda e^{\theta/\nu}. \quad . \quad . \quad . \quad . \quad . \quad . \quad . \quad . \quad (21)$$

(There are no other roots of (17) in this case, the remainder being given by an integral round the branch point $p=-\lambda$). We readily deduce that

$$\alpha=1/\nu, \qquad \Gamma^2=1/\nu, \quad . \quad . \quad . \quad . \quad . \quad . \quad . \quad . \quad (22)$$

so that $\Gamma^2<1$ for repulsive correlation, and >1 for attractive correlation.

(iii) Let $g(t)=\beta\delta(t)+(1-\beta)\lambda e^{-\lambda t}$; this means that there are finite probabilities β, β^2 . . . . of the simultaneous emission of 2, 3, events. Then

$$\alpha=1/1-\beta, \qquad \Gamma^2=1+\beta/1-\beta. \quad . \quad . \quad . \quad . \quad . \quad . \quad (23)$$

This is a particular case of a more general problem considered by Whittaker (1938).

§ 3. FORMAL GENERALIZATION TO EVENTS OF CLASS r.

We now suppose that if the intervals between the last r occurrences are $\xi_1, \xi_2, \ldots \xi_{r-1}$ the probability that an event occurs in the interval $[\eta, \eta+d\eta]$ from the last occurrence is $\lambda f(\xi_1, \xi_2 \ldots \xi_{r-1}; \eta)$ (this is a conditional probability). The relations (5) to (13) can be formally generalized, many of them now assuming the form of conditional probabilities. Thus

$$\left.\begin{aligned} &\phi(\xi_1, \ldots \xi_{r-1}; \eta)=e^{-\lambda \mathrm{F}(\xi_1, \ldots \xi_{r-1}; \eta)}, \\ &\left[\mathrm{F}(\xi_1, \ldots \xi_{r-1}; \eta)]=\int_0^\eta f(\xi_1, \ldots \xi_{r-1}; u)\,du\right]. \end{aligned}\right\} \quad . \quad (24)$$

and the probability $h(\xi_1, \ldots \xi_{r-1}; \eta)$ that the interval following a given event lies between η and $\eta+d\eta$, when the previous $(r-1)$ intervals are $\xi_1, \ldots \xi_{r-1}$ is

$$\lambda f(\xi_1, \ldots \xi_{r-1}; \eta) e^{-\lambda F(\xi_1, \ldots \xi_{r-1}; \eta)} d\eta. \quad . \quad . \quad . \quad . \quad (25)$$

As before $u_n(t)$ can be divided into mutually exclusive classes

$$u_n(t; \xi_1, \ldots \xi_{r-1}; \eta)$$

and we can define $w_n(t; \xi_1, \ldots \xi_{r-1})$ $[=u_n(t; \xi_1, \ldots \xi_{r-1}; 0]$. The operators P and Q are now given by

$$\left.\begin{aligned} \mathrm{P}w_n(t; \xi_1, \ldots \xi_{r-1}) &= \int_0^\infty d\xi_1 \ldots \int_0^\infty d\xi_{r-1} \int_0^t d\eta e^{-\lambda F(\xi_1, \ldots \xi_{r-1}; \eta)} \\ &\qquad \times w_n(t-\eta, \xi_1, \ldots \xi_{r-1}), \\ \mathrm{Q}w_n(t; \xi_1, \ldots \xi_{r-1}) &= \int_0^\infty h(\eta, \xi_1, \ldots; \xi_{r-1})\, d\eta \\ &\qquad \times w_n(t-\xi_{r-1}, \eta, \xi_1 \ldots \xi_{r-2})\, d\eta. \end{aligned}\right\} \quad . \quad . \quad . \quad (26)$$

Equation (13) now furnishes an integral equation for $w(\theta, \xi_1, \ldots \xi_{r-1})$, the operator Q being given by (26).

Unfortunately no transformation seems to be available in the general case to provide the analogue of the Laplace transform solution for events of class 1. On physical grounds we might expect the solutions to have a fairly simple asymptotic character, and we shall find this borne out in the next section.

§ 4. REFORMULATION IN TERMS OF INTERVAL DISTRIBUTIONS.

For event of class r any r adjacent intervals are correlated, but any intervals separated by r or more intervening intervals are uncorrelated. Let $t_n(\xi)d\xi$ be the probability that the sum of n adjacent intervals lies between ξ and $\xi+d\xi$. Then the probability that n events or more occur in a time t after a given occurrence is given by

$$q_n(t) = \int_0^t t_n(\xi)\, d\xi \qquad (n \geqslant 1). \quad . \quad . \quad . \quad . \quad . \quad (27)$$

Thus the probability that exactly n events occur is

$$p_n(t) = q_n(t) - q_{n+1}(t) \qquad (n \geqslant 1). \quad . \quad . \quad . \quad . \quad . \quad (28)$$

Hence the problem of determining the distribution of n is equivalent to determining $t_n(\xi)$.

The explicit evaluation of $t_n(\xi)$ is complicated; for large n we should expect $t_n(\xi)$ to be normally distributed, and it might be possible to derive asymptotic results on this basis. However, we shall find it more convenient to derive the moments of the $t_n(\xi)$ distribution (which can be done quite readily even for events of class r) and deduce results by analogy with events of class 1, for which an exact solution is available. For events of class 1, the cumulants of the $t_n(\xi)$ distribution are simply n times the cumulants of the $g(\xi)$ distribution, so that

$$\left.\begin{aligned} \mu_1^{(n)}&=ng_1, \\ \mu_2^{(n)}-\mu_1^{(n)2}&=n(g_2-g_1^2). \end{aligned}\right\} \quad . \quad . \quad . \quad . \quad . \quad . \quad . \quad (29)$$

We have seen that α and Γ^2 depend only on the two moments g_1 and g_2, and hence only on the two terms of (29). For events of class r let

$$g(\xi_1, \xi_2 \dots \xi_r)\, d\xi_1 \dots d\xi_r$$

be the joint probability distribution of r adjacent intervals, and denote the mean value of any interval, $\mathrm{E}(\xi_1)$, by g_1, and $\mathrm{E}(\xi_1\ \xi_i)$ by g_{1i}; thus if $i>r$, $\mathrm{E}(\xi_1\ \xi_i)=g_1^2$. Then

$$\mu_1^{(n)}=\mathrm{E}(\xi_1+\dots+\xi_n)=\mathrm{E}(\xi_1)+\mathrm{E}(\xi_2)+\dots \mathrm{E}(\xi_n)=ng_1 \quad . \quad (30)$$

$$\begin{aligned} \mu_2^{(n)}&=\mathrm{E}\left(\sum_{i=1}^{n} \xi_i\right)^2=\mathrm{E}\left(\sum_{i=1}^{n} \xi_i^2+2\sum_{i<j} \xi_i\xi_j\right) \\ &=ng_{11}+2(n-1)g_{12}+2(n-2)g_{13}+\dots 2(n-r+1)g_{1r} \\ &\qquad +\{n^2-n-2[(n-1)+\dots(n-r+1)]\}g_1^2. \quad . \quad . \quad . \quad (31) \end{aligned}$$

Hence

$$\begin{aligned} \mu_2^{(n)}-\mu_1^{(n)2}&=n[g_{11}+2g_{12}+\dots 2g_{1r}-\overline{2r-1}\,g_1^2] \\ &\qquad -2[g_{12}+2g_{13}+\dots(r-1)g_{1r}-\frac{r(r-1)}{2}g_1^2]. \quad . \quad . \quad (32) \end{aligned}$$

The second term of (32) does not involve n, and since r is a finite number, it will become negligible for sufficiently large n; in fact, it represents something in the nature of an end effect, and we should not expect it to influence the asymptotic distribution of the n's. With the exception of this term there is a complete analogy between (20) and (32), and (29), and the problem of class r is thus equivalent to a problem of class 1, in which g_2 is replaced by

$$g_{11}+2(g_{12}+\dots g_{1r})-(2r-2)g_1^2. \quad . \quad . \quad . \quad . \quad (33)$$

Using the result (19) for events of class 1, we deduce that, for events of class r,

$$\left.\begin{aligned} \alpha&=1/\lambda g_1, \\ \Gamma^2&=\frac{g_{11}+2g_{12}+\dots 2g_{1r}-(2r-1)g_1^2}{g_1^2}. \end{aligned}\right\} \quad . \quad . \quad . \quad . \quad (34)$$

We may also observe that there would be no difficulty in deriving higher moments in a similar manner.

§ 5. THE CORRELATION FUNCTION.

So far we have been dealing with asymptotic values for large intervals of time; we shall now consider an interval $[0, t]$ of finite length. Let us divide the interval $[0, t]$ into a large number N of sub-intervals of length δt, and denote the number of events occurring in the ith sub-interval, $[t_i\, t_i+\delta t]$, by δn_i. Then, since we have assumed that the process is in a "stationary" condition, E (δn_i) is independent of t_i, and E $(\delta n_i\, \delta n_j)$ depends only on (t_j-t_i) Therefore

$$E(n)=E\left[\sum_{i=1}^{N}\delta n_i\right]=\sum_{i=1}^{N}E(\delta n_i)=\lambda\alpha t, \qquad . \quad . \quad . \quad . \qquad (35)$$

so that this relation is the same for finite t. We now write

$$E(\delta n_i\delta n_j)=(\lambda\alpha\delta t)^2[1+\rho(t_i-t_j)], \qquad . \quad . \quad . \quad . \quad . \qquad (36)$$

where $(\rho\tau)$ can be regarded as a correlation function, indicating the time during which correlation is appreciable. Then

$$E(n^2)=E\left(\sum_{i=1}^{N}\delta n_i\right)^2=E\left(\sum_{ij=1}^{N}\delta n_i\delta n_j\right)=\sum_{ij=1}^{N}E(\delta n_i\delta n_j), \qquad . \qquad (37)$$

and as N tends to ∞, this can readily be transformed into

$$2(\lambda\alpha)^2\int_0^t(t-\tau)[1+\rho(\tau)]d\tau=\lambda^2\alpha^2t^2+2(\lambda\alpha)^2\int_0^t(t-\tau)\rho(\tau)d\tau. \qquad . \qquad (38)$$

Hence if we define $\gamma^2(t)$ by the relation

$$E(n^2)-[E(n)]^2=\gamma^2\alpha\lambda t, \qquad . \quad . \quad . \quad . \quad . \quad . \qquad (39)$$

for a finite interval t, we shall have

$$\gamma^2(t)=\frac{2\lambda\alpha}{t}\int_0^t(t-\tau)\rho(\tau)d\tau. \qquad . \quad . \quad . \quad . \quad . \quad . \quad . \qquad (40)$$

(It should be noted that $\rho(\tau)$ has a δ-function singularity at $\tau=0$ corresponding to $i=j$ in (36)).

It is not difficult to see that, if the probability of two events occurring in an interval δt is $0(\delta t^2)$, $\gamma^2(t)$ must tend to unity as $t\rightarrow 0$. On the other hand by definition $\gamma^2(t)\rightarrow\Gamma^2$ as $t\rightarrow\infty$, so that $\gamma^2(t)$ passes from 1 to Γ^2 as t goes from 0 to ∞. Letting $t\rightarrow\infty$ in (40),

$$\Gamma^2=2\lambda\alpha\int_0^{\infty}\rho(\tau)d\tau. \qquad . \quad . \quad . \quad . \quad . \quad . \quad . \quad . \qquad (41)$$

The above formulæ are well illustrated by the example considered previously of primary and secondary events separated by a fixed interval β, for which

$$2\lambda\alpha\rho(\tau)=\delta(\tau)+\delta(\tau-\beta). \qquad . \quad . \quad . \quad . \quad . \quad . \quad . \qquad (42)$$

Here,

$$\gamma^2(t)=\begin{cases}1 & t<\beta,\\ 2 & t>\beta,\end{cases}$$

so that for $t<\beta$, the events may be regarded as single and random, but for $t>\beta$ they are to be regarded as doublets.

We can readily make use of the correlation function to determine the correlation between any two finite intervals of lengths t_1 and t_2, separated by an interval of length u. If m refers to the number of events occurring in the first interval, and n to the number of events occurring in the second,

$$\mathrm{E}(mn)=\mathrm{E}\left[\left(\sum_{i=1}^{\mathrm{M}}\delta m_i\right)\left(\sum_{j=1}^{\mathrm{N}}\delta n_j\right)\right]=\sum_{i=1}^{\mathrm{M}}\sum_{j=1}^{\mathrm{N}}\mathrm{E}(\delta m_i\delta n_j\Big),$$

and this can readily be transformed into

$$\lambda^2\alpha^2\left[t_1t_2+\int_0^{t_1}\tau\rho(u+\tau)d\tau+t_1\int_{t_1}^{t_2}\rho(u+\tau)\,d\tau\right.$$
$$\left.+\int_{t_2}^{t_1+t_2}(t_2+t_1-\tau)\rho(u+\tau)d\tau\right](t_2\geqslant t_1). \quad . \quad . \quad . \quad (43)$$

For events of class 1, we can obtain an explicit solution for the correlation function by means of Laplace transforms. We require first to specify the value of $\mathrm{W}_1(p)$ in (15) to correspond to the " stationary " condition. This can most readily be determined by the condition that $\mathrm{E}(n)$ must be equal to $\lambda\alpha t$ for any finite t; hence $\mathrm{W}_1(p)=[1-\mathrm{G}(p)]/g_1p$. (An alternative derivation is given by Domb (1948)). We therefore deduce from (5) that the Laplace transform of $\mathrm{E}(n^2)$ is

$$\frac{1+\mathrm{G}(p)}{g_1p^2[1-\mathrm{G}(p)]}. \quad . \quad . \quad . \quad . \quad . \quad . \quad . \quad . \quad (44)$$

Let $\mathrm{R}(p)$ be the Laplace transform of $\rho(t)$. Then taking Laplace transforms in (38) and equating to (44) we have

$$\frac{2(\lambda\alpha)^2}{p^3}+\frac{2(\lambda\alpha)^2\mathrm{R}(p)}{p^2}=\frac{\lambda\alpha[1+\mathrm{G}(p)]}{p^2[1-\mathrm{G}(p)]}$$

or
$$\mathrm{R}(p)=\frac{1+\mathrm{G}(p)}{2\lambda\alpha[1-\mathrm{G}(p)]}-\frac{1}{p}=\frac{1}{2\lambda\alpha}-\frac{1}{p}+\frac{\mathrm{G}(p)}{\lambda\alpha[1-\mathrm{G}(p)]}. \quad . \quad . \quad (45)$$

The first term of the final expression in (45) corresponds to the δ-function singularity at $t=0$. When there is no correlation, so that $\mathrm{G}(p)=\lambda/p+\lambda$ the remaining terms in (45) vanish, as expected.

We now apply (45) to some particular cases considered previously in §2.

(i) For an α-particle counter of constant recovery time β

$$\mathrm{G}(p)=\lambda e^{-\beta p}/(p+\lambda) \qquad \text{and} \qquad \alpha=1/(1+\beta\lambda).$$

Therefore
$$\mathrm{R}(p)-\frac{1}{2\lambda\alpha}=\frac{(1+\beta\lambda)e^{-\beta p}}{p+\lambda-\lambda e^{-\beta p}}-\frac{1}{p} \quad . \quad . \quad . \quad . \quad . \quad . \quad (46)$$

and this can be expanded in the form

$$-\frac{1}{p}+\frac{(1+\beta\lambda)e^{-\beta p}}{p+\lambda}+\frac{\lambda(1+\beta\lambda)e^{-2\beta p}}{(p+\lambda)^2}+\ldots. \quad . \quad . \quad . \quad (47)$$

Thus we have an explicit expression for $\rho(t)$ in the form

$$\rho(t)-\frac{1}{2\lambda\alpha}\delta(t)$$
$$=-1+(1+\beta\lambda)\left[e^{-\lambda t_1}+\lambda t_2 e^{-\lambda t_2}+\frac{\lambda^2 t_3^2}{2\,!}e^{-\lambda t_3}+\ \ldots\right](t_r=t-r\tau), \quad . \quad (48)$$

where, if $(r-1)\tau\leqslant t\leqslant r\tau$, r terms are to be taken into account.

It is also of interest to consider the asymptotic behaviour of $\rho(t)$, and this can readily be obtained from the poles of (46). There is no pole at $p=0$, and hence the dominating term in an asymptotic series such as (16) is given by the real root, $-\eta$, of

$$p+\lambda-\lambda e^{-\beta p}=0.$$

Then
$$\rho(t)\sim\frac{(1+\beta\lambda)(1-\eta/\lambda)}{1+\beta(\lambda-\eta)}e^{-\eta t}. \quad . \quad . \quad . \quad . \quad . \quad . \quad (49)$$

(ii) Let

$$g(t)=\frac{\lambda^\nu t^{\nu-1}}{\Gamma(\nu)}e^{-\lambda t}, \qquad \text{so that} \qquad \mathrm{G}(p)=\left(\frac{\lambda}{p+\lambda}\right)^\nu \qquad \text{and} \qquad g_1=\nu/\lambda.$$

We have
$$\mathrm{R}(p)-\frac{\nu}{2\lambda}=\frac{\nu\lambda^{\nu-1}}{(p+\lambda)^\nu-\lambda^\nu}-\frac{1}{p}. \quad . \quad . \quad . \quad . \quad . \quad (50)$$

When ν is an integer, r, this can be readily evaluated explicitly as a sum of exponentials, the poles being given by $p/\lambda=-1+e^{2s\pi i/r}$; for example when $\nu=2$,

$$\rho(t)-\frac{\delta(t)}{\lambda}=-e^{-2\lambda t}. \quad . \quad . \quad . \quad . \quad . \quad . \quad . \quad . \quad (51)$$

The asymptotic form of $\rho(t)$ for general ν cannot be obtained as readily as in the previous example, since branch line integrals must be considered.

§ 6. THE GENERALIZATION OF CAMPBELL'S THEOREM.

For purely random events Campbell considered the distribution of amplitude in an instrument, when the effect of each event could be represented by an amplitude $s(t)$ after time t. We shall now consider the generalization of his results to correlated events. Let y be the amplitude at the time of observation, and let us measure time t backwards from this point; again we divide our time interval into a large number of small sub-intervals $[t_1, t_1+\delta t]$, and

$$y=\operatorname*{Lt}_{\delta t\to 0}\sum_i \delta n_i\, s(t_i). \quad . \quad . \quad . \quad . \quad . \quad . \quad . \quad . \quad (52)$$

Therefore
$$\mathrm{E}(y)=\operatorname*{Lt}_{\delta t\to 0}\sum_i \mathrm{E}(\delta n_i)s(t_i)=\lambda\alpha\int_0^\infty s(t)\,dt \quad . \quad . \quad . \quad . \quad (53)$$

and
$$\mathrm{E}(y^2)=\operatorname*{Lt}_{\delta t\to 0}\sum_i\sum \mathrm{E}(\delta n_i\delta n_j)s(t_i)s(t_j). \quad . \quad . \quad . \quad . \quad . \quad (54)$$

Substituting from (36) and proceeding as before, this double integral can be transformed into

$$(\lambda\alpha)^2\left[\int_0^\infty s(t)\,dt\right]^2+2(\lambda\alpha)^2\int_0^\infty d\tau\rho(\tau)\int_0^\infty s(t)s(t+\tau)\,dt \quad . \quad . \quad (55)$$

and thus

$$E(y^2)-[E(y)]^2=2(\lambda\alpha)^2\int_0^\infty \rho(\tau)d\tau\int_0^\infty s(t)s(t+\tau)\,dt. \quad . \quad . \quad (56)$$

This may be regarded as a generalized form of Campbell's theorem, the δ-function term in $\rho(\tau)$ giving rise to the usual term $\int_0^\infty s^2(t)\,dt$. As a particular example, if $\rho(t)$ is only significant during a time for which $s(t)$ does not change appreciably, the second integral in (56) can be replaced by $\int_0^\infty s^2(t)\,dt$, and using (41) we have

$$E(y^2)-[E(y)]^2=\lambda\alpha\Gamma^2\int_0^\infty s^2(t)\,dt. \quad . \quad . \quad . \quad . \quad . \quad (57)$$

This is the usual form of the theorem for the shot effect in the presence of space charge.

If we now take $s(t)$ to correspond to a sharply tuned circuit at frequency $\omega/2\pi$ $E(y^2)$ will correspond to a "power spectrum", and we obtain the standard formula

$$P(\omega)=\int_0^\infty 2\rho(\tau)\cos\omega\tau\,d\tau. \quad . \quad . \quad . \quad . \quad . \quad . \quad (58)$$

This is especially useful in considering events of class 1, since $R(p)$ has been evaluated explicitly in (45), and

$$P(\omega)=R(i\omega)+R(-i\omega). \quad . \quad . \quad . \quad . \quad . \quad . \quad (59)$$

As a particular case, for the α-particle counter we deduce from (46) that

$$P(\omega)=\frac{1+\beta\lambda}{\lambda}\left[1-\frac{1-\cos\beta\omega+\frac{\omega}{\lambda}\sin\beta\omega}{1-\cos\beta\omega+\frac{\omega}{\lambda}\sin\beta\omega+\omega^2/2\lambda^2}\right]. \quad . \quad (60)$$

It is interesting to note that as λ tends to ∞, this tends to zero for all frequencies other than multiples of $2\pi/\beta$, which is in accordance with what we would expect physically.

A rather interesting example is that of primary and secondary events separated by a fixed interval β. From (42) we readily deduce that

$$P(\omega)=\frac{1}{\lambda}\cos^2\frac{\beta\omega}{2}. \quad . \quad . \quad . \quad . \quad . \quad . \quad . \quad . \quad (61)$$

§7. THE PARTITIONING OF EVENTS

We now consider the effect of the random partitioning of correlated events into two groups. This problem has a physical application to valves containing two or more electrodes, and gives rise to the phenomenon of "partition noise." Let α_1 and α_2 be the probabilities that any given event falls into groups 1 or 2 respectively ($\alpha_1+\alpha_2=1$). Then the probability of an occurrence of n_1 events in group 1 and n_2 in group 2 in an interval $[0, t]$ is

$$\psi(n_1, n_2\,;\ t)=\frac{n\,!}{n_1!\ n_2\,!}\,\alpha_1^{n_1}\alpha_2^{n_2}u_n(t), \quad . \quad . \quad . \quad . \quad . \quad (62)$$

where $n=n_1+n_2$ and $u_n(t)$ is the probability of n events occurring in $[0, t]$. We have seen from §'s 2, 3 that $u_n(t)$ may be formally written as $PQ^{n-1}w_1(t)$ where P and Q are certain linear operators. The joint moment generating function of n_1 and n_2 is given by

$$\begin{aligned}\Psi(\theta_1, \theta_2\,;\ t)&=\sum_{n_1n_2}\psi(n_1, n_2\,;\ t)e^{(n_1\theta_1+n_2\theta_2)}\\ &=PQ^{-1}\sum_{n_1n_2}\frac{(n_1+n_2)\,!}{n_1!\ n_2\,!}(\alpha_1Qe^{\theta_1})^{n_1}(\alpha_2Qe^{\theta_2})^{n_2}w_1(t)\\ &=P\sum_{n}(\alpha_1e^{\theta_1}+\alpha_2e^{\theta_2})^nQ^{n-1}w_1(t). \quad . \quad . \quad . \quad . \quad . \quad . \quad . \quad (63)\end{aligned}$$

This is identical in form with the moment generating function for n except that e^{θ} is replaced by $\alpha_1e^{\theta_1}+\alpha_2e^{\theta_2}$. Hence if we know the expansion of the generating function for n we can immediately determine the corresponding expansion for n_1 and n_2 by replacing θ by

$$\ln\,[1+\alpha_1(e^{\theta_1}-1)+\alpha_2(e^{\theta_2}-1)].$$

In particular if we take into account only two terms of the cumulant generating function of n, we have

$$\ln u(\theta, t)\sim\lambda\alpha t(\theta+\Gamma^2\theta^2/2+\,\dots) \quad . \quad . \quad . \quad . \quad . \quad (64)$$

and the corresponding joint function is

$$\begin{aligned}\ln\Psi(\theta_1, \theta_2\,;\ t)=\lambda\alpha t\Big[&\alpha_1\theta_1+\alpha_2\theta_2+\frac{\theta_1^2}{2}(\alpha_1\alpha_2+\alpha_1^2\Gamma^2)\\ &+\frac{\theta_2^2}{2}(\alpha_1\alpha_2+\alpha_2^2\Gamma^2)+\alpha_1\alpha_2\theta_1\theta_2(\Gamma^2-1)+\,\dots\Big]. \quad . \quad (65)\end{aligned}$$

Thus, if we confine our attention to events of group 1,

$$\Gamma_1^2=\alpha_1\Gamma^2+\alpha_2\,; \quad . \quad . \quad . \quad . \quad . \quad . \quad . \quad . \quad . \quad . \quad (66)$$

and we may deduce the relation

$$\frac{E(n_1n_2)-E(n_1)E(n_2)}{\sqrt{(E(n_1)E(n_2))}}=\sqrt{(\alpha_1\alpha_2)}(\Gamma^2-1). \quad . \quad . \quad . \quad . \quad . \quad (67)$$

These latter results are standard in the theory of partition noise.

It has been pointed out to the author by Professor Pryce that all the above results can be deduced quite generally by an elementary process of averaging, since the partitioning process is independent of the correlating mechanism. In fact this is effectively the method used by Bakker (1938) to deduce the formulæ (66) and (67)*.

We now consider the interval distribution of partitioned events. We first observe that if the original series consists of events of class r, the partitioned series does likewise, since intervals separated by r intervening intervals remain uncorrelated. For events of class 1 the moment generating function of the partitioned series can readily be written down. The problem is then to determine the distribution of $\xi_1+\xi_2+\ldots\xi_r$, where the ξ's are independently distributed with probability $g(\xi)d\xi$, and r has distribution $\alpha_1\alpha_2^{r-1}$. This is a problem arising in many different fields (Kendall 1949) and the solution has been given independently by a number of writers (*e.g.* Woodward 1948). The moment generating function of the moment r's is $\alpha_1/(e^{-\theta}-\alpha_2)$, and that of the ξ's is $G(-\theta)$. Hence the generating function $G^{(1)}(-\theta)$ of the partitioned series is given by

$$G^{(1)}(-\theta)=\alpha_1/[G(-\theta)]^{-1}-\alpha_2. \qquad \text{(68)}$$

The first two moments can easily be determined from (68)

$$\left.\begin{aligned} g_1^{(1)}&=g_1/\alpha_1,\\ g_2^{(1)}&=(g_2-g_1^2)/\alpha_1-g_1^2\alpha_2/\alpha_1^2, \end{aligned}\right\} \qquad \text{(69)}$$

and we verify from (19) that (66) is satisfied.

For events of class r, although we cannot write down the complete generating function, we can determine the first and second moments. Thus

$$g_1^{(1)}=\underset{r\ \xi}{\mathrm{EE}}(\xi_1+\xi_2+\ldots\xi_r)=\underset{r}{\mathrm{E}}(rg_1)=g_1/\alpha_1. \qquad \text{(70)}$$

$$\begin{aligned} g_{11}^{(1)}&=\underset{r\ \xi}{\mathrm{EE}}(\xi_1+\xi_2+\ldots\xi_r)^2=\underset{r}{\mathrm{E}}[rg_{11}+2(r-1)g_{12}+2(r-2)g_{13}+\ldots]\\ &=\frac{1}{\alpha_1}[g_{11}+2\alpha_2g_{12}+2\alpha_2^2g_{13}+\ldots.]. \end{aligned} \qquad \text{(71)}$$

The correlations can be derived similarly, although the detailed evaluation of the various terms is rather cumbersome. We obtain

$$g_{1s}^{(1)}=\alpha_1^{s-2}\left[g_{1s}+s\alpha_2g_{1(s+1)}+\frac{s(s+1)}{2!}\alpha_2^2g_{1(s+2)}+\ \ldots(s\geq 2)\right]. \qquad \text{(72)}$$

the coefficients of the various terms being those in the expansion of $(1-x)^{-s}$.

---

* I am indebted to Dr. D. K. C. MacDonald for drawing my attention to this paper.

The series (71) (72) are not very convenient for manipulation, since the g_{1s} remain finite for large s. It is more convenient to take away the mean values, and put the results in the form

$$g_{11}^{(1)}-g_{1}^{(1)2}=\frac{\alpha_2}{\alpha_1^2}g_1^2+\frac{1}{\alpha_1}\Big[(g_{11}-g_1^2)+2\alpha_2(g_{12}-g_1^2)+2\alpha_2^2(g_{13}-g_1^2)+\ \ldots\Big]. \qquad (73)$$

$$g_{1s}^{(1)}-g_{1}^{(1)2}=\alpha_1^{s-2}\Big[(g_{1s}-g_1^2)+s\alpha_2(g_{1(s+1)}-g_1^2)+\frac{s(s+1)}{2\,!}(g_{1(s+2)}-g_1^2)+\ldots\Big]:$$

We can then easily verify, on substituting in (34), that the result (66) is obtained for the partitioned series, and this provides a useful check on the internal consistency of the formulæ derived.

ACKNOWLEDGMENT.

The author is indebted to Professor M. H. L. Pryce and Dr. D. K. C. MacDonald for helpful and stimulating discussion, and to the University of Oxford for the award of an I. C. I. Fellowship.

REFERENCES.

BAKKER, C. J., 1938, *Physica*, **5**, 581.
BATEMAN, H., 1910, *Phil. Mag.*, **20**, 698
DOMB, C., 1948, *Proc. Camb. Phil. Soc.*, **44**, 355.
FELLER, W., 1948, *Studies and Essays presented to R. Courant.* Interscience publishers, New York, p. 105.
KENDALL, D. G., 1949, *J. Royal Statist. Soc.*, B, **11**, 230.
NORTH, D. O., 1940, *R. C. A. Review*, **4**, 441.
OWEN, A. R. G., *Proc Roy. Soc.*, B, **136**, (1949) 67.
WHITTAKER, J. M., 1937, *Proc. Camb. Phil. Soc.*, **33**, 451; 1938, *Ibid.*, **34**, 158;
WOODWARD, P. M. 1948, *Proc. Comb. Phil. Soc.*, **44**, 404.

XC. *The Di-Iso-Electronic Row and the Effective Charge in the L Isorows.*

By Anthony Felix Richter,
Caroline University, Prague*.

[Received June 16, 1950.]

Summary.

The author's equation for the di-iso-electronic row enables us to compute by extrapolation the electron affinity of hydrogen, $E_H=0\cdot74$ eV. The author's equation is nearly identical with that of Hylleraas, but differs in an important term from that of Eucken. A relation is given between screening number and effective charge on one hand, and nuclear charge number Z and number of electrons in the isorow, i, on the other. Numerical values of the constants required to calculate screening numbers S_i in the K, L and M$-s$ isorows are given in Table I. It appears that with increasing Z, S_i approaches half the coefficient of the linear member of equation (10), *i. e.*, $S_i \sim \frac{1}{2}(2i-1-\bar{a}')$; when $Z \geqslant 20$, the screening constant for the di-iso-electronic row, $S_{II}=0\cdot631$, and that for the tri-iso-row, $S_{III}=1\cdot63$ and that for the ennea-isorow $S_{IX}=6\cdot01$, or $S'_{IX}=6\cdot40$ respectively.

In a previous paper on the K and L electrons (Richter 1948), the ionization potentials of iso-electronic atomic systems were expressed in a quadratic function of the variable $Z+1-i$, where Z is the charge number of the nucleus and i the number of electrons surrounding it ; the coefficients in the expression are functions of i only. The present work relates this method to the usual expression in terms of screening constants.

From the known experimental data we have derived the following expression for the ionization potentials J in a given iso-electronic row

$$J_i=\tfrac{1}{2}B_i(Z+1-i)^2+(A_i-\tfrac{1}{2}B_i)(Z+1-i)+D_i=(Z-S_i)^2R/n^2, \quad . \quad . \quad . \quad (1)$$

where B_i, A_i and D_i represent the quantum, row and correction constants respectively of the given row. Values of these constants in volts for the K and L iso-electronic rows are given in Table III. of the above-mentioned publication. Since B_i is very nearly the same for both K rows, and again for all L rows, we may take average values B'_K, B'_L, and the reduced constants corresponding to this choice are given in the same table ; these reduced constants are distinguished by a dash attached to the symbol. Usually the values of the individual and reduced constants differ little,

e. g. $B_{II}=27\cdot07$, $A_{II}=23\cdot72$, $D_{II}=0\cdot74$,
$B'_K=B'_{II}=27\cdot11$, $A'_{II}=23\cdot57$, $D'_{II}=1\cdot02$.

---

* Communicated by the Author.

The right-hand member of equations (1), where R denotes Rydberg's constant and n the principal quantum number, serves to evaluate the screening number S_i, or the effective charge. On inserting the individual constants for $i=2$ in equation (1) we obtain the equation for the di-iso-electronic row :

$$J_{II}=13{\cdot}535(Z-1)^2+10{\cdot}17(Z-1)+0{\cdot}74=R(Z-S_{II})^2. \quad . \quad . \quad (2)$$

It is worth noting that $10{\cdot}17=3R/4$, corresponding to the K$-\alpha$ line of the X-ray spectra, and further that extrapolation to $Z=1$ gives $E_H=0{\cdot}74$ eV. for the electron affinity of hydrogen. This value is identical with that determined by C. A. Hylleraas (Eucken 1938).

The difference between the di-isoelectronic formula and the quadratic hydrogen term is directly connected with the deviation of the screening number S_i from the value corresponding to "complete" screening, namely i. The screening number for the di-isoelectronic row derived from equation (2) is then given by

$$S_{II}=Z-[Z^2-1{\cdot}263Z+0{\cdot}317]^{\frac{1}{2}}=Z-Z^{*\frac{1}{2}}=Z-Z_{II} \quad . \quad . \quad . \quad (3)$$

or, using the reduced constants :

$$S'_{II}=Z-[Z^2-1{\cdot}260Z+0{\cdot}334]^{\frac{1}{2}}=Z-Z^{*\frac{1}{2}}=Z-Z_{II'}. \quad . \quad . \quad (3.2)$$

Then for $Z\geqslant 20$ we have the simple result

$$S_{II}=0{\cdot}631 \text{ and the effective charge } [Z^*_{II}]^{\frac{1}{2}}=Z-0{\cdot}631. \quad . \quad . \quad (4)$$

Two other equations have been elaborated for the di-isoelectronic row, one by C. A. Hyllerass (Eucken 1938) on wave-mechanical grounds :

$$J_{II}=R[Z^2-1{\cdot}250Z+0{\cdot}31488-0{\cdot}01752Z^{-1}+0{\cdot}00548Z^{-2}]=RZ^*, \quad . \quad . \quad . \quad . \quad . \quad . \quad (5)$$

and the other by Eucken (1938) :

$$J_{II}=R[Z^2-1{\cdot}250Z]. \quad . \quad . \quad . \quad . \quad . \quad . \quad . \quad . \quad (6)$$

It is clear that expressions (2) and (4) differ very little even for small Z, Hylleraas' result giving $S_{II}\sim 0{\cdot}625$. The strange-looking symbol $\sqrt{Z^*_{II}}$ is introduced to accord with the notation of Hylleraas and Hartree (Eucken 1938).

The analogous expressions for the tri-iso-electronic row are as follows :

$$J_{III}=3{\cdot}40(Z-2)^2+2{\cdot}54(Z-2)-0{\cdot}33 \quad . \quad . \quad . \quad . \quad . \quad (7)$$

and

$$S_{III}=Z-[Z^2-3{\cdot}254Z+2{\cdot}401]^{\frac{1}{2}} \quad . \quad . \quad . \quad . \quad . \quad . \quad . \quad (8)$$

It may be mentioned that the value 2·54 in equation (7) is 3R/16, corresponding to the L$-\beta$ line of the X spectra. As in the previous case, S becomes practically constant for $Z\geqslant 20$,

$$S_{III}\sim 1{\cdot}63 \quad \text{and} \quad \sqrt{Z^*_{III}}=Z-1{\cdot}63=Z_{III}. \quad . \quad . \quad . \quad (8.2)$$

Our picture of the dependence of the screening number S_i on Z and *i* becomes more intricate (Richter and Krestýnová 1947) whenever the quantum constant of the iso-row in question differs from that of the hydrogen L level, *i. e.* R/2=6·80. The simple picture may nevertheless be retained, substituting the value for the hydrogen L level either for the individual quantum constant of the L isoelectronic set under examination or for the reduced constant $B'_L(=6{\cdot}90)$. No very significant error is so introduced, the mean error of the reduced quantum constant ($\sigma=0{\cdot}033$) being less than that of any individual quantum constant in the L isorows with the sole exception of the tri-isoelectronic quantum constant with its $\sigma=0{\cdot}019$. To obtain the dependence in a simple algebraic form, we define quantities $\bar{a}_i$, $\bar{d}_i$, $\bar{a}'_i$, $\bar{d}'_i$, as follows :

$$\bar{a}_i=2A_i/B_i, \quad \bar{d}_i=2D_i/B_i, \quad \bar{a}'_i=2A'_i/B'_i, \quad \bar{d}'_i=2D'_i/B'_i. \quad . \quad . \quad (9)$$

Then the relations between Z and *i* on one hand and S_i or Z^*_i on the other are expressed by these equations :

$$\bar{S}_i=Z-[Z^2-(i-\bar{a}_i+i-1)Z+(i-\bar{a}_i)(i-1)+\bar{d}_i]^{\frac{1}{2}}=Z-Z_i^{*\frac{1}{2}}, \quad . \quad . \quad . \quad (10)$$

$$\bar{S}'_i=Z-[Z^2-(i-\bar{a}'_i+i-1)Z+(i-\bar{a}'_i)(i-1)+\bar{d}'_i]^{\frac{1}{2}}=Z-\sqrt{Z'^*_i}. \quad . \quad . \quad . \quad (10.2)$$

The calculated values of $\bar{a}_i$, $\bar{d}_i$, $\bar{a}'_i$, $\bar{d}'_i$ necessary to compute S_i and Z^*_i in the first twelve iso-electronic rows are given in Table I. On inserting the appropriate values we can write, *e. g.*

$$Z^*_{IX}=Z^2-12{\cdot}029Z+32{\cdot}35. \quad . \quad . \quad . \quad . \quad . \quad . \quad . \quad (11)$$

and $$Z_{IX}=[Z^2-12{\cdot}029+32{\cdot}35]^{\frac{1}{2}}=Z[1-12{\cdot}029Z^{-1}+32{\cdot}35Z^{-2}]^{\frac{1}{2}}.$$

If

$$|-12{\cdot}029Z^{-1}+32{\cdot}35Z^{-2}|=x_{IX}, \text{ then } Z_{IX}=Z(1+x_{IX})^{\frac{1}{2}}. \quad . \quad . \quad (11.2)$$

Under the supposition

$$-1<x<1$$

only the first two terms of Taylor's series are sufficient to determine the practically constant value of the screening power in the isorow inquired into, *i. e.* S_{IX}.

$$Z(1+x_{IX})^{\frac{1}{2}}=Z(1+\tfrac{1}{2}x_{IX}-\tfrac{1}{8}x^2_{IX}- \ . \ . \ . \ )=Z[1+\tfrac{1}{2}x_{IX}+R_2(x_{IX})]. \quad . \quad . \quad . \quad (11{\cdot}3)$$

The error caused by neglecting the remainder $R_2(x_{IX})$ of Taylor's series can be easily approximated by the inegality

$$R_2(x)<\frac{1}{8}\frac{|x|^2}{1-|x|}<\frac{1}{2}\frac{|x|^2}{1-|x|} \quad . \quad . \quad . \quad . \quad . \quad . \quad (12)$$

giving a more and less approximation.

As x depends on Z what we express by x_Z it is evident that

$$|x_{IX,20}| > |x_{IX,40}| > |x_{IX,80}|.$$

As $$|x_{IX,20}| = \left|\frac{-12{\cdot}029}{20} + \frac{32{\cdot}35}{400}\right| = 0{\cdot}68 < 1,$$

the formula (11·3) can be limited to the first two terms only without committing a significant error in evaluating S_{IX} for $Z \geqslant 20$.

Therefore $$Z_{IX} = Z(1 - 6{\cdot}01 Z^{-1}) \text{ and } S_{IX} = 6{\cdot}01. \quad . \quad . \quad . \qquad (11.4)$$

The evaluated error accounts to

$$|R_2(x_{IX})| < 0{\cdot}18 < 0{\cdot}72. \quad . \quad . \quad . \quad . \quad . \quad . \quad . \qquad (12.2)$$

In the table of O. Krestýnová (4) the values for Z=20, $S_{IX,20} = 6{\cdot}15$ and for Z=90, $S_{IX,90} = 6{\cdot}04$ are to be found.

TABLE I.

Constants serving to calculate the screening numbers and the effective charges in the K and L isoelectronic rows according to the formula :

$$S_i = Z - [Z^2 - (i - \bar{a}_i' + i - 1)Z + (i - \bar{a}_i')(i - 1) + \bar{d}_i]^{\frac{1}{2}} = Z - Z^{*\frac{1}{2}}.$$

The numbers with three decimals denote the constants of these isorows (i=2, 3, 8 and 9) the empirical quantum numbers of which agree with the hydrogen term exactly.

Isorow i	$\bar{a}_i = \frac{2A_i}{B_i}$	$i - \bar{a}_i$	$i - 1$	$\bar{d}_i = \frac{2D_i}{B_i}$	$\bar{a}_i' = \frac{2A_i'}{B_i'}$	$i - \bar{a}_i'$	$\bar{d}_i' = \frac{2D_i'}{B_i'}$
K 1	1	0	0		1	0	0
2	1·752	0·248	1	0·055	1·739	0·261	0·075
L 3	1·746	1·254	2	—0·097	1·62	1·38	—0·06
	1·749	1·251		—0·167			
4	2·40	1·60	3	0·44	2·49	1·51	0·26
	2·55	1·45		0·15			
5	2·54	2·46	4	—0·13	2·67	2·33	—0·35
6	3·33	2·67	5	—0·08	3·28	2·72	0·01
7	3·64	3·36	6	0·73	3·91	3·09	0·33
	3·80	3·20					
8	4·332	3·668	7	—0·435	4·16	3·84	0·17
9	4·971	4·029	8	0·118	4·81	4·19	0·25
10	5·46	4·54	9	0·76	5·45	4·55	0·86
M 11	4·26	6·74	10	—0·79	—	—	
12	5·09	6·91	11	—0·36	—	—	

The table contains in addition to values for the K and L isorows those for the M—s rows.

The quantum constant for the M$-s$ isoelectronic rows, determined from the available data for J, is 3·19, with mean error $\sigma=0{\cdot}04$, and is thus 6 per cent higher than the value of the hydrogen M term. This theoretical difficulty is increased by the fact that the quantum constant of the group M V seems to be clearly different from the constants of the groups M I to M IV; this opinion has been based on the study of the iso-electronic row of the 10th d electron, not only on the M level but also on N (Richter 1947).

From equation (10) it is obvious that the screening power S_i varies with both Z and i, but that for given i it becomes practically constant for all sufficiently large Z; its asymptotic value approaches half the coefficient of the linear term, $2i-1-a'_i$. Since the inter-relations of these iso-electronic equations with the X-ray spectra on one hand, and the screening numbers of A. Sommerfeld, N. Bohr, L. Pauling (Sommerfeld 1931) and J. C. Slater (Slater 1930) on the other, are not entirely elucidated, detailed discussion is reserved for a further paper.

ACKNOWLEDGMENT.

I should like to express my thanks to Miss Anna Berková, cand. med. Prague, and Miss Olga Krestýnová, cand. med. Olomouc, for their careful calculations needed for this and previous publications.

REFERENCES.

EUCKEN, A., 1938, *Lehrbuch der chem. Physik*, Bd. I, 243, 2nd edition.

RICHTER, A. F., 1947, *On the ionization potentials of the M and higher isoelectronic rows expressed as arithmetical progressions of the second degree.* XIth International Congress of pure and applied Chemistry, London. In print; 1948, *Phil. Mag.*, **39**, 303.

RICHTER, A. F., and KRESTÝNOVÁ OLGA, 1947, *Lékařské listy II*, 243.

SLATER, J. C., 1930, *Phys. Rev.*, 2, **36**, 57.

SOMMERFELD, A., 1931, *Atombau und Spektrallinien*, Bd. I, 5 umgearbeitete Auflage, Kap. 5, §4 and Kap. 7, §5.

XCI. *The Laminar Boundary Layer on Solids of Revolution.*

By L. G. WHITEHEAD, Ph.D., and G. S. CANETTI, Ph.D.
Aeronautical Department, Queen Mary College,
University of London *.

[Received June 20, 1950.]

§1. INTRODUCTION.

IMPROVED methods for calculating the laminar boundary layer flow for a cylindrical body were described in an earlier paper, Piercy, Whitehead and Tyler (1948). The purpose of the present paper is to show how these methods can be extended to the solution of the laminar boundary layer equations for the axial flow past a solid of revolution. This problem, which has received less attention than the two-dimensional case, has been examined previously by Millikan (1932) and by Tomotika (1935). In both of these papers a momentum integral relationship similar to von Kármán's two-dimensional equation has been employed to determine the boundary layer thickness. Millikan has assumed a quadratic velocity distribution through the boundary layer, which can give only a rough representation of the flow, while Tomotika has achieved somewhat greater accuracy by employing Pohlhausen's quartic velocity profile.

In the present paper the boundary layer equations for the flow past a solid of revolution are derived in a form similar to that employed in Piercy *et al.* (1948) for two-dimensional flow. Solutions of these equations are found for the flow past cones and are shown to be related to the corresponding two-dimensional flows past wedges given by Falkner and Skan (1930) and Hartree (1937). An approximate solution of general applicability is also presented, which is similar to the two-dimensional approximate solution described in section II. of Piercy *et al.* (1948). A velocity distribution involving three terms is used and these are chosen to give accurate velocity profiles in certain standard cases. Satisfactory results are achieved for the whole of the accelerated part of the boundary layer of slender bodies and for the earlier part of the retarded flow. Except for bluff bodies, a more elaborate solution employing four terms for the velocity profile would be required for the accurate determination of the laminar separation point. At practical Reynolds numbers, however, transition to turbulence will usually occur before the solution using three terms ceases to apply.

The approximate solution, which is exact in the vicinity of the stagnation point of a body with a rounded nose, is compared with the solutions for the flow past a cone and satisfactory agreement is found. The boundary layer flow has also been calculated for a sphere with theoretical and experimental pressure distributions and the results are compared with Tomotika's solutions. In these examples the present method is applicable to the whole laminar boundary layer up to the separation point.

---

*Communicated by Prof. N. A. V. Piercy.

As a final example the flow past an ellipsoid with a fineness ratio of 3 is considered. The boundary layer flow corresponding to the experimental pressure distribution is calculated and a satisfactory solution is obtained over the forward 80 per cent of the laminar layer. The method fails, however, to give a solution close to the laminar separation point.

§2. NOTATION.

The notation used is similar to that employed in the two-dimensional solutions described in Piercy *et al.* (1948) but due to the different nature of the problem the corresponding functions are defined differently in some cases.

A, B, C.	functions of ξ appearing in the series and approximate solutions of the boundary layer equations.
h'	irrotational flow velocity.
h	velocity ratio h'/U.
$h_1\ h_2\ h_3$	functions defining the curvilinear coordinate system.
K	a parameter defining the approximate velocity profile.
l	a representative length of the solid of revolution.
n	degree of the Legendre function $P_n(\mu)$.
p	static pressure.
q, w	component velocity ratios.
r, θ_1	spherical polar coordinates.
R	Reynolds number.
U	velocity of the undisturbed flow.
V	velocity vector.
x, y	cylindrical coordinates, x measured along the axis of symmetry and y perpendicular to it.
α'	velocity potential of flow with axial symmetry.
β'	Stokes' stream function.
α, β	α'/Ul and β'/Ul^2 respectively.
δ	boundary layer displacement thickness.
θ	boundary layer momentum thickness.
ϕ, ψ	functions of η.
μ	cos θ_1.
ν	kinematic viscosity.
τ	skin friction.
ξ, η	coordinates defined in terms of α and β.
ζ	vorticity.

§3. BOUNDARY LAYER EQUATIONS.

The exact equations for the incompressible viscous flow with axial symmetry past a solid of revolution are first derived in a modified form. An orthogonal system of independent variables α', β' and γ' are employed.

α'=constant defines an equipotential and β'=constant a streamline for the inviscid axisymmetric flow past the body while γ' is constant on a plane passing through the axis of symmetry. h' is the resultant velocity of the potential flow and q' and w' the velocity components of the viscous flow in directions perpendicular to surfaces α=constant and β=constant respectively. The velocity ratios $q=q'/h'$, $w=w'/h'$ and $h=h'/\mathrm{U}$ are employed in the equations and α' and β' are converted into the non-dimensional forms α and β by dividing by the undisturbed velocity U and by a power of a representative length l. Hence

$$\alpha=\alpha'/\mathrm{U}l\,, \qquad \beta=\beta'/\mathrm{U}l^2$$

and the Reynolds number for the flow is defined as

$$\mathrm{R}=\mathrm{U}l/\nu.$$

The vector form of the equation of motion for steady flow is

$$-\mathbf{V}\times\zeta=-\mathrm{grad}\,(p/\rho+\tfrac{1}{2}\mathbf{V}^2)+\nu\,(\mathrm{grad.\,div}\,\mathbf{V}-\mathrm{curl}\,\zeta)\,, \quad . \quad . \quad . \quad (1)$$

where **V** is the velocity vector and ζ the vorticity. The corresponding form of the equation of continuity for incompressible flow is

$$\mathrm{div}\,\mathbf{V}=0\,. \quad . \quad . \quad . \quad . \quad . \quad . \quad . \quad . \quad . \quad . \quad (2)$$

The transformation of these equations into curvilinear coordinates is readily carried out. General expressions for the components of the various terms in the two equations are given by Milne-Thomson (1937) in terms of three factors h_1, h_2, and h_3. The element of length along a line perpendicular to the surface α=constant is expressed as $h_1\delta\alpha$ and the corresponding values in the two other directions are $h_2\delta\beta$ and $h_3\delta\gamma$ respectively. It follows therefore that for the present system of orthogonal coordinates

$$h_1=1/h, \quad h_2=1/yh \quad \text{and} \quad h_3=y,$$

where y is the radial distance from the axis of symmetry divided by the representative length l. Substitution in (1) yields the equations

$$\frac{1}{h}\frac{\partial h}{\partial\alpha}(q^2+\omega^2)+q\frac{\partial q}{\partial\alpha}+y\omega\frac{\partial q}{\partial\beta}+\frac{\omega^2}{y}\frac{\partial y}{\partial x}$$
$$=-\frac{1}{\rho\mathrm{U}^2h^2}\frac{\partial p}{\partial\alpha}+\frac{1}{\mathrm{R}h^2}\left[\frac{\partial}{\partial x}\cdot h^2\left\{\frac{\partial q}{\partial\alpha}+\frac{\partial}{\partial\beta}(y\omega)\right\}-\frac{\partial}{\partial\beta}\cdot y^2h^2\left\{\frac{\partial}{\partial\alpha}\left(\frac{\omega}{y}\right)-\frac{\partial q}{\partial\beta}\right\}\right], \quad . \quad . \quad . \quad (3)$$

and

$$\frac{1}{h}\frac{\partial h}{\partial\beta}(q^2+\omega^2)+q\frac{\partial\omega}{\partial x}+y\omega\frac{\partial\omega}{\partial\beta}-\frac{q\omega}{y}\frac{\partial y}{\partial\alpha}$$
$$=-\frac{y}{\rho\mathrm{U}^2h^2}\frac{\partial p}{\partial\beta}+\frac{1}{\mathrm{R}h^2}\left[\frac{\partial}{\partial\beta}\cdot h^2\left\{\frac{\partial q}{\partial\alpha}+\frac{\partial}{\partial\beta}(y\omega)\right\}+\frac{\partial}{\partial\alpha}\cdot y^2h^2\left\{\frac{\partial}{\partial\alpha}\left(\frac{\omega}{y}\right)-\frac{\partial q}{\partial\beta}\right\}\right]. \quad . \quad . \quad . \quad (4)$$

A third equation does not arise as there is no flow normal to the planes γ=constant. The equation of continuity takes the form

$$\frac{\partial q}{\partial \alpha}+\frac{\partial(y\omega)}{\partial \beta}=0. \quad . \quad . \quad . \quad . \quad . \quad . \quad . \quad . \quad . \qquad (5)$$

Equations (3) and (4) are simplified by applying the usual assumptions appropriate to flow with a thin viscous boundary layer. In addition the change of y through the boundary layer is neglected so that it can be replaced by y_0, its value on the boundary. This latter assumption will introduce small local errors close to the stagnation point on a solid of revolution with a conical nose since in this region y is comparable with the boundary layer thickness. This does not, however, affect the validity of the solution over the major part of the body. With these approximations equation (4) reduces to

$$q^2 \frac{1}{h} \frac{\partial h}{\partial \beta}=-\frac{y_0}{\rho U^2 h^2} \frac{\partial p}{\partial \beta},$$

so that the change of pressure through the boundary layer is negligible. Hence the value of $\partial p/\partial \alpha$ in (3) can be calculated from the irrotational flow just outside the boundary layer, giving

$$\frac{\partial p}{\partial x}=-\rho U^2\left(h \frac{dh}{d\alpha}\right)_{\beta=0}.$$

Equation (3) therefore reduces to

$$q \frac{\partial q}{\partial \alpha}+w y_0 \frac{\partial q}{\partial \beta}=\left(\frac{1}{h} \frac{dh}{d\alpha}\right)_{\beta=0}(1-q^2)+\frac{y_0^2}{R} \frac{\partial^2 q}{\partial \beta^2}. \quad . \quad . \quad . \qquad (6)$$

This equation is to be solved in conjunction with the equation of continuity (5) for the boundary conditions $q=w=0$ on the solid of revolution, which forms part of the streamline $\beta=0$, and $q=1$ for large values of β.

New variables ξ and η are now introduced in order to simplify the boundary conditions. They are defined in terms of α and β by

$$\xi=\frac{\beta}{2y_0}\left[\frac{R}{\alpha-\alpha_0}\right]^{\frac{1}{2}} \quad \text{and} \quad \eta=\alpha-\alpha_0, \quad . \quad . \quad . \quad . \quad . \qquad (7)$$

where α_0 is the value of α at the front stagnation point. The part of the streamline $\beta=0$ lying downstream of the stagnation point corresponds to $\xi=0$ so that the boundary conditions are taken as $q=0$ for $\xi=0$ and $q=1$ for large values of ξ. With this change of variables (6) becomes, after substituting from (5) for w

$$\frac{\partial^2 q}{\partial \xi^2}+\left[2+\frac{4\eta}{y_0} \cdot \frac{dy_0}{d\eta}\right] \frac{\partial q}{\partial \xi} \int_0^\xi q\, d\xi$$
$$=-4\left(\frac{\eta}{h} \cdot \frac{dh}{d\eta}\right)_{\beta=0}(1-q^2)+4\eta \frac{\partial q}{\partial \eta} \cdot q-4 \frac{\partial q}{\partial \xi} \int_0^\xi \frac{\partial q}{\partial \eta}\, d\xi, \quad . \quad . \quad . \quad . \quad . \quad . \qquad (8)$$

an equation which differs only from the two-dimensional form by the inclusion in the second term on the left hand side of the additional factor $4\eta/y_0\,(dy_0/d\eta)$. A function ϕ employed in the two-dimensional solution is reintroduced here together with an additional function ψ. They are defined by

$$\phi=2\left[1-\frac{2\eta}{h}\frac{dh}{d\eta}\right]_{\beta=0} \quad\text{and}\quad \psi=2\left[1-\frac{2\eta}{y_0}\frac{dy_0}{d\eta}\right]_{\beta=0}.$$

Both ϕ and ψ are functions of η only and are zero at the stagnation point of a body with a rounded nose. Equation (8) therefore becomes finally

$$\frac{\partial^2 q}{\partial\xi^2}+(4-\psi)\frac{\partial q}{\partial\xi}\cdot\int_0^\xi q\,d\xi=(\phi-2)(1-q^2)+4\eta\frac{\partial q}{\partial\eta}.q-4\frac{\partial q}{\partial\xi}\int_0^\xi\frac{\partial q}{\partial\eta}.d\xi. \quad . \quad (9)$$

§4. FLOW PAST CONES.

General solutions of the boundary layer equation (9) give a velocity profile which varies along the surface, but when ϕ and ψ are both constant a solution for q is found which is independent of η. It is readily shown that the flow past a cone is of this type. The velocity potential α is expressed generally in terms of Legendre functions by the relation

$$\alpha=r^n\mathrm{P}_n(\mu)\,,$$

where $\mu=\cos\theta_1$ and r and θ_1 are spherical polar coordinates. θ_0 the value of θ_1 on the conical boundary, is found from the condition $\partial\alpha/\partial\theta_1=0$ and hence is given by the solution of the equation

$$\frac{d}{d\mu}\,[\mathrm{P}_n(\mu)]=0.$$

θ_0 is the external angle between the axis and the wall of the cone, it has the value $\pi/2$ for $n=2$ giving the flow up to a stagnation point. When $n=1$, $\theta_0=\pi$ and a cone of vanishing thickness results. Values of θ_0 for intermediate values of n, between these two limits, are plotted against π/n in fig. 1. On the conical boundary, η and y_0 are given therefore by

$$\eta=r^n\mathrm{P}_n\,(\cos\theta_0) \quad\text{and}\quad y=r\sin\theta_0.$$

Hence

$$\phi=-\psi=4/n-2. \quad . \quad . \quad . \quad . \quad . \quad . \quad . \quad . \quad (10)$$

With these values of ϕ and ψ substituted in (9), the equation for q, as a function of ξ only, takes the form

$$\frac{\partial^2 q}{\partial\xi^2}+\left(2+\frac{4}{n}\right)\frac{\partial q}{\partial\xi}\int_0^\xi q\,d\xi=4\left(1-\frac{1}{n}\right)(q^2-1). \quad . \quad . \quad . \quad (11)$$

This equation is transformed by the further substitution $\xi_1=\xi(2+4/n)^{-\frac{1}{2}}$ into

$$\frac{\partial^2 q}{\partial\xi_1^2}+\frac{\partial q}{\partial\xi_1}\int_0^{\xi_1}q\,d\xi_1=\frac{2(n-1)}{n+2}\,(q^2-1)$$

and if $z'=q$ and $\lambda=2(n-1)/n+2$ it becomes identical with the equation

$$z'''+z''\,z+\lambda(1-z'^2)=0\,. \quad . \quad . \quad . \quad . \quad . \quad . \quad . \quad . \quad (12)$$

which has been solved by Hartree for the corresponding two-dimensional problem of the flow past a wedge. Hartree gives accurate numerical values for z for a series of values of the parameter λ. The flow up to the stagnation point on a plane wall ($n=2$) corresponds to $\lambda=\frac{1}{2}$ so that the velocity profile will differ appreciably from that near a two-dimensional stagnation point for which $\lambda=1$. The solution is not valid for values of n close to unity for the boundary layer thickness on the slender cones which occur in this range is comparable with y_0.

Fig. 1.

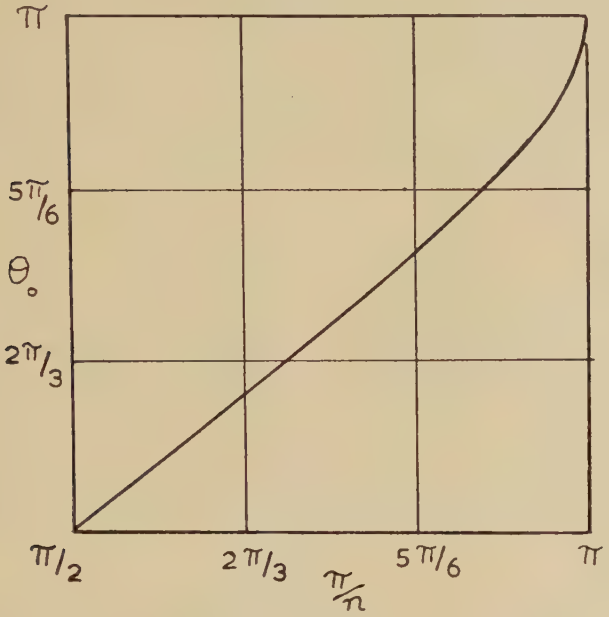

Variation of cone angle with n.

§5. Series Solution for a Body with a Rounded Nose.

A series solution starting from the front stagnation point can be constructed in a manner similar to that described in Piercy *et al.* (1948) but, due to the presence of the additional function ψ, it will involve, for equal accuracy, the use of a larger number of terms. An expansion for q is assumed in the form

$$q=A+B\phi+C\phi^2+\ldots\ldots, \qquad (13)$$

and each function B, C, etc. is further expanded into series involving functions of ξ multiplied by powers and products of the coefficients in the expansions

$$\eta\frac{d\phi}{d\eta}=a\phi+b\phi^2+c\phi^3+\ldots\ldots,$$

and

$$\psi=a_1\phi+b_1\phi^2+c_1\phi^3.$$

Only the function A and the term in B which is independent of these coefficients have been examined as they are required in the approximate solution given later. They satisfy the equations

$$A''+4A'\int_0^\xi A\,d\xi-2(A^2-1)=0,$$

and

$$B_0''+4A'\int_0^\xi B_0\,d\xi+4B_0'\int_0^\xi A\,d\xi-4AB_0=1-A^2.$$

The boundary conditions for A are $A=0$ for $\xi=0$ and $A=1$ for ξ large. The equation for A is identical with (11) if n is put equal to 2 so that the solution is given in Hartree's paper. For B_0 the boundary conditions are $B_0=0$ at $\xi=0$ and $B_0=0$ for ξ large. The equation for B_0 has been solved by a method of successive approximations and its values together with A are given in Table I. The second derivatives for all the further functions vanish at $\xi=0$ but otherwise the boundary conditions are identical with those of B_0.

§6. THE APPROXIMATE SOLUTION.

An approximate solution which can be employed over the greater part of a laminar boundary layer is next considered. An expression for q is assumed which contains three terms. The first two of these are the initial terms of the series solution and a third term, multiplied by a variable parameter, is used to represent approximately the remaining terms of the series. This type of velocity distribution has given good results for two-dimensional flow and is justified by the fact that the third term replaces terms which have the same boundary conditions and vary in a similar manner throughout the range. Therefore q is expressed as

$$q=A+B_0\phi+K.f(\xi), \qquad (14)$$

where the parameter K is a function of η only, and is determined from a momentum integral relationship. A more elaborate solution using a fourth term and two integral relationships would give more accurate results in the retarded region, as is shown in Piercy *et al.* (1948) but the single term used here is adequate for accelerated flow. K is chosen arbitrarily as unity for the flow past a cylindrical tube with its axis lying along the stream. For this case equation (10) reduces to the two-dimensional form for the flat plate since, as y_0 and h are constant, $\phi=\psi=2$. Thus the velocity profile is given by the well known Blasius solution for zero pressure gradient. $f(\xi)$ is chosen therefore so that q takes this form for $\phi=2$ and $K=1$, its values are given in Table I.

The appropriate form of the momentum integral relationship is obtained by integrating (9) through the boundary layer, leading to

$$\left(\frac{\partial q}{\partial \xi}\right)_{\xi=0}=(4-\psi)\int_0^\infty (q-q^2)\,d\xi+(2-\phi)\int_0^\infty (1-q^2)\,d\xi+4\eta\frac{d}{d\eta}\int_0^\infty (q-q^2)\,d\xi. \qquad (15)$$

This equation may be expressed in terms of the two functions

$$\bar{\theta}=\int_0^\infty (q-q^2)\,d\xi \quad\text{and}\quad \bar{\delta}=\int_0^\infty (1-q)\,d\xi,$$

which are related to the momentum thickness θ and the displacement thickness δ of the boundary layer respectively, by

$$\frac{\theta}{l}=\frac{2}{h}\cdot\left(\frac{\eta}{\mathrm{R}}\right)^{\frac{1}{2}}\bar{\theta} \quad\text{and}\quad \frac{\delta}{l}=\frac{2}{h}\left(\frac{\eta}{\mathrm{R}}\right)^{\frac{1}{2}}\bar{\delta}. \quad . \quad . \quad . \quad . \quad . \quad (16)$$

Table I.

ξ	A	$-\mathrm{B}_0$	$f(\xi)$
0·0	0·0	0·0	0·0
0·2	0·3311	0·0510	0·0963
0·4	0·5834	0·0674	0·1839
0·6	0·7615	0·0605	0·2467
0·8	0·8760	0·0432	0·2728
1·0	0·9421	0·0257	0·2609
1·2	0·9760	0·0130	0·2210
1·4	0·9913	0·0056	0·1686
1·6	0·9974	0·0020	0·1173
1·8	0·9993	0·0006	0·0748
2·0	0·9999	0·0002	0·0440
2·2	1·0000	0·0000	0·0241
2·4	.	.	0·0122
2·6	.	.	0·0058
2·8	.	.	0·0025
3·0	.	.	0·0010
3·2	1·0000	0·0000	0·0004

Equation (15) therefore takes the form

$$\left(\frac{\partial q}{\partial \xi}\right)_{\xi=0}=4\eta\frac{d\bar{\theta}}{d\eta}+(6-\phi-\psi)\bar{\theta}+(2-\phi)\bar{\delta}, \quad . \quad . \quad . \quad . \quad (17)$$

and the numerical values of $\bar{\theta}$, $\bar{\delta}$ and $(\partial q/\partial\xi)_{\xi=0}$ appropriate to the chosen velocity distribution are

$$\bar{\theta}=0\cdot1752+0\cdot0192\phi-0\cdot0027\phi^2+0\cdot2425\mathrm{K},$$
$$-0\cdot0219\phi\mathrm{K}-0\cdot0692\mathrm{K}^2, \quad . \quad . \quad . \quad . \quad . \quad . \quad . \quad (18)$$

$$\bar{\delta}=0\cdot4022+0\cdot0550\phi+0\cdot3481\mathrm{K}, \quad . \quad . \quad . \quad . \quad . \quad . \quad . \quad (19)$$

$$(\partial q/\partial\xi)_{\xi=0}=1\cdot8554-0\cdot3523\phi-0\cdot4868\mathrm{K}, \quad . \quad . \quad . \quad . \quad . \quad . \quad . \quad (20)$$

The non-dimensional skin friction coefficient $\tau\mathrm{R}^{\frac{1}{2}}/\frac{1}{2}\rho\mathrm{U}^2$ is expressed in terms of $(\partial q/\partial\xi)_{\xi=0}$ by the relation

$$\frac{\tau\mathrm{R}^{\frac{1}{2}}}{\frac{1}{2}\rho\mathrm{U}^2}=\frac{h^2}{\eta^{\frac{1}{2}}}\left(\frac{\partial q}{\partial\xi}\right)_{\xi=0}.$$

A differential equation for K is obtained by substituting these numerical values in (17) and it is solved for each example by a step by step method of integration. The equation is

$$\begin{aligned}4\eta\, d\mathrm{K}/d\eta\, &(0{\cdot}2425-0{\cdot}0219\phi\ -0{\cdot}1384\mathrm{K})\\ &=0{\cdot}0904\phi^2 -2{\cdot}6379\mathrm{K} +0{\cdot}4150\mathrm{K}^2 +0{\cdot}7221\phi\mathrm{K}\\ &\quad -4\eta\, d\phi/d\eta\ (0{\cdot}0192\ -0{\cdot}0054\phi\ -0{\cdot}0219\mathrm{K})\\ &\quad +\psi\,(0{\cdot}1752\ +0{\cdot}0192\phi\ +0{\cdot}2425\mathrm{K})\\ &\quad -(\phi+\psi)\ (0{\cdot}0027\phi^2 +0{\cdot}0219\phi\mathrm{K} +0{\cdot}0692\mathrm{K}^2).\end{aligned}$$

A first check on the accuracy of the approximate solution is made by a comparison with the accurate solutions for the flow past a cone found in §4. For these examples, as ϕ and ψ are constant, K is also constant and equation (21) reduces to the simple quadratic for K

$$0{\cdot}4150\mathrm{K}^2+\left(\frac{1{\cdot}9184}{n}-3{\cdot}5971\right)\mathrm{K}+\frac{1{\cdot}1392}{n^2}-\frac{1{\cdot}8400}{n}+0{\cdot}6352=0.$$

Values of K for a range of n between 1 and 2 are given in Table II. and the approximate values of $(\partial q/\partial\xi)_{\xi=0}$ are compared with values found by Tomotika's method and with the accurate values obtained by Hartree. The accuracy for the present approximate solution is seen to be superior to that of Tomotika's solution, the maximum error for the range considered being 0·6 per cent compared with 1·8 per cent.

TABLE II.

λ	n	K	$\left(\frac{\partial q}{\partial\xi}\right)_{\xi=0}$ Present method	$\left(\frac{\partial q}{\partial\xi}\right)_{\xi=0}$ Tomotika	$\left(\frac{\partial q}{\partial\xi}\right)_{\xi=0}$ Hartree
0·1	1·159	−0·0529	1·369	1·380	1·371
0·2	1·333	−0·0477	1·526	1·525	1·536
0·3	1·530	−0·0343	1·655	1·639	1·665
0·4	1·750	−0·0176	1·763	1·736	1·768
0·5	2·000	0·0000	1·855	1·832	1·855

§7. THE LAMINAR BOUNDARY LAYER ON A SPHERE.

The boundary layer flow on a sphere has been calculated previously by Tomotika for the potential flow pressure distribution and by Tomotika and Imai (1938) for an experimental pressure distribution measured by Fage (1936). Solutions for these examples have been calculated by the present method and are compared with these earlier results.

For the irrotational flow past the sphere the velocity near the boundary is given by $h=\frac{3}{2}\sin\theta_1$ and, if the representative length is taken as the diameter, $\eta=\frac{3}{4}(1-\cos\theta_1)$ and $y_0=\frac{1}{2}\sin\theta_1$. The corresponding values of ϕ, ψ and $\eta\ (d\phi/d\eta)$ are therefore

$$\phi=\psi=\frac{2(1-\cos\theta_1)}{1+\cos\theta_1},\qquad \eta\frac{d\phi}{d\eta}=\frac{4(1-\cos\theta_1)}{(1+\cos\theta_1)^2},$$

and it is convenient to change the variable η in equation (21) to θ_1 for the step by step integration. A series solution for small values of θ_1 shows that only even powers arise and the starting value of K is given by

$$K=0{\cdot}01365\,\theta_1^2+\ldots\ldots$$

The skin friction coefficient $\tau R^{\frac{1}{2}}/\frac{1}{2}\rho U^2$ is plotted as the continuous line in fig. 2 and the dotted line shows Tomotika's solution. The separation point is found to be 107° from the front stagnation point compared with 108° for his solution.

Fig. 2.

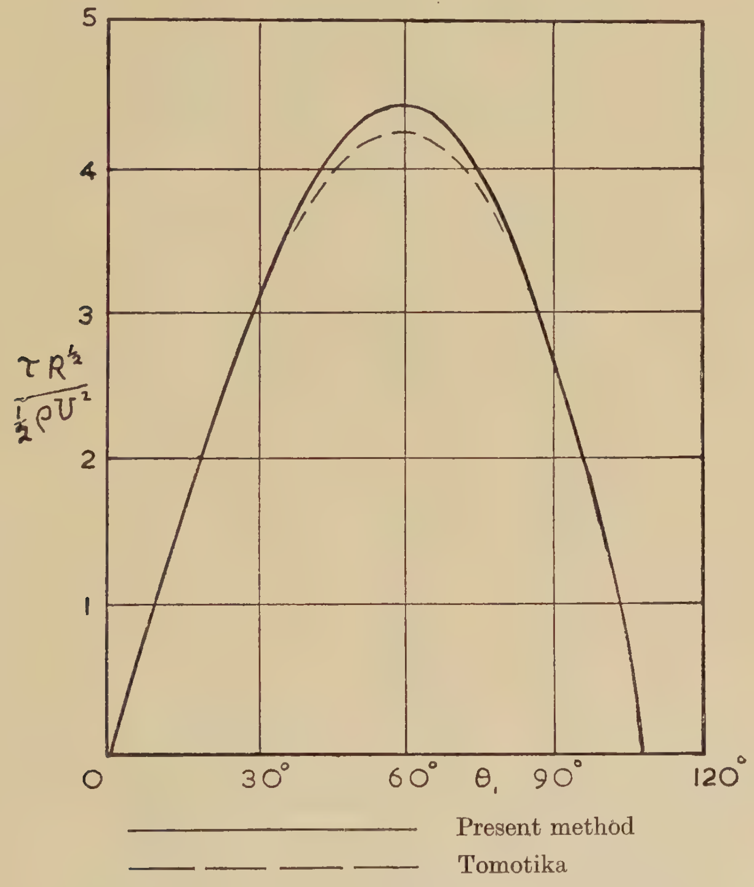

Skin friction on sphere, theoretical pressure distribution.

Tomotika and Imai have expressed the experimental velocity distribution on a sphere measured by Fage for an entirely laminar boundary layer as

$$h=1{\cdot}5\,\theta_1-0{\cdot}43707\,\theta_1^3+0{\cdot}148097\,\theta_1^5-0{\cdot}042329\,\theta_1^7,$$

and this form is retained for the calculation of ϕ and ψ in the present solution, though it differs slightly from the measured values in the immediate vicinity of the separation point. ϕ, ψ and $\eta\ (d\phi/d\eta)$ are calculated from the relations

$$\eta=\int h d\theta_1,$$

$$\phi=2-\frac{4\eta}{h^2}\frac{dh}{d\theta_1},$$

$$\psi=2-\frac{4\eta}{h}\,.\cot\theta_1,$$

and

$$\eta\frac{d\phi}{d\eta}=\frac{4\eta}{h^2}\left\{\frac{2\eta}{h^2}\left(\frac{dh}{d\theta_1}\right)^2-\left(\frac{dh}{d\theta_1}\right)-\frac{\eta}{h}\frac{d^2h}{d\theta_1^2}\right\}.$$

Fig. 3.

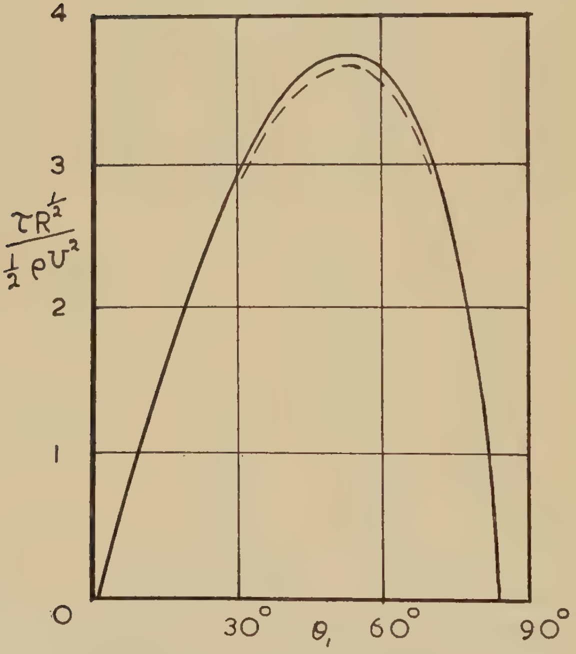

———————— Present method

— — — — Tomotika and Imai

Skin friction on sphere, experimental pressure distribution.

The inital values for the step by step integration of (21) are given by $K=-0{\cdot}00035\ \theta_1^2$ in this case. The skin friction coefficient for the experimental pressure distribution is plotted as the continuous line in fig. 3 and the dotted line gives Tomotika and Imai's solution. Somewhat higher values for the skin friction are given by the present method for both pressure distributions. Tomotika's method is a development of

Pohlhausen's two-dimensional solution which has been compared by Bairstow (1939) with more accurate solutions for the flow past a circular cylinder. In this two-dimensional problem it is found that Pohlhausen's method underestimates the friction and it is likely that Tomotika's solution for the sphere will involve similar errors. The separation point calculated from the experimental pressure distribution is 83·3° from the front stagnation point compared with 84° for Tomotika's solution and the experimental value of 83° found by Fage.

§8. Flow Past an Ellipsoid.

The boundary layer flow past an ovary ellipsoid of fineness ratio 3 is next considered. This example involves much smaller pressure gradients than occur on the sphere over the major part of the boundary layer and in this respect it is more representative of a practical streamline shape. The experimental pressure distribution has been measured at a Reynolds' number of $2{\cdot}5\times10^5$ based on the major axis, which is 1 ft. long. The ellipsoid was mounted in a 4 ft. square wind tunnel and supported by a tube 1 in. diameter which formed a rearward extension of the ellipsoid and which was faired into it. All pressure connections were carried through this tube and the pressures were recorded after carefully aligning the axis of the ellipsoid along the stream. In fig. 4, values of h calculated from these pressure readings are plotted against x, the distance from the nose divided by the major axis. The readings are plotted as far as the laminar separation point which is located at $x=0{\cdot}76$. The skin friction calculated by the present method is shown in fig. 5. The solution has not been carried beyond $x=0{\cdot}65$ as its accuracy is considered doubtful further downstream. A difficulty arises in the retarded part of the flow when K approaches a value of about 1·4 as the coefficient of $d\mathrm{K}/d\eta$ decreases rapidly

Fig. 4.

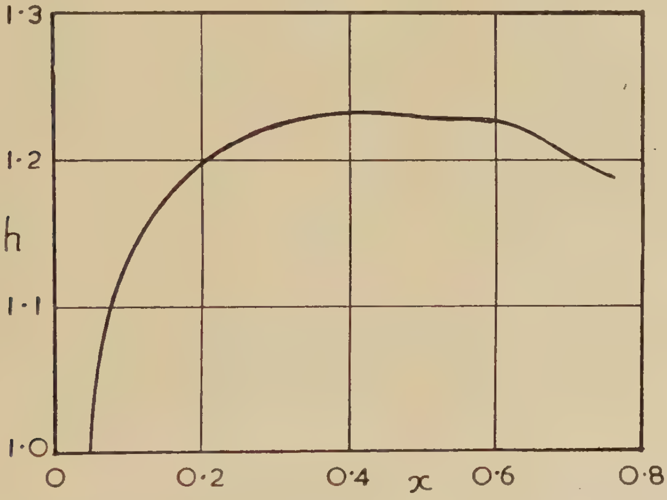

Velocity outside the boundary layer of the ellipsoid.

and becomes negative for larger values of K. For this reason the method fails to give a solution near the laminar separation point in the present example.

§ 9. CONCLUSION.

Solutions for the laminar boundary layer flow on a solid of revolution are described which employ methods previously applied successfully in two-dimensional flow. An approximate solution is obtained which is superior in accuracy to earlier methods for accelerated boundary layer flow. The approximate solution is compared with accurate solutions for the flow past cones and satisfactory agreement is found. Comparisons with Tomotika's solutions for the flow past a sphere show that the skin friction calculated by the present method is larger over most of the laminar layer.

Fig. 5.

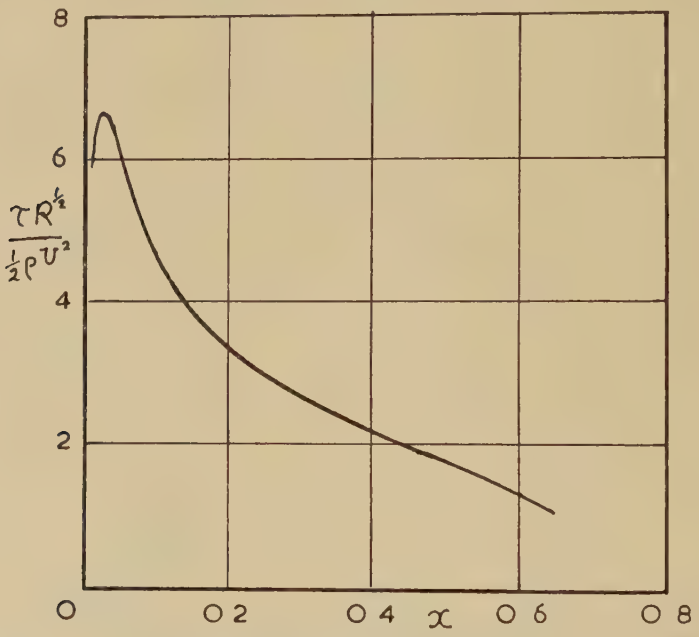

Skin friction for flow past ellipsoid.

REFERENCES

L. BAIRSTOW, 1939, *Applied Aerodynamics* (2nd Edition) (London : Longmans, Green and Co.) pp., 524, 543.

A. FAGE, 1936, *A.R.C.R. & M.*, No. 1766.

V. M. FALKNER and S. W. SKAN 1930, *A.R.C.R. & M.*, No. 1314.

D. R. HARTREE 1937 *Proc. Camb. Phil. Soc.*, **33,** 223-239.

C. B. MILLIKAN 1932, *Trans. Amer. Soc. Mech. Eng., Appl. Mech. Sec.*, **54,** 29.

L. MILNE-THOMSON, 1937, *Theoretical Hydrodynamics* (1st Edition) (London : Macmillan) pp. 55-58.

PIERCY, N.A. V., WHITEHEAD, L. G., and TYLER, R. A., 1948, *Aircraft Engineering*, **20,** 354-359.

TOMOTIKA, S., 1935, *A.R.C.R. & M.*, No. 1678.

TOMOTIKA, S, and IMAI, I, 1938, *Proc. Phys.-Math. Soc. Japan*, 3rd Ser. **20,** 287-303.

XCII. *A Theory of Radar Information.*

By P. M. Woodward, B.A. and I. L. Davies, M.A.,
T.R.E., Ministry of Supply *.

[Received April 13, revised July 18, 1950.]

Summary.

The theoretical accuracy and certainty with which range may be determined by radar is obtained quantitatively by applying the principle of inverse probability. In agreement with experience, the theory yields two fundamental criteria for satisfactory radar reception. First, the total received signal energy must always be larger than the effective noise power per unit bandwidth. Secondly, there is a more stringent threshold of unambiguous reception which depends not only on the quantity of received energy but also on the bandwidth of the transmitted waveform, for as this is increased the minimum energy required for the certain detection of an echo also increases. The quantity of information obtainable at the receiver, as measured by reduction of entropy, is evaluated for comparison with that given by Shannon's general theory of communication (Shannon 1948). It is found that as the time of observation and hence the received energy increases, information is initially obtained at a roughly uniform rate which is not far removed from the absolute limit for an ideal communication system, but that after crossing the threshold of unambiguous reception, additional received energy contributes little further information.

Since only stationary echoing objects are considered, phase-coherent integration is implied in the theory and the problem of post-detection integration is not discussed. Apart from obviously unsuitable waveforms, the theory is applicable to any type of modulation.

§1. Introduction.

It has long been recognized that the amount of information which can be obtained from any physical observation is fundamentally limited by random fluctuations. In communication problems, for example, the physicist or engineer always strives to work with signals which are large compared with the background of noise. Superficially, one might be tempted to conclude that information can be communicated at a satisfactory rate only when the signal power P is greater than the noise power N in the system. There is, however, no such abrupt limitation, for Shannon (1948, 1949) has shown that the limiting rate at which information can be communicated, in the presence of a uniform spectrum of Gaussian noise, is given by

$$C=W \log_2\left(1+\frac{P}{N}\right) \quad . \quad . \quad . \quad . \quad . \quad . \quad . \quad . \quad . \quad (1)$$

---

* Communicated by the Authors.

binary choices per unit time, when no frequencies higher than W are utilized. Nevertheless, many practical systems do exhibit a threshold of intelligibility when P is equal to N, but this is only due to the manner of coding the information. It is not revealed by equation (1) because this assumes ideal coding, which might be somewhat complicated if P were less than N. A threshold is especially pronounced when the information is encoded by a non-topological increase in its natural number of dimensions (Shannon 1949).

The simplest information sought from a radar system is the range of an echoing object, presumed stationary in this paper. Such information has only a single dimension, but it is coded (perforce) in a special manner which increases its dimensionality. A repetitive waveform, not necessarily a sequence of pulses, is transmitted, echoed, and received. Observation is assumed to last only for a finite time—any integral number of repetition periods—during which only a finite quantity of signal energy is available at the receiver : the observer compares the transmitted and received waveforms and tries to determine the time-delay between them. The presence of noise in the received waveform prevents him doing so with unlimited precision. Both transmitted and received waveforms occupy a substantial area of the time-frequency information diagram as defined by Gabor (1946), and therefore encompass a large number of elementary cells. In Shannon's terminology, their dimensionality is high. But since the shape of the transmitted waveform is fixed at the outset and contains no information at all, and the received waveform is only a delayed copy, it is not obvious that this time-frequency area can be utilized to the same advantage as in an ordinary communication system. One of the objects of this paper is to show that radar can be fairly efficient in this fundamental sense. The primary purpose of the work, however, is to determine the threshold of intelligibility, which we might expect to be quite marked in view of the nature of the coding. Under conditions of intelligible reception, it is further possible to determine the inherent accuracy with which target range may be ascertained.

The mathematical analysis centres round one important concept, the *a posteriori* probability distribution for the time-delay τ between transmission and reception. This probability distribution describes all that can possibly be known about range after a radar observation has been made, and is formally derived in §3 after a preliminary statement of terminology in §2. The distribution will be found to depend on two significant functions of τ, for which the terms signal function and noise function are adopted. They are, effectively, the signal auto-correlation and signal-noise cross-correlation functions (Wiener 1949). Both of them depend on the known shape of the transmitted waveform and on the known statistical characteristics of the noise, but apart from this, they depend separately on the signal and noise actually received. Their relative importance is discussed in §4, where certain of their properties are derived for subsequent reference. The so-called signal function shows to what extent the accuracy of a range determination is, in the presence of noise inherently limited (§5), but the limitation it describes is merely the "topological uncertainty" of the observation, because it refers to a connected region of uncertainty in the neighbourhood of the true value of the range. The noise function, on the other hand, may produce spurious peaks in the probability distribution, representing "non-topological uncertainty" or ambiguity which may exist as the result of an observation, and which may render the observation valueless from a practical point of view. Such ambiguity arises from the non-topological mapping referred to earlier. The conditions under which ambiguity occurs in a radar system are examined in §6, where a formula for the threshold of intelligibility is derived—fig. 1 illustrates the effect. Finally, in §7, the entropy of the *a posteriori* distribution is obtained: after subtraction from the *a priori* entropy it represents the information content of the observation (fig. 2), and it is interesting to compare this with Shannon's general formula for the information capacity of a communication channel. The main features of the results are briefly discussed in the concluding section.

§ 2. REPRESENTATION OF WAVEFORMS.

The transmitted radio-frequency waveform will be denoted by the complex function $\psi(t)$, and the received waveform by

$$\gamma(t)=\alpha\psi(t-\tau)+\nu(t). \qquad (2)$$

Upon reception, $\psi(t)$ will have suffered a change in amplitude and a delay of τ in its passage to and from the target, while $\nu(t)$ is a complex random function representing added noise. These complex functions are all formed from the physical waveforms by the addition of an imaginary quadrature component in the manner described, for instance, by Gabor (1946). Doing the analysis in terms of such complex waveforms introduces no spurious information, and it is only necessary to remember that the energy which would be dissipated in a unit resistance is no longer the time integral of the square of the waveform, but half the integral of the squared modulus. As a matter of purely mathematical convenience, it will be presumed that the noise energy is confined within a finite band of frequencies. As long as this band is sufficiently wide to include the whole spectrum of ψ, there is no loss of generality, for it is merely equivalent to assuming that $\gamma(t)$ has been filtered so as to reduce the noise while leaving the signal unaffected. Such curtailing of the noise, which is assumed uniformly distributed in frequency, has no bearing on the problem of optimum filtering.

Since γ, ψ, and ν are all high-frequency functions, they may be written in the form

$$\left.\begin{aligned}\gamma&=y(t)\exp(2\pi i f_0 t),\\ \psi&=u(t)\exp(2\pi i f_0 t),\\ \nu&=n(t)\exp(2\pi i f_0 t),\end{aligned}\right\} \qquad (3)$$

where y, u and n are complex low-frequency functions, and f_0 is the carrier frequency defined by

$$f_0 = \frac{1}{2\pi i} \frac{\int \psi^* \frac{d}{dt} \psi \, dt}{\int \psi^* \psi \, dt}. \quad . \quad . \quad . \quad . \quad . \quad . \quad . \quad . \quad (4)$$

It may be shown (Gabor 1946) that this definition makes f_0 the centroid of the power spectrum of ψ. When ψ is periodic, it is equivalent to

$$\int |\psi|^2 (f - f_0) \, dt = 0, \quad . \quad . \quad . \quad . \quad . \quad . \quad . \quad . \quad . \quad (5)$$

where the integral is taken over one period and f denotes the instantaneous frequency, or rate of change of phase, of $\psi(t)$. The above definitions have the merit of applying equally well to any form of modulation, and are essential to the subsequent analysis.

Further, it is convenient to introduce here the vectorial representation of waveforms (Shannon 1949, Oswald 1949). Suppose that $z(t)$ is a complex function of t, whose complex frequency spectrum $s_z(f)$ is zero outside the range of frequencies $(-\mathrm{W}, \mathrm{W})$, as is assumed for the particular functions y, u, and n defined above. It is well known that $z(t)$ may be completely specified by a set of sample values $z(r/2\mathrm{W})$, and may therefore be represented by a complex multi-dimensional vector $\mathbf{z}$ with these components. The Hermitian product of two such vectors $\mathbf{z}$ and $\mathbf{w}$, is

$$\mathbf{z}^\dagger \mathbf{w} = \sum_r z_r^* w_r = 2\mathrm{W} \int z^*(t) w(t) \, dt. \quad . \quad . \quad . \quad . \quad . \quad . \quad . \quad (6)$$

The second equation may be proved by applying Parseval's theorem (Titchmarsh 1939) successively to the Fourier Integrals representing $z(t)$ and $w(t)$ and to the Fourier Series representing $s_z(f)$ and $s_w(f)$ in the interval $(-\mathrm{W}, \mathrm{W})$. It follows immediately from equation (6) that

$$\mathbf{u}^\dagger \mathbf{u} = |\mathbf{u}|^2 = 2\mathrm{W} \int |u(t)|^2 \, dt = 4\mathrm{WE}, \quad . \quad . \quad . \quad . \quad . \quad (7)$$

where E denotes the energy of the waveform u, or ψ, within the range of integration. Further, if $\mathbf{u}'$ represents the waveform du/dt, we may define an effective bandwidth β by the equation

$$|\mathbf{u}'|^2 = \beta^2 |\mathbf{u}|^2. \quad . \quad . \quad . \quad . \quad . \quad . \quad . \quad . \quad . \quad . \quad (8)$$

This bandwidth β is, apart from a constant factor, the effective bandwidth as defined by Gabor (1946), who has shown that $\beta^2/4\pi^2$ is the second moment of the power spectrum of u about the origin, or ψ about f_0.

Vector notation is especially convenient when dealing with noise characteristics, and the results quoted in this section will be used in vector and integral form indiscriminately, since each may be transformed into the other by equation (6).

§ 3. Basic Theory of Radar Observation.

The central problem is to form, from any particular received waveform and from a knowledge of the transmitted waveform, the probability distribution for the target range, measured in terms of the time-delay τ. Suppose that, on some typical occasion, the actual value of the time-delay is τ_0 and of the coefficient α is α_0; the received waveform is then

$$\gamma(t)=\alpha_0\psi(t-\tau_0)+\nu(t). \qquad (9)$$

In order to form the probability distribution for τ (and in general α also) when only $\gamma(t)$ and $\psi(t)$ are known, one must first determine the probability density for the observed $\gamma(t)$ on the assumption of any guessed τ and α. This depends solely on the noise which would be necessary to satisfy the assumption. On a hypothesis (τ, α), the noise would in fact have to be

$$\gamma(t)-\alpha\psi(t-\tau),$$

or in terms of the low-frequency functions defined in equation (3),

$$\{y(t)-\alpha u(t-\tau)\exp(-2\pi i f_0\tau)\}\exp(2\pi i f_0 t). \qquad (10)$$

The expression in large brackets may be represented by the vector

$$\mathbf{y}-\alpha\mathbf{u}(\tau)e^{-i\omega\tau}, \qquad (11)$$

where $u(t-\tau)$ has become a continuous vector function of τ, and ω stands for $2\pi f_0$. The vector (11) uniquely determines the high frequency noise fluctuation, and assuming Gaussian noise, its multi-dimensional probability density is proportional to

$$\exp\{-|\mathbf{y}-\alpha\mathbf{u}(\tau)e^{-i\omega\tau}|^2/2\mathrm{N}\}. \qquad (12)$$

Here N is the mean physical noise power, and is the mean square value of both the real and imaginary part of the noise fluctuation at each sampling point. All these values are uncorrelated because the noise is assumed to extend *uniformly* over a high-frequency band of width 2W.

If the *a priori* probability distribution for τ and α is denoted by $p_0(\tau, \alpha)$, then by the principle of inverse probability (Jeffreys 1939) their *a posteriori* distribution is

$$p(\tau, \alpha)\propto p_0(\tau, \alpha)\exp\{-|\mathbf{y}-\alpha\mathbf{u}(\tau)e^{-i\omega\tau}|^2/2\mathrm{N}\}. \qquad (13)$$

This is the frequency distribution of the true values of τ and α over an ensemble in which the received waveform $\gamma(t)$ is fixed. The *a priori* distribution, on the other hand, is the corresponding frequency over the ensemble of all waveforms received, and must be precisely formulated before one can proceed to analyse the problem further.

Since this paper is concerned with the information content of received signals of given energy, it is assumed that the coefficient α is constant, and hence that its *a priori* distribution is given by

$$p_0(\alpha)=\delta(\alpha-\alpha_0). \qquad (14)$$

Further, it is assumed that the *a priori* distribution of τ is uniform over a fixed interval T, less than or equal to the repetition period of the transmitted waveform. Such an assumption is not only the simplest but also the most non-commital one to make, because it represents a state of least prior knowledge (Jeffreys 1939) between the limits of the distribution. Within the interval T we therefore write

$$p_0(\tau, \alpha)=\frac{1}{\mathrm{T}}\delta(\alpha-\alpha_0). \quad \ldots\ldots\ldots \quad (15)$$

It follows from equation (13) that the *a posteriori* distribution for τ is

$$p(\tau)=\int_0^\infty p(\tau, \alpha)\,d\alpha \propto \exp\{-|\mathbf{y}-\alpha_0\mathbf{u}(\tau)e^{-i\omega\tau}|^2/2\mathrm{N}\}, \quad . \quad (16)$$

within the *a priori* interval T, and zero elsewhere.

This expression will now be reduced to a more convenient form. By expanding, and omitting terms independent of τ, we obtain

$$p(\tau)\propto \exp\left[\frac{\alpha_0}{\mathrm{N}}\mathscr{R}\,\mathbf{y}^\dagger\{\mathbf{u}(\tau)e^{-i\omega\tau}\}\right]. \quad \ldots\ldots \quad (17)$$

Of the terms which have disappeared, $|\mathbf{y}|^2$ is dependent on τ_0 but not on τ, whilst the term $|\mathbf{u}(\tau)|^2$ is proportional to the energy of the signal over the interval of observation, and is independent of τ because it extends over an integral number of periods. Converting now into integral form,

$$p(\tau)\propto \exp\left\{\frac{\alpha_0}{\mathrm{N}_0}\mathscr{R}\int y^*(t)u(t-\tau)e^{-i\omega\tau}\,dt\right\}, \quad \ldots \quad (18)$$

where

$$\mathrm{N}=2\mathrm{WN}_0 \quad \ldots\ldots\ldots\ldots \quad (19)$$

and N_0 is the mean noise power per unit bandwidth.

From equations (3) and (9), substitution for y gives

$$p(\tau)\propto \exp\mathscr{R}\left[\frac{1}{\mathrm{N}_0}e^{-i\omega(\tau-\tau_0)}\int\{\alpha_0^2u^*(t-\tau_0)u(t-\tau) + \alpha_0 n^*(t)u(t-\tau)e^{-i\omega\tau_0}\}\,dt\right]. \quad \ldots \quad (20)$$

Since $n(t)$ is a complex random quantity, the constant $\exp(-i\omega\tau_0)$ may be absorbed into it without altering its statistical properties, and is in future omitted. Denoting the phase of the integral by θ, and writing

$$g(\tau)=\frac{\alpha_0^2}{\mathrm{N}_0}\int u^*(t-\tau_0)u(t-\tau)\,dt \quad \ldots\ldots \quad (21)$$

$$h(\tau)=\frac{\alpha_0}{\mathrm{N}_0}\int n^*(t)u(t-\tau)\,dt, \quad \ldots\ldots\ldots \quad (22)$$

one obtains equation (20) in the form

$$p(\tau)\propto \exp[\cos\{\omega(\tau-\tau_0)-\theta\}.|g(\tau)+h(\tau)|]. \quad \ldots \quad (23)$$

The cosine is a high-frequency function of τ, while θ and also the modulus are low-frequency functions. This means that the *a posteriori* distribution consists of a closely-packed sequence of peaks under a slowly varying envelope ; these peaks arise from the comparison which the observer could make between the carrier phases of transmitted and received waveforms.

The information which this fine structure represents is of no value when there is ambiguity between one peak and another ; the realistic distribution for τ, denoted $\mathrm{P}(\tau)$ is consequently given by smoothing $p(\tau)$ to remove fine structure. It is important, however, to realize that, although the information which could be obtained by comparing the phase of the transmitted and received carriers will be discarded, phase-coherence from one repetition cycle of the modulation to the next is assumed throughout the interval of observation. In other words, variation of phase yields useful information but absolute magnitude does not. The smoothed distribution is easily obtained by integrating equation (23), with respect to τ, from τ to $\tau+(2\pi/\omega)$, and assuming that the variation of θ and the modulus are negligible over this interval. This is not equivalent to taking the envelope of $p(\tau)$, because the fine structure is not of a sinusoidal nature. Integration gives, in fact,

$$\mathrm{P}(\tau)=\lambda \mathrm{I}_0(|g+h|), \quad . \quad . \quad . \quad . \quad . \quad . \quad . \quad . \quad (24)$$

where I_0 is a modified Bessel function, and λ is a normalizing constant. It should be emphasized that the integrals g and h extend over the whole interval of observation.

The characteristics of $\mathrm{P}(\tau)$ depend markedly on the relative importance of g and h, which may be regarded as the contributions of the signal and noise to the probability distribution. For convenience, they are termed the signal and noise function respectively : they are, in effect, the signal auto-correlation and signal-noise cross-correlation functions (Wiener 1949).

§ 4. The Signal and Noise Functions.

In this section, some of the properties of $g(\tau)$ and $h(\tau)$ will be formulated, and there will emerge, incidentally, a criterion for the amount of energy which must be received from an echo before satisfactory radar observation is possible.

We should expect $\mathrm{P}(\tau)$ to have a peak in the vicinity of the true range τ_0 ; this will arise from the signal function $g(\tau)$. Elsewhere, $g(\tau)$ will in practice be negligible because, in effect, radar waveforms are specially chosen to ensure it. Near τ_0 one may expand $u(t-\tau)$ by Taylor's theorem, and obtain from equation (21)

$$g(\tau)=\frac{\alpha_0^2}{\mathrm{N}_0}\int u^*(t-\tau_0)\{u(t-\tau_0)-(\tau-\tau_0)u'(t-\tau_0) \\ +\tfrac{1}{2}(\tau-\tau_0)^2u''(t-\tau_0)\}\,dt, \quad . \quad . \quad . \quad (25)$$

neglecting higher powers of $\tau-\tau_0$ and denoting du/dt by u'. Writing

$$\rho^2 \doteq 2\mathrm{E}/\mathrm{N}_0, \tag{26}$$

where E is now the energy of the received signal $\alpha_0\psi$, one may obtain from equations (7), (4) and (8) the following useful relations :

$$\frac{\alpha_0^2}{\mathrm{N}_0}\int u^*(t-\tau_0)u(t-\tau_0)\,dt=\rho^2, \tag{27}$$

$$\frac{\alpha_0^2}{\mathrm{N}_0}\int u^*(t-\tau_0)u'(t-\tau_0)\,dt=0, \tag{28}$$

$$\frac{\alpha_0^2}{\mathrm{N}_0}\int u^*(t-\tau_0)u''(t-\tau_0)\,dt=-\rho^2\beta^2. \tag{29}$$

These are definite integrals, extending over an integral number of repetition periods of $u(t)$. The second relation depends on the definition (4) of carrier frequency, while the third is obtained after an integration by parts. Consequently,

$$g(\tau)=\rho^2-\tfrac{1}{2}\rho^2\beta^2(\tau-\tau_0)^2+\mathrm{O}(\tau-\tau_0)^3. \tag{30}$$

It will be seen that the peak in $g(\tau)$ is of height ρ^2 occurring at τ_0, and in this neighbourhood $g(\tau)$ is purely real. This quantity ρ^2 is important because it is the dimensionless energy parameter which constantly recurs in the theory. The expansion of $g(\tau)$ outlined above is required later, when determining the accuracy of range measurement.

It is now necessary to consider the noise function $h(\tau)$ and its influence on $g(\tau)$. Transformation of equation (22) into vector notation gives

$$h(\tau)=\frac{\alpha_0}{\mathrm{N}}\mathbf{n}^\dagger\mathbf{u}(\tau). \tag{31}$$

This Hermitian product is a linear function of the components of **n**, and the resultant is a stationary random function whose distributions in real and imaginary parts are independent and Gaussian about zero. By using the additive property of mean square deviations, one may readily show that

$$\overline{\{\mathscr{R}h(\tau)\}^2}=\overline{\{\mathscr{I}h(\tau)\}^2}=\alpha_0^2\,|\,\mathbf{u}(\tau)\,|^2/\mathrm{N}=\rho^2. \tag{32}$$

Furthermore, it is well known (Rice 1945) that the amplitude distribution for such a function is given by

$$q(\,|\,h\,|\,)=\frac{1}{\rho^2}|\,h\,|\exp\left(-\,|\,h\,|^2/2\rho^2\right), \tag{33}$$

and that $|\,h\,|$ has a mean square value $2\rho^2$.

When $\mathrm{E}<\mathrm{N}_0$, the root mean squared modulus, $\rho\sqrt{2}$, of $h(\tau)$ is greater than the peak value ρ^2 of $g(\tau)$, and the signal and noise functions will not be distinct in $\mathrm{P}(\tau)$. A necessary, though insufficient, criterion for satisfactory observation is therefore that the total received energy should be greater than the noise power per unit bandwidth, and for convenience in the mathematics it will be assumed much greater. The condition

$$\rho^2 \gg 2, \quad \text{or} \quad E \gg N_0 \quad . \quad . \quad . \quad . \quad . \quad . \quad . \quad . \quad . \quad (34)$$

applies, in fact, throughout the remainder of this paper. It is insufficient because it does not of itself ensure that the area under $P(\tau)$ is all near τ_0.

An immediate consequence of this condition is that the peak of the signal function $g(\tau)$ will be large compared with unity, and it can be seen from equation (24) that this feature is accentuated in $P(\tau)$, since asymptotically $I_0(x)$ increases exponentially with x. Thus, for practical radar waveforms, the peak in the normalized probability distribution due to the signal function will be concentrated near τ_0 and in equation (30) the higher powers of $(\tau-\tau_0)$ may be neglected. Except near this peak, the signal function will have a negligible influence on $P(\tau)$ and the noise function (if it is of sufficient magnitude) will alone affect it. The total interval T over which $P(\tau)$ is defined will thus be considered in two parts: one which includes the peak of $P(\tau)$ due to the signal function, where $P(\tau)$ will be denoted by $P_g(\tau)$, and the remainder, of a length nearly equal to T, where $P(\tau)$ will be denoted by $P_h(\tau)$ since g makes a negligible contribution. It is possible to demarcate the two regions satisfactorily because $P_h(\tau)$ itself consists (when ρ^2 is large) of a sequence of isolated and randomly occurring peaks. The first region will determine the accuracy with which range can be measured, whilst the area under the second region represents the degree of *ambiguity* of the observation. It is the probability that, in the ensemble of observations with fixed received waveform, the actual range does not lie anywhere near τ_0.

The more important features of the signal and noise functions have now been enunciated, and it has been seen that, if the total received energy is not large compared with the noise power per unit bandwidth, only a negligible quantity of information can be obtained from the system. This result is not, of course, confined to radar and may be seen quite generally from Shannon's formula, equation (1).

§ 5. RANGE ACCURACY.

There are two distinct statistical approaches to the problem of observational error. The first (and here deceptively simple) approach is to fix the true value and evaluate the spread of the estimates. The other, which has been adopted in this paper, is to fix on a typical received waveform resulting from a true range τ_0, and to consider the spread of the true values τ which could have produced it. The latter approach, involving the inverse distribution $P(\tau)$, eliminates consideration of how the observer estimates the true value when confronted with the received waveform.

Since $P(\tau)$ represents the properties of an ensemble in which the received waveform γ is fixed, it is *particular*, inasmuch as it depends on the specific choice of γ. It will therefore be necessary, on occasion, to consider average statistical properties of $P(\tau)$ by varying γ while keeping τ_0 fixed (see equation (9)). Averages over this fixed-τ_0 ensemble will be distinguished from averages in the fixed-γ ensemble by using the symbol A*v* instead of a bar. We shall then demonstrate that $P_g(\tau)$ is approximately Gaussian near τ_0 and calculate its standard deviation.

For the present, any ambiguity arising from the behaviour of $h(\tau)$ outside the g-region around τ_0 is ignored, but its influence inside it is interesting and is considered as follows. By equation (31) and the Taylor expansion of $u(t-\tau)$, the noise function near τ_0 is

$$h(\tau)=\frac{\alpha_0}{N}\{\mathbf{n}^\dagger\mathbf{u}(\tau_0)-(\tau-\tau_0)\mathbf{n}^\dagger\mathbf{u}'(\tau_0)+O(\tau-\tau_0)^2\}. \quad . \quad . \quad (35)$$

It may be shown that, if ρ^2 is sufficiently large, neglect of all but the linear and constant terms is not serious in spite of the necessity for including the quadratic term in the corresponding expansion of $g(\tau)$. Thus we may write

$$h(\tau)=\xi+i\eta=\{\xi_0+(\tau-\tau_0)\xi'\}+i\{\eta_0+(\tau-\tau_0)\eta'\}, \quad . \quad . \quad (36)$$

where ξ_0, η_0, ξ' and η' are random in the fixed-τ_0 ensemble and have Gaussian distributions about zero. From equation (32),

$$\mathrm{A}v(\xi_0^2)=\mathrm{A}v(\eta_0^2)=\rho^2, \quad . \quad . \quad . \quad . \quad . \quad . \quad . \quad . \quad (37)$$

and by a similar argument, it is easy to show that

$$\mathrm{A}v(\xi'^2)=\mathrm{A}v(\eta'^2)=\rho^2\beta^2. \quad . \quad . \quad . \quad . \quad . \quad . \quad . \quad . \quad (38)$$

Thus $|g+h|$ may be approximately evaluated in the neighbourhood of τ_0 for substitution into equation (24). Expanding the modulus and neglecting powers of $(\tau-\tau_0)$ higher than the second, one obtains from equations (30) and (36),

$$|g(\tau)+h(\tau)|=\rho^2+\xi_0+\frac{\eta_0^2}{2\rho^2}+\frac{\xi'^2}{2\rho^2\beta^2}-\tfrac{1}{2}\rho^2\beta^2\left(\tau-\tau_0+\frac{\xi'}{\rho^2\beta^2}\right)^2+O\left(\frac{1}{\rho^2}\right). \quad . \quad . \quad . \quad (39)$$

This may be written more simply as

$$|g+h|\approx\rho^2+\chi-\tfrac{1}{2}\rho^2\beta^2(\tau-\tau_m)^2, \quad . \quad . \quad . \quad . \quad (40)$$

where from equations (37) and (38)

$$\mathrm{A}v\,\chi=1, \quad . \quad . \quad . \quad . \quad . \quad . \quad . \quad . \quad . \quad . \quad (41)$$

$$\mathrm{A}v\,\tau_m=\tau_0, \quad . \quad . \quad . \quad . \quad . \quad . \quad . \quad . \quad . \quad . \quad (42)$$

$$\mathrm{A}v(\tau_m-\tau_0)^2=1/\rho^2\beta^2. \quad . \quad . \quad . \quad . \quad . \quad . \quad . \quad . \quad (43)$$

Near τ_0, one therefore has from equation (24)

$$P_g(\tau)=\lambda I_0\{\rho^2+\chi-\tfrac{1}{2}\rho^2\beta^2(\tau-\tau_m)^2\}. \quad . \quad . \quad . \quad . \quad . \quad . \quad . \quad (44)$$

The asymptotic expansion for I_0 is

$$I_0(x)\sim\frac{e^x}{\sqrt{(2\pi x)}}\left\{1+\frac{1}{8x}+O\left(\frac{1}{x^2}\right)\right\}, \quad . \quad . \quad . \quad . \quad (45)$$

and a trivial application of it shows $P_g(\tau)$ to be approximately Gaussian near τ_0 with

$$\tau=\tau_m, \qquad (46)$$

$$\overline{(\tau-\tau_m)^2}=1/\rho^2\beta^2. \qquad (47)$$

Thus the standard deviation of τ from its mean in $P_g(\tau)$ is given by

$$\delta\tau=1/\rho\beta, \qquad (48)$$

and this represents the *a posteriori* uncertainty in the measurement of range. That the mean value of τ in $P_g(\tau)$ has itself the same uncertainty with respect to τ_0 (equation (43)) is no mere coincidence, and is what one would expect from an application of inverse probability: both spreads really represent the same effect.

Equation (48) is the first result of practical interest. The uncertainty is independent of the frequency response of the receiver because it has been established without reference to any particular receiving mechanism and represents optimum performance.

§6. AMBIGUITY.

It was remarked at the end of §4 that the degree of ambiguity of an observation is the probability that, in the ensemble of observations with fixed received waveform, the actual range τ does not lie anywhere near τ_0. The ambiguity, A, may therefore be expressed as the area under that portion of $P(\tau)$ which is due only to $h(\tau)$, *i. e.* which excludes the signal peak discussed in the previous section. This will be calculated by multiplying the expected area per unit range of τ due to h alone, by the whole of the *a priori* interval T. This in fact includes a small range of integration near τ_0 which should strictly be omitted, but since for any practical system one has the inequality

$$T\gg 1/\rho\beta \qquad (49)$$

this approximation is justified.

It is convenient to define $P_h(\tau)$ precisely, by the relation

$$P_h(\tau)=\lambda I_0(|h|), \qquad (50)$$

and this is identical with $P(\tau)$ defined in equation (24), except near τ_0. The "expected area per unit range" under $P_h(\tau)$ is, of course, the expected value of P_h and may be obtained by considering the probability distribution for $|h|$ given by equation (33). Thus

$$\mathrm{Av}P_h=\overline{P}_h=\int_0^\infty P_h Q(P_h)dP_h, \qquad (51)$$

where

$$Q(P_h)dP_h=q(|h|)d|h|. \qquad (52)$$

The two forms of average in (51) are equal because $h(\tau)$ is a stationary random function. The integral may be evaluated by substituting for q from equation (33), P_h from equation (50), and using the expansion (45) for the Bessel function. Finally, one obtains

$$\overline{P}_h=\lambda e^{\rho^2/2}(1+O(\rho^{-4})), \quad \ldots \ldots \quad (53)$$

and the ambiguity, given by the average area under $P_h(\tau)$ is

$$A=T\overline{P}_h. \quad \ldots \ldots \quad (54)$$

It only remains to determine the normalizing constant, λ, of $P(\tau)$, which depends also on the area under $P_g(\tau)$ due to the signal function.

This area is obtained by integrating the distribution given by equation (44), and using again the Bessel expansion. The result is*

$$\int_T P_g(\tau)d\tau=\frac{\lambda e^{\rho^2+1}}{\rho^2\beta}\left\{1-\frac{1}{8\rho^2}+O\left(\frac{1}{\rho^4}\right)\right\}. \quad \ldots \quad (55)$$

Fig. 1.

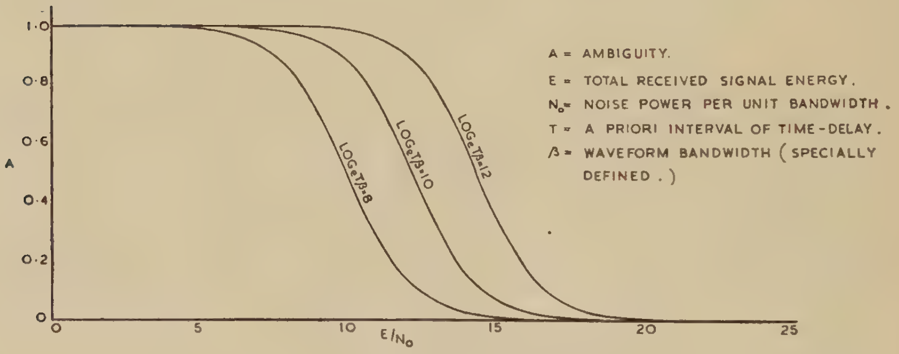

The threshold of intelligibility.

Neglecting terms of order ρ^{-4} compared with unity, the normalizing equation is

$$\begin{aligned}1&=\int_T P_g(\tau)\,d\tau+\int_T P_h(\tau)\,d\tau\\ &=\lambda\left\{\frac{e^{\rho^2+1}}{\rho^2\beta}\left(1-\frac{1}{8\rho^2}\right)+Te^{\rho^2/2}\right\}. \quad \ldots \ldots \quad (56)\end{aligned}$$

Hence, approximately,

$$A=\frac{T\rho^2\beta}{T\rho^2\beta+\exp\left(\frac{1}{2}\rho^2+1\right)}. \quad \ldots \ldots \quad (57)$$

---

* An average has been adopted in the exponent—see equation (41)—as a matter of expedience. The consequences in later parts of the theory are unimportant except when $A\approx 0{\cdot}5$, where additional approximations are, in any case, unavoidable.

Thus, keeping T and β constant, as the ratio $\frac{1}{2}\rho^2$ of the received signal energy to the noise power per unit bandwidth increases, the ambiguity diminishes to zero from a value near unity. The transition is fairly abrupt as shown in fig. 1, and forms the threshold of intelligibility. This may be defined conventionally by $A=0{\cdot}5$, and is therefore given by

$$\tfrac{1}{2}\rho^2+1=\log \mathrm{T}\rho^2\beta. \qquad (58)$$

When $\frac{1}{2}\rho^2+1 \gg \log \mathrm{T}\rho^2\beta$, unambiguous reception is ensured. This is the second criterion for a useful radar observation.

§7. INFORMATION.

The quantity of information obtainable from a radar observation is the difference of the entropies (Shannon 1948) of the *a priori* and *a posteriori* probability distributions for range. Since the *a priori* distribution has been assumed rectangular of width T, its entropy, defined by *

$$\mathrm{H}=-\int p \log p \, d\tau, \qquad (59)$$

is given by

$$\mathrm{H}_0=\log \mathrm{T}. \qquad (60)$$

The *a posteriori* entropy required is the average entropy of $\mathrm{P}(\tau)$ over the total ensemble of received waveforms. Since, however, the entropy is independent of τ_0, it is sufficient to consider an average over the fixed-τ_0 ensemble. As before, that portion of the distribution near τ_0, viz. $\mathrm{P}_g(\tau)$, and the remainder, $\mathrm{P}_h(\tau)$, will be considered separately, the total entropy being given by addition.

A difficulty arises, however, in evaluating the entropy of any particular distribution $\mathrm{P}(\tau)$ because, in doing so, the correct normalizing constant for that distribution should be used, and this will vary throughout the fixed-τ_0 ensemble. This makes the integrations difficult to perform, and to simplify the treatment a fixed normalizing constant λ, dependent on average properties of $\mathrm{P}(\tau)$ and given by equation (56), is used.

Fluctuations in λ are due, when $\rho^2 \gg 1$, almost entirely to $\mathrm{P}_h(\tau)$ and their neglect is justified in either of two circumstances:

(*a*) When the total area under $\mathrm{P}_h(\tau)$ is small, *i. e.* $A \sim 0$, and the entropy is approximately that of $\mathrm{P}_g(\tau)$ alone, or

(*b*) When the total interval, T, over which $\mathrm{P}_h(\tau)$ extends, is sufficiently large for P_h to include an adequate statistical sample of those of its ensemble properties which influence the entropy. This condition amounts to $A \sim 1$, though the derivation is lengthy and is here omitted. The entropy then arises almost entirely from $\mathrm{P}_h(\tau)$.

Thus one may first calculate the average entropy due to $\mathrm{P}_g(\tau)$ alone, which will represent that of $\mathrm{P}(\tau)$ when $A \sim 0$; then that due to $\mathrm{P}_h(\tau)$ alone, giving the entropy of $\mathrm{P}(\tau)$ when $A \sim 1$; finally, an approximation in the intervening (threshold) region will be made by ignoring fluctuations of the normalizing constant.

---

* Here $p(\tau)$ signifies any probability distribution.

The contribution of $P_g(\tau)$ to the entropy, is obtained by substituting the averaged expression for $P_g(\tau)$ given by equations (44) and (41) into equation (59), using the expansion for I_0, and integrating. This leads to

$$Av(H_g)=-\frac{\lambda e^{\varrho^2+1}}{\rho^2\beta}\left\{\left(1-\frac{1}{8\rho^2}\right)\log\frac{\lambda}{\rho\sqrt{(2\pi)}}+\rho^2+\tfrac{3}{8}+O\left(\frac{1}{\rho^2}\right)\right\}. \quad . \quad (61)$$

But if $A\sim0$, from equation (55) the normalizing constant is given by

$$\frac{\lambda e^{\varrho^2+1}}{\rho^2\beta}\left(1-\frac{1}{8\rho^2}\right)=1, \quad . \quad . \quad . \quad . \quad . \quad . \quad . \quad . \quad (62)$$

whence from equation (61)

$$AvH_g=\log\frac{\sqrt{(2\pi e)}}{\rho\beta}+O\left(\frac{1}{\rho^2}\right). \quad . \quad . \quad . \quad . \quad . \quad . \quad (63)$$

The information content is given by the difference of the *a priori* and *a posteriori* entropies, viz.

$$I=H_0-H_1=\log T-H_1 \quad . \quad . \quad . \quad . \quad . \quad . \quad . \quad (64)$$

and hence

$$I\sim\log\frac{T\rho\beta}{\sqrt{(2\pi e)}}, \quad (A\sim0). \quad . \quad . \quad . \quad . \quad . \quad . \quad . \quad (65)$$

Since $P_h(\tau)$ is a stationary random function, one may calculate its average contribution to the total entropy by multiplying the expected value of $P_h \log P_h$ by the interval T of integration. Thus, ignoring fluctuations of λ,

$$AvH_h=-T\int_0^\infty Q(P_h)P_h\log P_h dP_h. \quad . \quad . \quad . \quad . \quad (66)$$

Hence, substituting for $Q(P_h)$ and P_h from equations (52), (33) and (50), using the expansion for I_0, and integrating, one obtains

$$AvH_h=-\lambda Te^{\varrho^2/2}\left\{\log\frac{\lambda}{\rho\sqrt{(2\pi)}}+\rho^2+\tfrac{1}{2}+O\left(\frac{1}{\rho^2}\right)\right\}. \quad . \quad . \quad (67)$$

But when $A\sim1$, using equations (53) and (54), the normalizing constant λ is given approximately by

$$\lambda e^{\varrho^2/2}=1/T. \quad . \quad . \quad . \quad . \quad . \quad . \quad . \quad . \quad . \quad (68)$$

Thus,

$$AvH_h=\log(T\rho\sqrt{(2\pi)})-\tfrac{1}{2}\rho^2-\tfrac{1}{2}+O\left(\frac{1}{\rho^2}\right) \quad . \quad . \quad . \quad (69)$$

and

$$I\sim\tfrac{1}{2}\rho^2-\log(\rho\sqrt{(2\pi)})+\tfrac{1}{2}, \quad (A\sim1). \quad . \quad . \quad . \quad . \quad . \quad (70)$$

Equations (65) and (70) thus give the asymptotic approximations to the information content under conditions of unambiguous and ambiguous reception, except in the vicinity of the threshold at $A=0{\cdot}5$.

When A approximates neither to zero nor unity, it is, of course, necessary to normalize $P(\tau)$ taking into account both $P_g(\tau)$ and $P_h(\tau)$, and incidentally to ignore—as explained above—normalizing fluctuations which should in this region be included. The value of λ taken from equation (56) is substituted into equations (61) and (67), addition of which gives the approximate average *a posteriori* entropy H_1. Finally subtraction from H_0 gives

$$I \approx -\log\left\{\sqrt{(2\pi e)}\left(\rho e^{-\frac{1}{2}\rho^2-1}+\frac{1}{T\rho\beta}\right)\right\}+O\left(\frac{1}{\rho^2}\right). \quad . \quad . \quad (71)$$

It will be seen that this expression reduces, as it must, to equations (65) or (70) according as the second or first terms in the logarithm predominate, *i.e.* $A \sim 0$ or 1. It represents a better approximation to the total quantity of information than either of the previous equations, even though fluctuations of the normalizing constant are ignored.

Fig. 2.

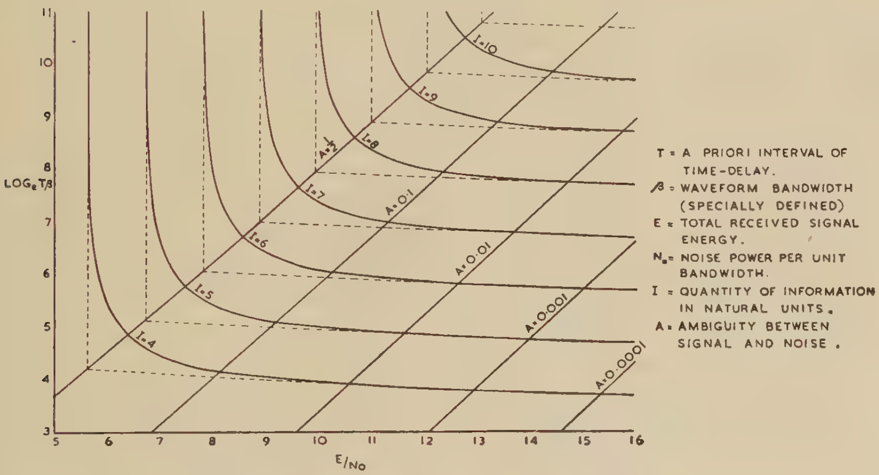

Information and ambiguity contours.

§8. Discussion.

The chief results of the foregoing theory are illustrated in fig. 2, where contours of information content I, given by equation (71), and ambiguity A, given by equation (57), are plotted against the quantities $\log_e(T\beta)$ and E/N_0. It will be seen that the I-contours behave in a markedly different manner on either side of the threshold of intelligibility ($A=0{\cdot}5$). When the ambiguity A is small, the I-contours are asymptotic to dotted curves given by equation (65). The information here represents almost unambiguous knowledge of target range, subject to a "topological" error which is shown in §5 to have a standard deviation of

$$\delta\tau = 1/\rho\beta,$$

where

$$\rho = \sqrt{(2E/N_0)}$$

and β is the "effective bandwidth" of the transmitted waveform. As would be expected, the error diminishes as the total received energy E increases, if the noise power N_0 per unit bandwidth is constant. It also diminishes as β increases, but increasing β alone in order to obtain high resolution, has its drawbacks because the observation gradually becomes more ambiguous.

When the ambiguity is greater than a half, the I-contours are asymptotic to the dotted vertical lines given by equation (70), which represent the upper bound to the information content when the total received energy is fixed. In Shannon's general theory of communication (Shannon 1948) there is a similar upper bound, with which comparison may be made. Quite generally, the quantity of information I which can be extracted from any received message of energy E is limited to E/N_0 natural units. This result is obtained from equation (1) by writing

$$I = Ct = Wt \log\left(1 + \frac{E}{N_0 Wt}\right) \text{ nat. units,}$$

where t is the duration of the message. As $Wt \to \infty$, I approaches the asymptotic value

$$I_s = E/N_0 = \tfrac{1}{2}\rho^2.$$

The corresponding radar limit, as $\beta \to \infty$, is less than this by $\log(\rho\sqrt{(2\pi)}) - \frac{1}{2}$ natural units of information, and the discrepancy may be shown to correspond to the fine-structure information which was deliberately discarded in passing from equation (23) to (24). If radar could operate without a high-frequency carrier, this effect would not arise and the asymptotes in the ambiguous region of fig. 2 would exactly equal Shannon's theoretical limit.

In normal reception, the quantities β, N_0, and the *a priori* interval T are constant, while E increases with the time of observation. One therefore starts beyond the left of the diagram and moves steadily to the right along a horizontal path. At first, the amount of information increases rapidly as the ambiguity is steadily removed. After crossing the threshold into the useful region, however, the information increases only very slowly and represents a progressive improvement in accuracy. This phenomenon is in full accord with the ideas underlying information theory. Once the approximate position of the target is known without ambiguity, further incoming energy is continually contributing information which is already partly known ; the resolution in range is increased by continued emphasis rather than by a systematic process of elimination. For this reason, the most efficient radar system should work as close to the threshold of intelligibility as possible—how close depending upon the degree of ambiguity which can be tolerated.

It must be emphasized that a phase-coherent received waveform is assumed in this paper, and this severely limits the practical application of the theory. If the range parameter τ were itself a function of time, the time-integrals in the theory would have to be evaluated differently. As matters stand, the total period of observation must be restricted to an interval which is sufficiently short for τ to be treated as a constant. Under these circumstances, there is nothing to choose (except on practical grounds) between concentrating the available energy into one repetition period of the modulation or spreading it out over several. There is little doubt, however, that the latter course is wasteful of energy when long-term phase-coherent integration cannot be utilized (Lawson and Uhlenbeck 1950).

The bandwidth of the receiver does not appear in the results of the theory. As long as it is sufficiently wide to include the whole of the transmitted spectrum, no information is gained or lost by increasing it, and none can be gained by reducing it. The choice of frequency response at the receiver depends only on the best way to extract, and present to the observer, all the latent information in the incoming waveform, with which practical problem this paper is not concerned.

§9. ACKNOWLEDGMENT.

Acknowledgment is made to the Chief Scientist, Ministry of Supply, and the Controller, H.M. Stationery Office, for permission to publish this paper.

§10. REFERENCES.

GABOR, D., 1946, *Jour. Inst. Elect. Eng.*, **93**, Pt. III, 429.
JEFFREYS, H., 1939, *Theory of Probability* (Oxford).
LAWSON, J. L., and UHLENBECK, G. E., 1950, *Threshold Signals*, Chap. 7.
OSWALD, J., 1949, *Comptes Rendus* (l'Académie des Sciences), **229**, 21.
RICE, S. O., 1945, *Bell. Sys. Tech. Jour.*, **24**, 46.
SHANNON, C. E., 1948, *Bell Sys. Tech. Jour.*, **27**, 379 and 623 ; 1949, *Proc. Inst. Radio Eng.*, **37**, 10.
TITCHMARSH, E. C., 1939, *Theory of Fourier Integrals* (Oxford).
WIENER, N., 1949, *Interpolation, Extrapolation, and Smoothing of Stationary Time Series.*

XCIII. *Some Optical Properties of Evaporated Layers of Silver, Copper and Tin.*

By D. G. Avery, Ph.D.,
Royal Holloway College, London University*.

[Received July 21, 1950.]

[Plates XXXII. & XXXIII.]

Summary.

In an earlier work (Tolansky 1944), a description was given of the use of multiple-beam interferometry to determine relative phase changes on reflection at the silvered surfaces of an interferometer. This method has been extended and critically examined. It is shown that the method does not approach the accuracy of the older polarimetric methods, and that its optimum use is restricted to reflecting surfaces of fairly high reflection coefficient. Within its limitations the method has advantages.

Measurements of the relative phase changes on reflection at a number of layers of silver, copper, and tin have been made, together with measurements of the ellipticity of the light reflected at these layers. The variation of these quantities with the thickness of some layers of silver has been discussed in relation to the use of evaporated layers for the measurement of the optical constants of bulk materials, and the optical constants of evaporated layers of copper and tin have been determined and the results discussed.

Part I: The Interferometric Technique for the Measurement of Relative Phase Changes.

In 1944 Tolansky described the appearance of the multiple-beam interference fringes formed by a highly silvered lens and plate combination, when the angle of incidence of monochromatic light falling on to the interferometer varied from 0° to 80°. At normal incidence the fringes took the form of rings (Newton's rings), but as the angle of incidence increased these of course became elliptical, but further each became a doublet, the separation of the doublet components increasing with the angle of incidence. The components were found to be polarized in mutually perpendicular directions and the origin of the doubling was shown to be the effective difference in gap of the interferometer for the two components, due to the difference between the phase changes suffered on reflection by the light polarized parallel and perpendicularly to the plane of the incidence.

---

* Communicated by Professor S. Tolansky.

It was apparent that this was a new method for the measurement of the relative phase changes occurring on reflection, and Tolansky measured this quantity for the particular silvered surfaces of his interferometer. No further examination of this method has been reported and it is the purpose of this paper to study the method critically both theoretically and in the light of a number of measurements of relative phase changes made by this technique.

The Theory of the Method.

Although Tolansky's original experiments were carried out on silver-modified Newton's rings it is advantageous to treat the simpler case of straight line fringes formed in a wedge interferometer composed of two plane reflecting surfaces, inclined at a small angle.

Consider first monochromatic light, of wavelength λ, incident at angle θ on a wedge interferometer with an air gap. The fringes (of equal thickness) will take the form of lines parallel to the line of intersection of the two reflecting surfaces. If the angle of incidence is not zero, each fringe will in fact have two components, and if the fringes occur at distances x_s, x_p x'_s, x'_p, etc. along the wedge, it can be shown that the relative phase change Δ can be determined from

$$\Delta(\theta, \lambda)=\lambda/2 \,.\, (x_s-x_p)/(x'_p-x_p). \qquad (1)$$

An equation from which Δ may be determined can also be derived in the case of fringes of equal chromatic order (Tolansky 1945). These fringes are formed when an interferometer is illuminated with white light, and a small section of the interferometer is projected on to the slit of a spectrograph. The section is small enough for the value of t to be assumed constant over it, if the wedge apex is parallel to the spectrograph slit. In the focal plane of the spectrograph fringes appear, which in this case take the form of straight lines parallel to the slit. Again, if θ is not zero, the fringes are doubled, the components having different wavelengths.

Let the wavelengths of the components of two adjacent doublets be λ_p, λ_s, λ'_p, λ'_s. Then the relative phase changes given by

$$\Delta(\theta, \lambda)=m/2(\lambda_p-\lambda_s), \qquad (2)$$

and hence Δ can be found from measurements of λ_p and λ_s if m, the order of the fringe, is known.

The order, m, is given by

$$m\lambda_p-(m+1)\lambda'_p=2\Phi_p(\theta, \lambda_p)-2\Phi_p(\theta, \lambda'_p) \qquad (3)$$

where the function Φ_p represents the change of phase suffered on reflection by the parallel component. In the absence of published data describing the variation of the function with wavelength and with angle of incidence, the order of the fringe m cannot be determined without making an assumption of the form of Φ_p. This is true not only for fringes at other than normal incidence but also for all uses of fringes of equal chromatic order.

If we assume $2\Phi_p(\theta, \lambda)=\beta\lambda$ where β is a constant fraction, then as, closely enough,

$$\lambda_p \simeq \tfrac{1}{2}(\lambda_p+\lambda_s) \equiv \lambda, \ldots$$

gives

$$m-\beta=\lambda'/(\lambda-\lambda'). \quad \ldots \ldots \ldots \quad (4)$$

Now m, the order of the fringe, is integral, and the quantity $m-\beta$, which can be determined from measurements of the mean wavelengths λ and λ', is in general not integral. Moreover, the sign of the fractional part is indeterminate.

However, from measurements on fringes of equal thickness we can find the relative phase change Δ for one wavelength unambiguously from equation (1), and so if the value of m for a fringe of equal chromatic order at that wavelength be chosen to give the correct value for Δ, the values for the orders of the other fringes of equal chromatic order at different wavelengths can readily be assigned, and the fringes used to measure the variation of the relative phase change with wavelength. In addition fringes of equal chromatic order, being formed in a very small section, of the interferometer of assumed constant thickness, have a constant dispersion leading to improved accuracy of measurement. As against this latter point however, it should be noted that when fringes of equal thickness are used, the whole surface of the interferometer is covered, with perhaps a desirable averaging effect of the properties of the films.

The experimental arrangement and the interferometric technique have been adequately described elsewhere (Tolansky 1948) and no treatment will be given here. The discussion which follows of the accuracy of measurement of relative phase changes from measurements of the doubling of interference fringes of non-normal incidence will assume that the interferometer has been used in such a manner as to give the best interference fringes obtainable with the particular reflecting surfaces employed.

The Errors in Measurement.

In figs. 1 (*a*), (*b*) and (*c*) (Pls. XXXII. & XXXIII.) are shown photographs of fringes formed at varying angles of incidence in interferometers whose surfaces had reflection coefficients 90, 50, and 20 per cent respectively. The photographs are all of fringes of equal thickness, using light of wavelength 5461 Å.

The previously established increase in separation of the fringe doublet as the angle of incidence increases from zero is clearly shown.

Three striking features of these fringes are immediately apparent, all of which are of importance in assessing the accuracy with which the doubling can be measured, and the relative phase change determined.

First, comparison of figs. 1 (*a*), (*b*) and (*c*) (Pls. XXXII. & XXXIII.) shows that the width of both components of the fringe doublets increases rapidly with decreasing reflection coefficient. This of course is to be expected and constitutes one serious drawback to the generalized use of the technique, since the highest accuracy is only obtainable when measuring the effect on surfaces of reflection coefficients of over 85 per cent.

Secondly, as the angle of incidence increases there is a considerable difference in fringe width for the two components for all values of the reflection coefficient, and thirdly, the maximum intensity of the sharper component decreases rapidly at the higher angle of incidence.

Tolansky suggested that the difference in the intensities was evidence for the existence of some preferential absorption by the silver film. However, reference to fig. 2, which shows the variation with incidence angle of the reflection and transmission coefficients of a typical silver film, shows that for these films, whilst some slight preferential absorption exists at the higher angles, it is in the opposite sense to the effect observed. The difference in the maximum intensities of the two components arises mainly from the difference in the transmission coefficients in the two cases, the maximum intensity being governed by the ratio $1/1+(A/T)^2$ where A is the absorption given by $A=1-(R+T)$. The values shown in fig. 2 are typical for silver films of high reflection coefficient. The

Fig. 2.

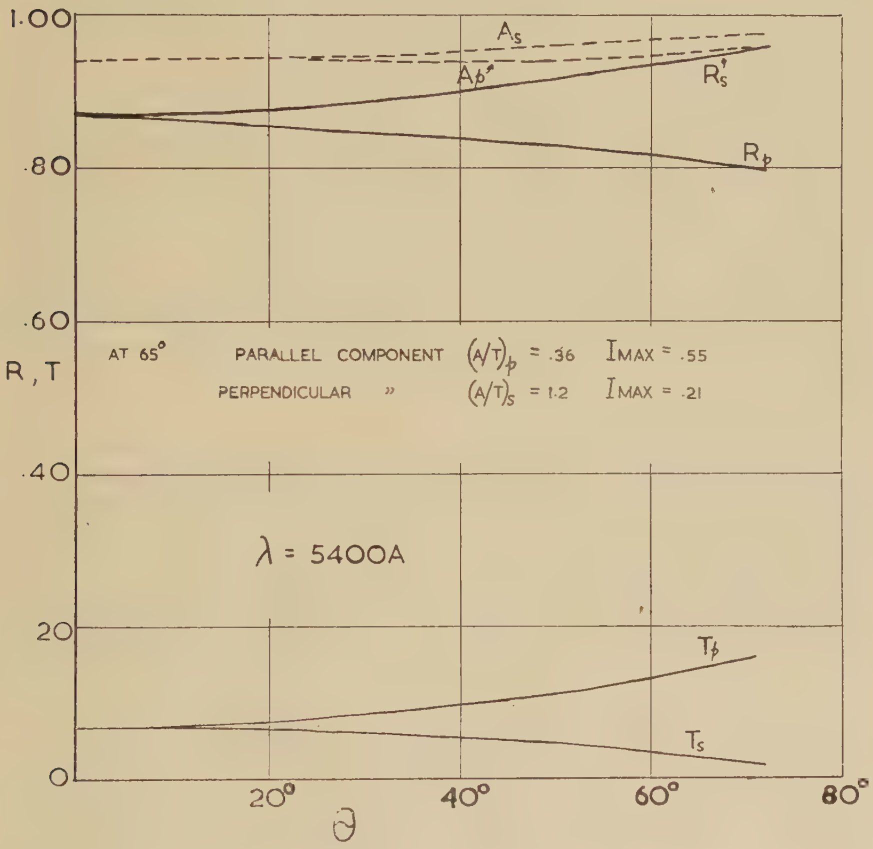

The variation with incidence angle of the reflection and transmission coefficients of a typical silver film.

differences in fringe width are of course due to the widely differing values of the reflection coefficient for the components. This effect increases with decreasing normal incidence reflection coefficient.

The accuracy with which the doublet separation can be measured is affected by the differences in width and intensity of the components in two ways. Not only is it impaired by the increase in fringe width due to the lower reflection coefficient of the "parallel" component, but also this width, coupled with the weaker intensity of the "perpendicular" component, causes the visibility of the latter to be poor. This obscuring of the weaker component is not serious for high reflection coefficient films, but becomes so when the reflection decreases to values of 50 per cent or less (fig. 1 (*c*), Pl. XXXIII.).

The errors all increase with decreasing reflection coefficients. With fringes of equal thickness and fringes of equal chromatic order, in transmission, determinations of relative phase change have been made for surfaces of reflection coefficient varying between 20 and 94 per cent. The experimental error in the determination of relative change of phase, expressed as a fraction of the wavelength of the incident light, varies from $\pm 0{\cdot}002\,\lambda$ for the optimum case of $R > 80$ per cent, to $\pm 0{\cdot}005\,\lambda$ for $R < 30$ per cent. If the relative phase change is expressed as an angle this corresponds to $\pm 0{\cdot}7^\circ$ for the optimum, and $\pm 2^\circ$ for the worst case studied.

The Limitations of the Technique.

The accuracy obtainable with this method for measuring relative phase changes ($\pm 0{\cdot}7^\circ$) is inferior to the figures of $\pm 0{\cdot}001\,\lambda = 0{\cdot}36^\circ$ readily obtainable by Drude's method (Hass, 1938) and with the error of $\pm 0{\cdot}1^\circ$ in the estimation of the angle of principal incidence by O'Bryan (1936).

From the point of view of the use of the measurements for the determination of optical constants, however, the higher accuracies obtainable in the older optical methods are not always required, since large local irregularities often arise in the preparation of the reflecting surfaces employed. Clearly under such conditions high intrinsic accuracy of measurement is meaningless physically. It was to overcome these errors that the use of evaporated layers as characteristic reflecting surfaces of metals was introduced (O'Bryan, Hass, *loc. cit.*). However, this technique does not allow of one main advantage of the use of evaporated layers to be gained, namely the measurement of the properties of such layers *in vacuo*. Possible deterioration of the layers by atmospheric corrosion during measurement could be avoided by the introduction of an oil between the interferometer plates.

However, a principal limitation of the method remains. Relative phase changes occurring on reflection at low reflectivity metals such as copper, tin, chromium, etc. can only be measured with half the accuracy available for measurements on silver and aluminium, due to the increase of the errors with decreasing reflection coefficient.

As against these limitations must be set some advantages over the earlier method. The method requires no expensive polarimetric equipment and the experimental arrangement is simple. The doubling of the fringes can be photographically recorded and measurements made at leisure, as opposed to the need for laborious visual observations necessary with most of the polarimetric methods. This is particularly the case when it is desired to measure the variation of the relative change of phase with wavelength, since the whole visible range can be covered with a single photograph of fringes of equal chromatic order, whereas a dozen or more visual observations with a half-shade device would be necessary with the older methods.

PART II: THE OPTICAL MEASUREMENTS.

The interferometric data are coupled with measurements of the ellipticity of the light reflected at the layers, made with a simple photoelectric photometer. An investigation was made as to whether the magnitude of the effects occurring on reflection at evaporated layers having the finite transmission required for the multple-beam method were the same as those associated with reflection at the bulk metal. The variation of the phase and intensity quantities with the thickness of the evaporated layers has been measured to supplement existing information regarding the normal incidence reflection characteristics of evaporated layers.

Measurements have been made for a number of evaporated layers of silver of varying thickness and the results served to define the limits within which the thickness of a metallic layer must lie if it is to be used for the determination of the optical constants of the metal. With the increasing use of evaporated layers in this connection (*e. g.* O'Bryan 1936, Hass 1938, Archard 1949) these limits are a matter of some significance, particularly when the interference method is used for the measurement of the relative phase changes.

The layers of silver, and of the other metals used, were all produced by vacuum evaporation from molybdenum filaments at pressures less than 5×10^{-5} mm. of Hg, after the glass disks on to which they were deposited had been cleaned both by hand and by ionic bombardment in the evaporation chamber. The rates of evaporation were such that opaque layers of the metals could be formed in thirty seconds.

Measurement of Relative Phase Changes and Ellipticities for Reflection at Silver Layers.

The first series of silver layers produced were all of the order of thickness used for usual interferometric work, *i. e.* between 400–500 A. thick and having transmission coefficients of up to 4 or 5 per cent. The variation of the ellipticity ρ with the angle of incidence of light for one of these layers is shown in fig. 3, and the variation of the relative phase changes with incidence angle for several layers in fig. 4. The error in the measurement of the ellipticity throughout the work was $\pm 0{\cdot}01$, the error in the measurement of the relative phase change, Δ, varied with the reflection coefficient of the layers, and for the present series was $\pm 0{\cdot}002\,\lambda$. The measurements of ellipticity were made for the light passed by a filter giving a mean wavelength of 5400 Å. and a band width of roughly 300 Å., and of relative phase change for the mercury green line 5461 Å.

Taking the values found by Hass (1938) for the optical constants of silver ($n=0{\cdot}177$, $k=18{\cdot}60$, $\lambda=5461$ Å.) the ellipticities and relative phase changes to be expected on reflection at a silver surface have been calculated using formulæ due to Drude (1890). These theoretical values have been plotted in figs. 3 and 4, and in addition, the angle of principal incidence for silver (for which the relative phase change on reflection is equal to $\lambda/2$ or 0·25) found by O'Bryan (1936) is also shown in fig. 4.

Fig. 3.

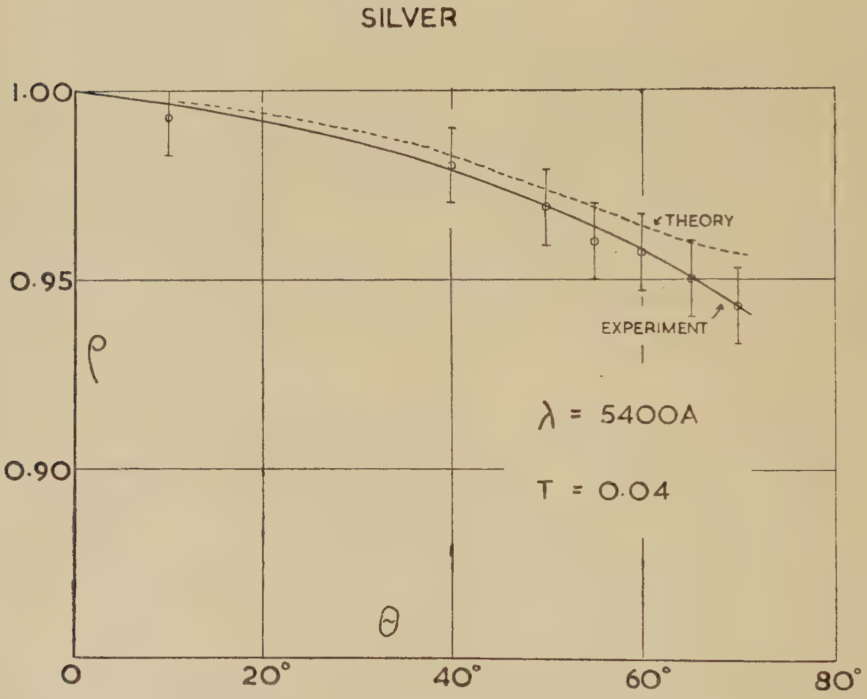

The variation with incidence angle of the ellipticity of the light reflected from a silver film.

It is seen from these curves that whilst the ellipticity for a layer having a transmission coefficient of 0·04 differs from the theoretical value for reflection at bulk silver by nearly one per cent at the higher angles of incidence, the relative phase change values, taken for some ten layers having transmission coefficients between 0·01 and 0·07 do not differ from the theoretical value to this extent. This indicates that the value of the ellipticity of the light reflected from evaporated layers is more sensitive to film thickness than is the relative change of phase on reflection. This will be borne out completely when the measurement of the variation of these quantities with thickness is considered.

In fig. 4 are plotted the earlier measurements made by Tolansky (1944) for the relative phase changes occurring on reflection with a given silver layer. In the neighbourhood of 65° incidence, there is a sudden change in the slope of Tolansky's curve. This effect has not been observed with any of the films examined in this work, and has not been completely explained. One possible explanation is that the films used by Tolansky were comparatively old (at least one month after preparation) and the effect may be due to surface contamination of the layer due to age. In the present work measurements were made on the layers within one hour of production in each case. Below 65° there is reasonably close agreement between the two sets of data.

Fig. 4.

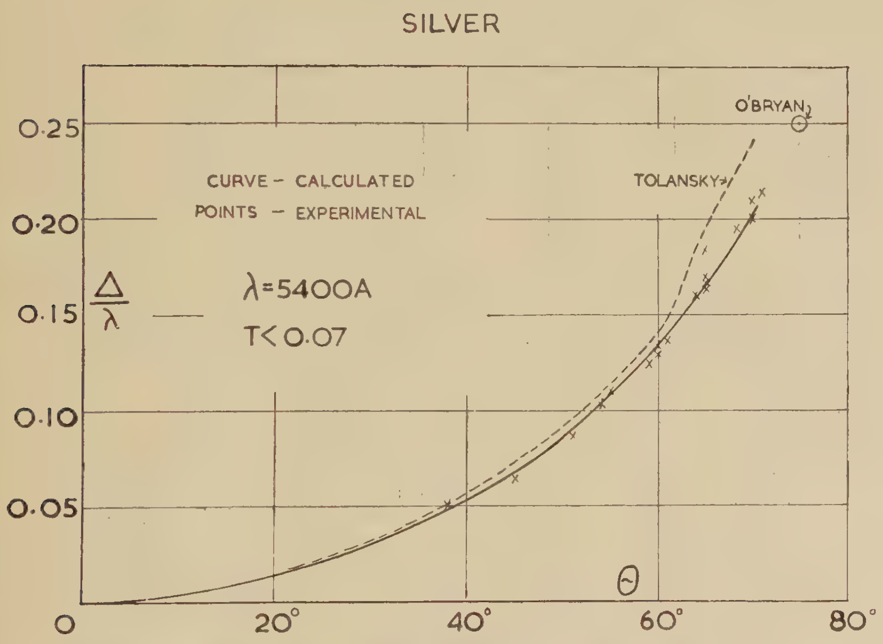

The variation of the relative phase change on reflection at "thick" silver films with the angle of incidence.

The variations of the quantities ρ and Δ with the thickness of the silver layer varying between 100 Å. and 500 Å. are shown in figs. 5 and 6 for an angle of incidence of 65°. The errors in the values for ρ are $\pm 0{\cdot}01$, but the errors in the relative phase changes increase from $\pm 0{\cdot}002\,\lambda$ for the thickness layers, to $\pm 0{\cdot}005\,\lambda$ for the thinnest ones, due to the decreasing reflection coefficient of the layers. The thicknesses of the layers were measured by the interferometric technique developed by Khamsavi and Donaldson (1947), and the values are accurate to ±15 Å. The mass of silver present per unit area of the film is also given, since the thickness measurements may be open to question (Avery 1949).

Fig. 5.

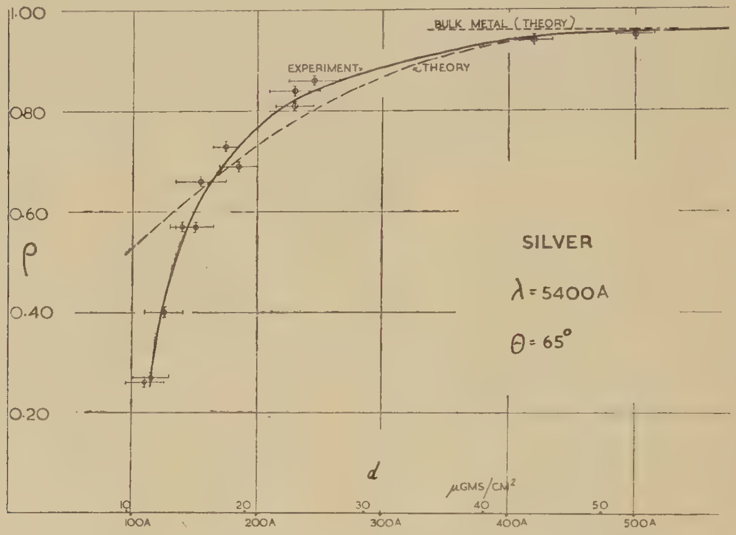

The variation of ellipticity with thickness for silver films.

Fig. 6.

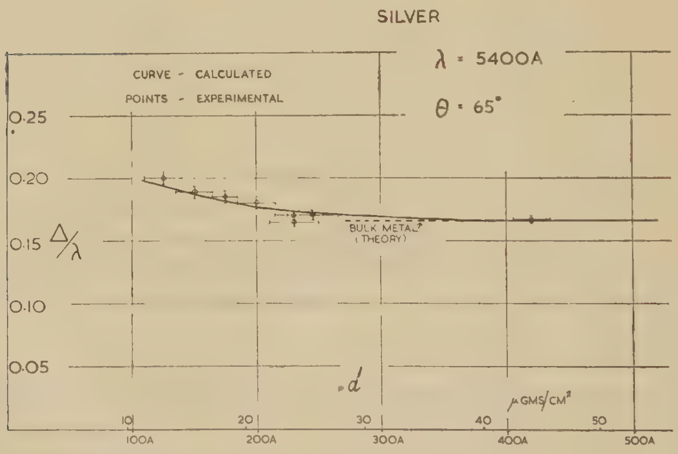

The variation of relative phase change with thickness for silver films.

The theoretical values of ρ and Δ were calculated using formulæ similar to those developed by Winterbottom (1948).

Apart from a slight divergence in the thickness region about 250 Å., the values of the ellipticity measured agree with the theoretical values down to layers of about 150 Å. in thickness, and marked differences between theory and experiment first appear at thicknesses below this value. This agrees well with the variation of the normal incidence coefficients with thickness as measured by a number of workers (Rouard 1949), and the deviation of experiment from theory at the lower thickness values is in accord with the observed changes in the optical constants of silver layers of lesser thickness. The relative phase changes (fig. 6) show no similar divergence, though the measurement of d for the thinner films is correct only to 5 per cent.

If reflection at an evaporated layer is treated as equivalent to reflection at the metal in bulk when the values of ρ and Δ do not differ from the values characteristic of the bulk metal by more than one per cent, then fig. 6 shows that as far as the measurement of relative phase change is concerned, the layers need be no more than 350 Å. thick for this. For silver this corresponds to a transmission coefficient of 6 to 8 per cent. Such a thickness gives bright good multiple-beam interference fringes. Since the deviation of the value of Δ from the bulk metal value as the thickness decreases is probably due to interference effects within the layer, this implies that the optical transmission of the layer is the deciding factor of the usefulness of the film for " bulk " measurements, not the physical thickness.

Fig. 5 shows that the variation of the ellipticity with thickness is more rapid, and deviations of one per cent from the bulk metal value are found for thicknesses below 450 Å., that is for silver, for transmissions of no more than one or two per cent. Whilst for silver this represents no hindrance to the use of the same layers for the measurement of both the quantities ρ and Δ, metals which form layers of a greater absorption than silver layers need a greater transmission than this if reasonably intense interference fringes are to be obtained.

If a simple photometer to measure ρ, combined with an interference technique to measure Δ, is used to determine optical constants, or for other reflection studies, it seems that it is most suitable to prepare two sets of layers. One set should be opaque or very nearly so, and used for the measurement of the ellipticity, and the other set should have transmissions of the order of five per cent, and used in the interferometer to measure the relative phase changes. Where a polarimetric method is being used to determine ρ and Δ in one operation and the layers are produced and measured immediately *in vacuo*, the layers must have transmission of less than one or two per cent for the layer characteristics to be within one per cent of those of the bulk metal.

Electron microscope investigations have shown (Levinstein 1949) that not all metals can be deposited on to substrates at room temperature to give layers with structures corresponding to the bulk metal. Thus the optical properties of evaporated layers, particularly those of the low melting point metals, may differ from those of the bulk metal due to differences in crystalline structure, even in layers thick enough for the interference effects within the films to be neglected.

The Optical Constants of some Evaporated Layers of Copper.

Copper films were deposited by evaporation, four layers being prepared almost opaque and four with transmissions of up to five per cent. The values of the ellipticity found from the thick layers are plotted against incidence angles in fig. 7 and the values of relative phase change found interferometrically from the slightly transparent layers are shown in fig. 8. The errors in Δ are $\pm 0{\cdot}003\,\lambda$ due to the relatively low reflection coefficient of copper (0·57 at normal incidence).

Taking the values of ρ and Δ for four angles of incidence, 50°, 55°, 60°, 65°, the optical constants for the layers were determined using the formulæ of Drude. The value derived for the refractive index is $n=1{\cdot}10\pm0{\cdot}07$, and for the absorption coefficient $k=2{\cdot}3\pm0{\cdot}1$.

Fig. 7.

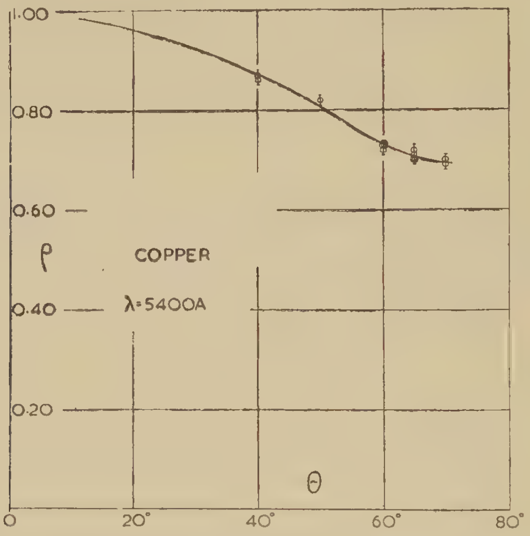

The variation of ellipticity with incidence angle for thick copper films.

Also included in fig. 8 are two values for Δ for evaporated layes of copper reported by Lowery, Wilkinson and Sware (1936). Good agreement exists within the present values. However the values of the optical constants calculated by Lowery, $n=0{\cdot}90$, $k=2{\cdot}1$, for a single angle of incidence differ from those quoted above.

These are in close agreement with the values quoted in the *International Critical Tables* for $\lambda=5400$ Å., $n=1{\cdot}07$, $k=2{\cdot}25$, and with those given by Winterbottom (1936) for bulk copper, $n=1{\cdot}00$, $k=2{\cdot}40$. However, as Lowery has demonstrated, values found from measurements on copper surfaces prepared by polishing are extremely susceptible to differing methods of surface preparation, hence the agreement is fortuitous. The values for electrolytically deposited copper are $n=1{\cdot}38$, $k=1{\cdot}78$, and for cathodically sputtered layers $n=0{\cdot}90$, $k=2{\cdot}70$, and so it seems that the layers produced by evaporation resemble the structure of the massive metal more closely than layers made by electrolytic deposition or cathodic sputtering.

The Optical Constants of Evaporated Layers of Tin.

Eight evaporated layers of tin were examined at one angle of incidence only, 65°. The reflection coefficient at normal incidence was 0·70, and the layers were stable in air.

Fig. 8.

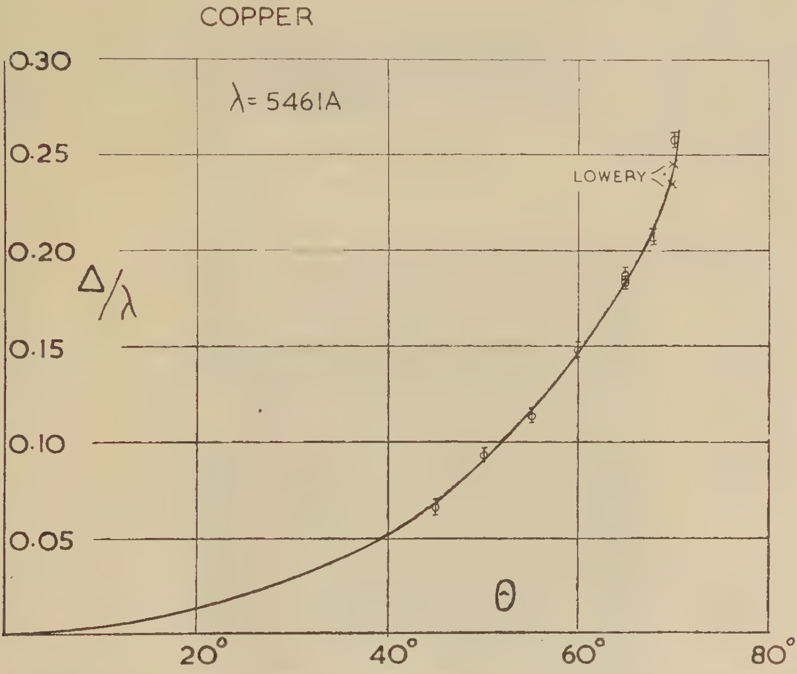

The variation of relative phase change with incidence angle for thick copper layers.

The optical constants derived for a wavelength of 5400 Å. were $n=2{\cdot}4\pm0{\cdot}2$, $k=1{\cdot}9\pm0{\cdot}1$. The accuracy of the values for the constants of copper cannot be claimed here since these measurements were made at one angle of incidence only. The optical constants for bulk tin (Hedges and Homer 1937) are given as $n=1{\cdot}0$, $k=4{\cdot}2$, and even allowing for considerable variations in the values for the bulk metal (tin is soft and so its surface would be susceptible to conditions of polish etc.) there exists considerable difference between the optical constants of the layers and of the bulk.

The constants for the bulk metal yield theoretical values for ρ and Δ of 0·82, and $0{\cdot}130\,\lambda$. These values were checked experimentally. Some plane surfaces of tin were prepared by allowing drops of the molten metal to fall on a hot glass plate, and to cool there slowly. When separated from the glass the tin surface had the finish of the glass plate, and also was presumably free from any distortion due to cold working. The ellipticity of the light reflected from these surfaces was measured, and the relative phase change was determined using the interferometric technique in reflection.

A photograph of the interference fringes obtained by reflection in an interferometer formed between a freshly prepared evaporated silver layer (R=0·88, T=0·06) and the cast tin surface (R=0·80) is shown in fig. 9. In order to use reflection fringes in this connection it is desirable to improve the visibility by polarizing the two halves of the field at right angles to one another and to observe the doubling along the line between the halves. The accuracy of measurement on these fringes is not equal to that obtainable with transmission fringes, but it is sufficient for the present case.

Fig. 9.

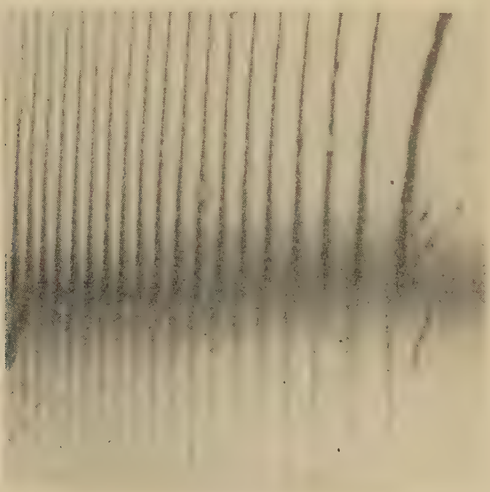

Reflection fringes at 65° incidence in the surface of a cast tin specimen.

The results of this experiment together with the experimental values for the layers, and the theoretical values for bulk tin are included in the Table below.

TABLE.

	ρ	Δ/λ	R	n	k
Theory Bulk	0·84	0·133	0·82	1·0	4·2
Exp. Bulk (cast)	0·82±0·01	0·13±0·01	0·80		
Exp. Layers	0·73±0·01	0·101±0·003	0·70	2·4	1·9

Fig. 1 (*a*).

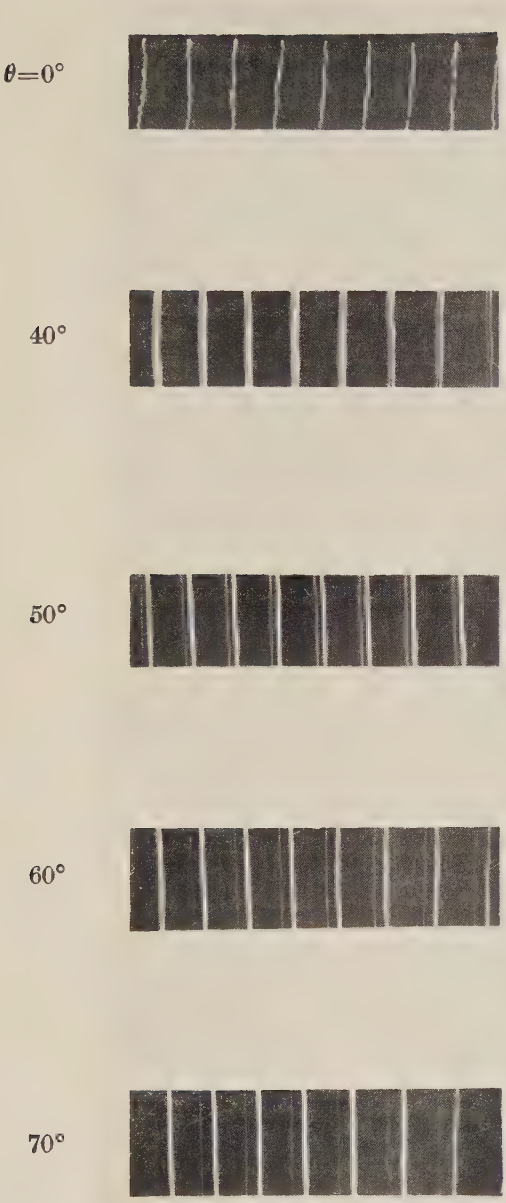

Fringes of equal thickness in an interferometer at various incidence angles, for reflection coefficients of 90 per cent.

Fig. 1 (*b*).

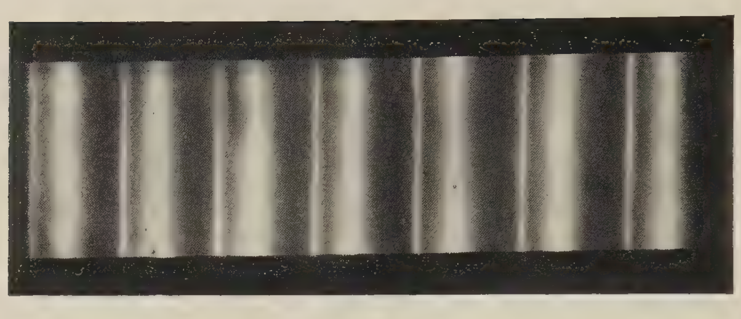

Fringes of equal thickness in an interferometer at various incidence angles, for reflection coefficients of 50 per cent.

Fig. 1 (*c*).

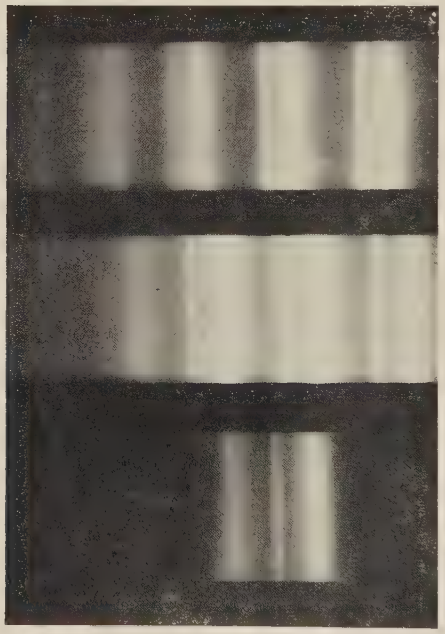

Fringes of equal thickness in an interferometer at various incidence angles, for reflection coefficients of 20 per cent.

The surface structure of the evaporated layers of tin would thus appear to differ from that of the metal in bulk.

Three possible explanations can be put foward to explain the discrepancy. First it may be that an oxide film was present on all the layers of tin examined, and its presence changed the optical properties of the layer. However, the layers were very stable in air, and the values of the ellipticity and relative phase change were found to be unaltered after several days, during which an oxide film might have been expected to grow and to cause further changes in the optical properties.

The second possibility (suggested by Dr. Hedges of the Tin Research Institute) is that an alloying action took place between the tin and the molybdenum filament used for the evaporation. The percentage of molybdenum in the alloy would be very small, since the filament used was of strip 0·004 in. thick, and was not visibly affected after fourteen separate evaporations from it, but the possibility remains.

A third possibility is that tin, whilst it forms a stable layer at room temperature, exhibiting specular reflection, being a low melting point layer might not form layers of a structure similar to that of the metal in bulk, even when they are opaque.

ACKNOWLEDGMENTS.

I must express my thanks to Professor S. Tolansky for suggesting these problems and for much helpful guidance throughout the work described. I am also indebted to Dr. Hedges of the Tin Research Institute for the supply of samples of very pure tin. The work was made possible by a Department of Scientific and Industrial Research maintenance grant.

REFERENCES.

ARCHARD, J., 1949, *Ph.D. Thesis* (University of London).

AVERY, D. G., 1949, *Nature, Lond.*, **163**, 916.

DRUDE, P., 1890, *Wied. Ann.*, **34**, 480.

HASS, G., 1938, *Ann. der. Phys.*, **31**, 245.

HEDGES and HOMER, 1937, *The properties of Tin*, 3rd Edition.

KHAMSAVI and DONALDSON, 1947, *Nature, Lond.*, **159**, 228.

LEVINSTEIN, 1949, *J. App. Phys.*, **20**, 306.

LOWERY, WILKINSON and SMARE, 1936, *Phil. Mag.*, **22**, 149.

O'BRYAN, H. M., 1936, *Journ. Opt. Soc. Amer.*, **26**, 122.

ROUARD, P., 1949, *Rev. d'Optique*, **28**, 569.

TOLANSKY, S., 1944, *Phil. Mag.*, **35**, 120 ; 1945, *Ibid.*, **36**, 225 ; 1948, *Multiple-beam interferometry of surfaces and films* (Clarendon Press).

WINTERBOTTOM, A. S., 1936, Private communication ; 1948, *Journ. Opt. Soc. Amer.*, **38**, 12.

XCIV. *The Magnetic Deflection of Fast Charged Particles in the Photographic Emulsion**.

By C. C. Dilworth†, S. J. Goldsack‡, Y. Goldschmidt-Clermont†, and F. Levy‖.

[Received Aug. 1, 1950.]

[Plate XXXIV.]

§ I. SUMMARY.

Electron Sensitive Nuclear Research Emulsions have been exposed at sea level, and at the Pic du Midi (2800 m.) in magnetic fields of the order of 34,000 gauss, in order to test the possibilities of curvature, within the emulsion itself, of the tracks of charged cosmic ray particles.

The existence of measurable deflections of long tracks has been established by comparison of the results of measurements on field and no field plates, and the method has been applied to determine the sign of particles in a group of cosmic ray phenomena in the exposures at high altitude.

§ II. INTRODUCTION.

In a dense medium such as the photographic emulsion, the multiple scattering of a charged particle is so high as to mask the continuous curvature produced by a magnetic field except under high fields and on long tracks.

The angle of magnetic curvature θ_m is given by

$$\theta_m=\frac{180}{\pi}\cdot\frac{3\times10^{-4}}{p}\,\mathrm{H}t \text{ degrees,}$$

where H is the magnetic field in gauss, p is the momentum in MeV./c, t is the track length in cms.

The arithmetic mean angle of scattering is given by $\bar{\theta}_s=100{\cdot}4\sqrt{t}\mathrm{G}/p\beta$ degrees where 100·4 is a constant calculated for the emulsion, β is the ratio of the velocity to that of light, and G is a slowly varying function of β and t of the order of 4. Hence the ratio of the magnetic deviation to the mean scattering angle is

$$\theta_m/\theta_s=\beta\mathrm{H}\sqrt{t}/6050\,\mathrm{G}=\gamma_0\beta\sqrt{t}. \quad . \quad . \quad . \quad . \quad . \quad . \quad (1)$$

---

* Communicated by Professor P. M. S. Blackett, F.R.S.

† Centre de Physique Nucléaire, Université Libre de Bruxelles.

‡ University of Manchester.

‖ University of Manchester, on leave of absence from Centre National de la Recherche Scientifique, Paris.

where γ_0 is a slowly varying function of track length and of β and is proportional to the field H *.

For a field H=34,000 gauss, and for a relativistic particle of track length 1 cm. $\gamma_0 \simeq 1{\cdot}46$.

In fig. 1 the sloping line shows the quantity $\bar{\theta}_s E/t = 100{\cdot}4\phi/\sqrt{t}$ as a function of track length. The horizontal lines show $\theta_H E/t$ for relativistic particles, for various field strengths. The figures show that for H=30,000 gauss the ratio $\theta_H/\theta_s = 1$ when $t \simeq 5$ mm. This indicates the order of length of track required to separate the magnetic deflection from the scattering deflection for relativistic particles. For slower particles the length must be greater by a factor $1/\beta^2$.

Fig. 1.

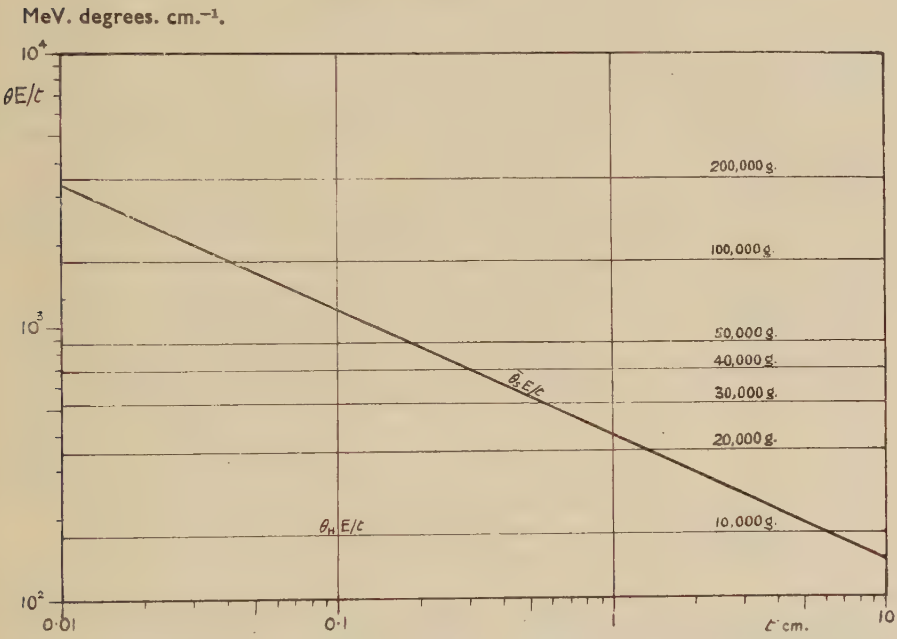

Plot of $\bar{\theta}_s E/t$ as a function of track length t. The horizontal lines show $\theta_m E/t$ for relativistic particles.

In the following paragraphs we discuss how the magnetic deflection may be separated from the scattering and used to determine the sign of the particle, to improve the estimate of momentum, and to estimate the ratio of deflection to scattering $\beta\gamma_0\sqrt{t}$. Since γ_0 is nearly independent of the type of particle and of its momentum, its mean value for a number of tracks may be regarded as a test of the scattering theory, or as a calibration of the plates.

---

* This definition of $\bar{\theta}_s$ and of γ_0 differs from that of Moyal (1950) by a factor $\sqrt{\pi}/2$ since $\bar{\theta}_s$ is the root mean square scattering angle in his paper.

§ III. METHODS OF ANALYSIS.

(1) *Estimation of the Curvature.*

To measure magnetic deflection and scattering we use the customary method of dividing the track into a set of equal cells, and we measure the direction θ_i of the track in the ith cell with respect to an arbitrary origin. The deviation $\xi_i=\theta_{i+1}-\theta_i$ between two successive tangents to the track is the sum of a constant magnetic deflection and a random scattering deflection with zero mean.

Except at highest momenta we may neglect measurement errors for the present discussion. If we assume the distribution of scattering to follow a Gaussian law, the best estimate for the curvature is the sum of this set of independent measured deviations $\sum_1^n \xi_i$.

This sum is equal to the total deviation between tangents at the two ends of the track* $\phi=(\theta_n-\theta_0)$.

This result is confirmed by a more refined analysis, taking into account small measurement errors (Moyal 1950) or using sagitta measurements (Scott 1949).

The actual distribution of scattering is closely similar to a Gaussian distribution, but has a rather large "single scattering tail". The effects of this tail are most simply eliminated by subtracting large deviations from the total deflection in estimating the curvature.

The standard error on the estimate of the magnetic deflection θ_m from the total deviation ϕ is the sum of the independent errors, the scattering error $(\frac{1}{2}\pi)^{\frac{1}{2}}\bar{\theta}_s$ and the measurement error s_0 on each of the first and last settings.

$$i.\,e.\ \ \theta_m=\phi\pm(\tfrac{1}{2}\pi\bar{\theta}_s^2+2s_0^2)^{\frac{1}{2}}.$$

In most cases $2s_0^2\ll\frac{1}{2}\pi\bar{\theta}_s^2$, so we may write

$$\theta_m=\phi\pm(\tfrac{1}{2}\pi)^{\frac{1}{2}}\bar{\theta}_s.$$

The relative error on the determination of the momentum p from the magnetic deflection is therefore approximately

$$\frac{\epsilon(p)}{p}=\frac{\epsilon(\theta_m)}{\theta_m}=\sqrt{\frac{\pi}{2}}\cdot 1/\beta\gamma_0\sqrt{t}. \quad . \quad . \quad . \quad . \quad . \quad (2)$$

---

* This result depends on the statistical independence of the successive deflections ξ_i. If the track were a perfect arc, and measurement errors were the only cause of scattering, the actual observations θ_i, and not the deflections ξ_i would be independent. The best estimate for the curvature would then be given by the mean value of the deflection over half track distances, $\frac{2}{n}\sum_1^{n/2}\left(\theta_{\frac{n}{2}+i}-\theta_i\right)$ since this statistic involves each of the n independent observations with equal weight. These conditions are encountered in cloud-chamber measurements on particles of high momentum, and may exist for such particles in the plate if higher fields become available.

The errors on the determination of momentum from scattering are discussed in paragraph (5). The variation of these errors with energy of the particle is shown in fig. 7, where $\frac{\epsilon(p\beta)}{p\beta}\sqrt{t}$ is plotted against $p\beta$ for typical values of the measurement errors. The horizontal lines show the relative error from magnetic curvature, together with the form of the curves for protons and π mesons, allowing for their becoming non-relativistic.

Fig. 2.

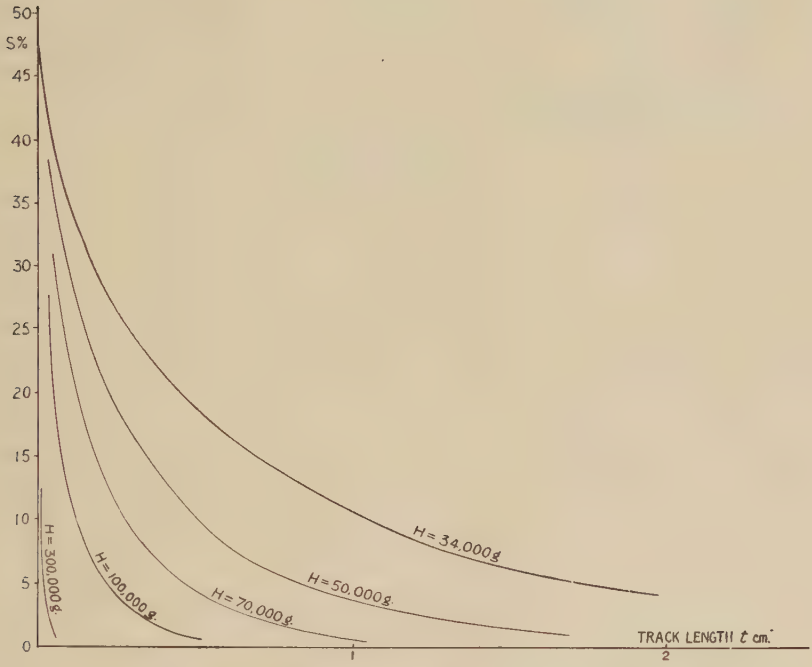

The proportion S per cent of particles of track length t, which, owing to multiple scattering, will give a total deflection in the wrong sense, as a function of t for various field strengths.

It can be seen that over wide ranges of energy the momentum is determined with greater precision from scattering observations than from magnetic deflection in moderate fields. However, for very high fields (of the order of 100,000 gauss), and for high momentum particles, the estimate from magnetic deflection is more accurate.

(2) *Determination of the sign of particles.*

In many tracks from cosmic-ray events the direction of motion of the particle is known. The determination of its sign then depends simply on the sense of its deflection in the magnetic field. Owing to the superposed scattering there exists a certain probability that a particle will have a total deflection in the wrong sense. This probability is a function of track length and of magnetic field, and is plotted in fig. 2. Here it will be noticed that for a track of 1 cm. and a field of 34,000 gauss, the probability is 12 per cent.

If, however, the momentum can be determined with fair accuracy from scattering measurements, or from other considerations, we may frequently assess the sign with greater accuracy. For consider fig. 3. Here are shown two distributions representing the probability distribution for the total deflection ϕ if the particle has a positive or negative sign respectively, the mean value θ_H being predetermined from the knowledge of the momentum. If we observe for some particular track, a total deviation ϕ, then clearly the ratio of the probabilities of the sign being positive or negative is given by the ratio of the ordinates of the two distributions at the position ϕ, *i. e.*

$$\frac{\mathrm{P}(+|\phi)}{\mathrm{P}(-|\phi)}=\mathrm{AN}/\mathrm{BN}.$$

Fig. 3.

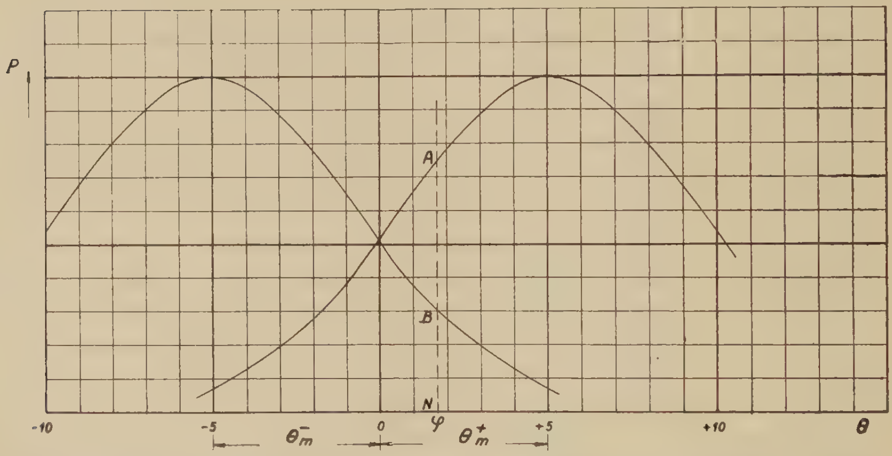

The probability distributions for the total deviation for a positive or negative particle whose mean is known from scattering measurements to be θ_H.

This assumes that a priori there are equal chances of the particle having either sign. A more rigorous analysis of the situation is given by Moyal. With $p(+)/p(-)$ the ratio of the a priori sign probabilities, his conclusion is expressed by

$$\mathrm{P}(+|\phi)=\left\{1+\frac{p(+)}{p(-)}\exp-\frac{4\beta^2}{\pi}\gamma_0\gamma t\right\}^{-1}, \quad . \quad . \quad . \quad . \quad (3)$$

where $\gamma=\phi/\bar{\theta}_s\sqrt{t}$ is the estimated value of γ_0.

In the present experiment we assume the ratio $p(+)/p(-)$ to be always unity. Fig. 4 shows the proportion of positive particles of length t which will yield a positive sign with probability $P(+|\phi)$ greater than the fixed values marked on the curves for a field of 34,000 gauss.

It should be pointed out that in the event of a track occurring during the inevitable "no-field time" and being believed to be a field track, one will, in general, attribute a sign with a probability greater than 50 per cent. The fraction of no field tracks which would give sign probabilities greater than the same fixed values as in fig. 4 is shown in fig. 5. It will be seen that this fraction can be rather high for long tracks. For this reason it is important to reduce to a minimum the no-field time, and to keep the plates horizontal while out of the field.

Fig. 4.

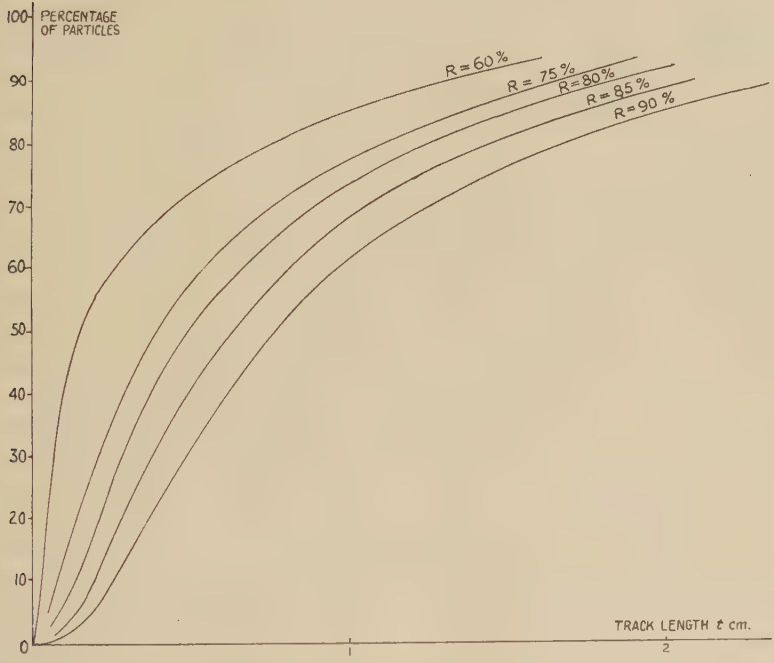

The proportion of particles, of track length t, which will give the correct sign with probabilities greater than R per cent for H = 34,000 gauss and for various values of R, as a function of t.

(3) *Estimation of Scattering.*

To estimate the multiple scattering, the direction of the mean line through the grains in each cell is carefully measured, using an accurate eyepiece goniometer, fitted with a suitable graticule*.

---

* The method of measurement of sagitta, described recently by Fowler (1950), could also be used for these measurements. We are now investigating the advantages of the two methods.

Two methods are available for the calculation of the momentum from the measured angles. Either the arithmetic mean deviation, or the root mean square is calculated. In either case the effects of the single scattering tail are eliminated by applying suitable weighting functions, as for example, for the mean deviation, a sharp cut off of all angles greater than four times the mean. Such a sharp cut off can be shown to introduce a much greater uncertainty in the root mean square than in the mean deviation.

Fig. 5.

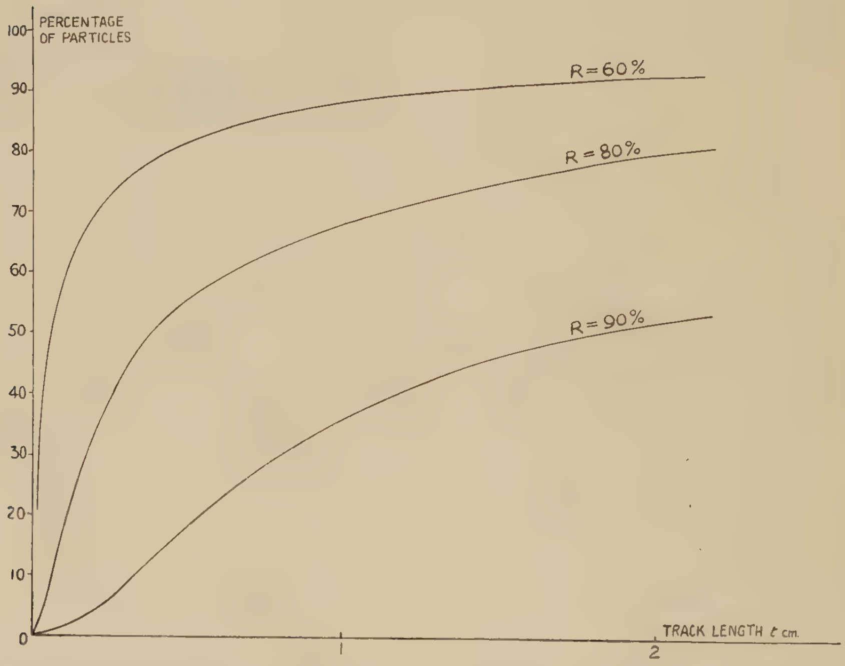

The proportion of particles of track length t which, in the absence of a field, may be expected to yield a sign probability (correct or incorrect) greater than R per cent for various values of R. The proportion which will yield the incorrect sign with these probabilities is, of course, just one-half those given by these curves.

(4) *Determination of the Errors.*

Errors of two types occur in the measurements of multiple scattering and of the total deflection.

(*a*) Distortion of the emulsion and inaccuracy of the microscope stage.

(*b*) Measurement errors, which we call spurious scattering or noise ; statistical errors, due to the finite number of cells available ; and an uncertain amount of " smoothing", a systematic reduction in scattering angles due to the treatment of the track as a straight line within each cell.

The first type of error is more serious for determination of the magnetic deflection, the second in the determination of multiple scattering. The emulsion, especially when wet, is easily distorted. Even slight distortions could limit the measurements to particles of low momentum. Their effects can be reduced by using thin emulsions, but only at the expense of the frequency of long tracks. Thin plates were used for the sea level exposure, but recent advances in the processing of thick emulsions (Dilworth *et al.* 1948 and 1950) and in the measurement of distortion (Cosyns *et al.* 1950) made possible the use of thicker emulsions for some of the later experiments. Measurements of distortion on both sets of plates are described in § IV., where it is shown that they have been reduced to a satisfactory level. For the measurements on high energy tracks the movement of the microscope stage is controlled throughout the measurements by an optical method. Both Cooke and Baker microscopes show a deflection less than 0·4′ over a displacement of 20 mm.

The determination of the second type of error depends on the method of analysis used.

In using the root mean square determination of scattering, systematic effects of smoothing and of spurious scattering may be eliminated by the method suggested by Moyal. He points out that true and spurious scattering have a different statistical nature. True scattering yields a set of independent deflections ξ_i while the presence of measurement errors on each setting θ_i is shown to introduce a negative correlation between the successive ξ_i's. On the other hand, smoothing introduces a positive correlation of a similar nature. Both effects are eliminated on the average by using as an estimate for the scattering

$$\tfrac{1}{2}\pi\bar{\theta}_s^2=(\Sigma\xi_i^2-\phi^2/n)+2(\Sigma\xi_i\xi_{i+1}-\phi^2/n). \quad . \quad . \quad . \quad . \quad (4)$$

The terms containing the total deviation ϕ are small corrections to allow for the mean deflection, and the second bracket term is a correction to the sum of squares to allow for the combined effects of noise and smoothing.

It is shown by Moyal that neglecting the departure of the scattering law from the Gaussian Law, the relative error on this estimate of $\bar{\theta}_s^2$ is given by

$$\epsilon(\bar{\theta}_s^2)/\bar{\theta}_s^2=(2/n)^{\frac{1}{2}}\left\{\left(1+\frac{4w}{\pi\bar{\theta}_s^2}\right)^2+2\right\}^{\frac{1}{2}}, \quad . \quad . \quad . \quad . \quad . \quad . \quad (5)$$

where w is the mean value of $(\Sigma\xi_i\xi_{i+1}-\phi^2/n)$.

Alternatively, using the arithmetic mean as an estimate for $\bar{\theta}_s$ the systematic effects of noise and smoothing are eliminated by the methods described by Goldschmidt-Clermont *et al.* (1948).

Smoothing is taken into account by using the angle between cells separated by one cell distance, *i. e.* $(\theta_{i+2}-\theta_i)=(\xi_i+\xi_{i+1})$, and then increasing the measured scattering by 4 ± 2 per cent *. The noise level for the track is not known, but is estimated from measurements on similar tracks of such high momentum that the true scattering is negligible, and the observed scattering is reduced accordingly.

---

* If this method were applied to the root mean square estimate we would have to calculate $\tfrac{1}{2}\Sigma(\xi_i+\xi_{i+1})^2=\Sigma\xi_i^2+\Sigma\xi_i\xi_{i+1}$. The second term is just half the correction suggested by Moyal.

The $(n-1)$ measured angles are not statistically independent. This effect is allowed for by treating $\frac{2}{3}$ of the observations as independent. Corrected for the effect of cutting off large angles, the statistical error is

$$0{\cdot}54\,[\tfrac{2}{3}(n-1)]^{-\frac{1}{2}}.$$

Fig. 6.

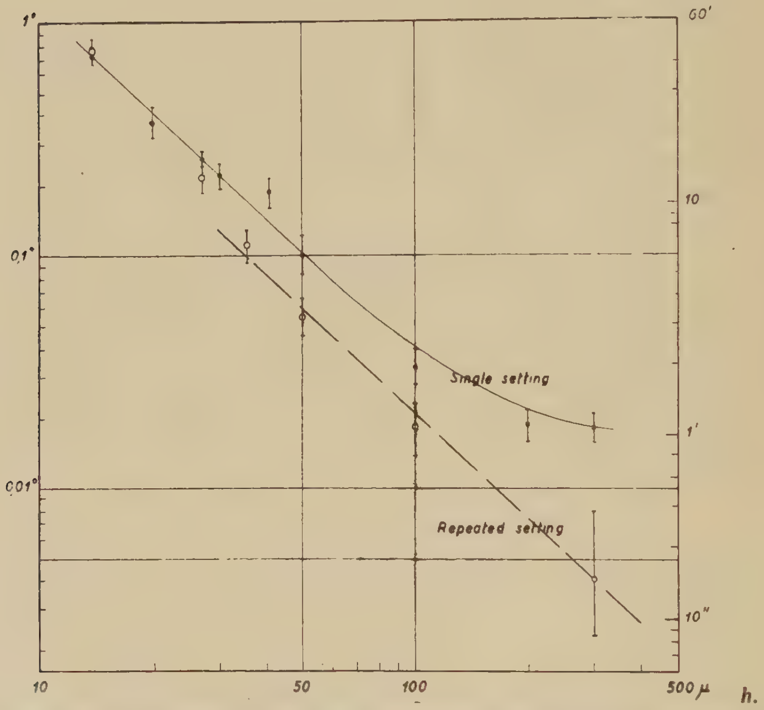

The experimentally observed spurious scattering per cell as a function of cell length for single settings and for multiple settings.

(5) *Choice of Cell Length.*

The choice of cell length results from a compromise between two conflicting requirements: a short cell reduces the statistical errors while a long cell decreases the noise level. The optimum value is that which renders minimum the total error and can be calculated from the empirical law of variation of noise level with cell length. Measurements have been made on high energy tracks to determine the magnitude of the spurious scattering and its approximate variation with cell length.

Analysis of the experimental results shows that the noise may be divided in two parts :

(1) One component, which we may call setting error, is introduced by the inability of the observer to set the line of the graticule accurately along the mean line of the grains. This error can be determined by repeated settings on a cell, and may be reduced to as low a level as is required by averaging a sufficiently large number of settings.

(2) The second and more fundamental source of spurious scattering is the spread of the grains about the true direction of the track. The mean angle $\bar{\epsilon}$ between the track and the best mean line which can be drawn through the grains can be calculated by supposing the grains to lie at random on either side of the track and at a mean distance r from it. It is found that

Fig. 7.

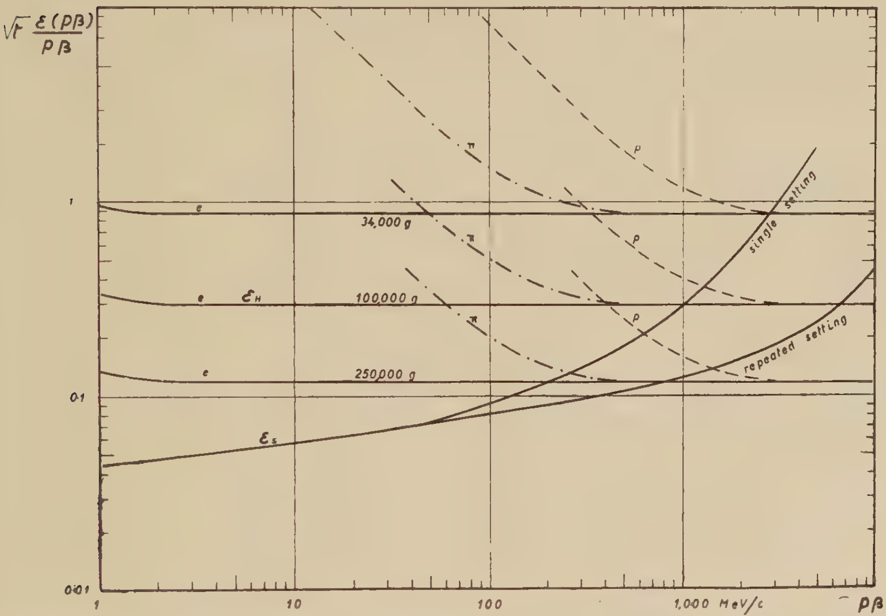

The relative error of estimation of energy at optimum cell length from scattering using single and multiple settings as a function of energy. The auxiliary lines show the error in the estimate of momentum from magnetic deflection for electrons, protons and π mesons, given by equation (2).

$$\bar{\epsilon} = \frac{Ar}{\sqrt{d}} h^{-3/2}.$$

Where d is the grain density, and h the cell length; r may be assumed to be of the order of the radius of a grain, and $A \simeq 1$.

Fig. 6 shows the observed variation of noise level with cell length. The upper curve gives the spurious scattering for single settings, the lower one that for averages of several settings. The number of settings to be averaged increases as the cell length increases. The lower curve may be assumed to represent the noise level arising from the second source. It will be seen that it is less than 1′ for cell length of 200 μ.

The value of the optimum cell length depends on the type of analysis used. With Moyal's method, where the noise level is calculated from the set of observations, it can be shown that the minimum error is obtained when the total mean square scattering is the sum of two nearly equal terms due to noise and true scattering

$$\frac{1}{n}\cdot\frac{1}{2}\cdot\pi\bar{\theta}_s^2 = s_0^2/\rho,$$

Fig. 8.

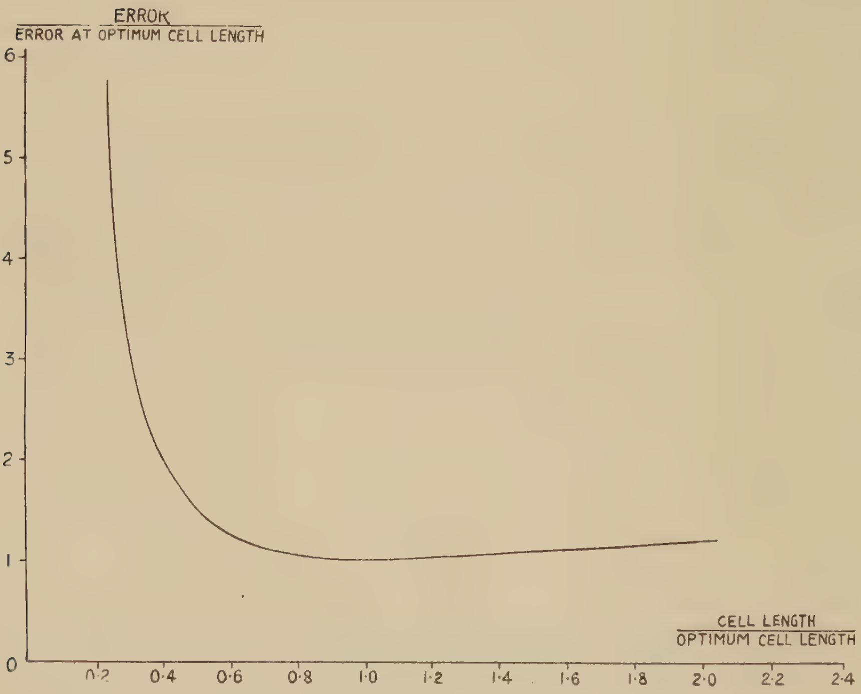

The variation of total error of momentum estimate by scattering with cell length.

where ρ is a constant of the order of 0·5. The values calculated for the total error for a single setting and for multiple settings are presented in fig. 7 as a function of momentum.

Fig. 8 shows the theoretical variation with cell length of total errors. Owing to the rapid variation of spurious scattering with cell length the total error is seriously increased by using too short a cell length. On the contrary, the use of somewhat too large a cell length will increase it only slightly. It will be seen from the figure that the use of a cell length equal to twice optimum increases the error by only 20 per cent.

For the alternative method of analysis it is necessary to use a somewhat greater cell length, since the effect of setting errors is estimated from measurements on other tracks, and we require that the uncertainty introduced should be small. As shown, however, this does not seriously increase the total error.

§IV. EXPERIMENTAL METHODS.

(1) *Exposure and Processing of the Plates.*

(A) *Sea level plates.*

The photographic plates were exposed in a vertical position in an electromagnet being built for the University of Colombo, Ceylon, at the firm of Metropolitan Vickers Ltd., Manchester. The electromagnet was similar in design to that described by Blackett (1934) for use in cloud chamber studies of cosmic ray events, having poles of 10 in. diameter. For the present experiments the poles were coned down at an angle of 60° with good quality high permeability steel (kindly supplied by Metropolitan Vickers Ltd.) to a diameter of 1 in. The gap used was 1 cm. With this arrangement and a power consumption of 6 kilowatts the field was 34,000 gauss.

The plates were Kodak NT4 plates 200 μ thick emulsions and 2 in. × 2 in. dimensions. They were carried in a horizontal position from London as soon as they were dry, and two were put in the magnetic field. Two other plates were kept in a vertical position in the Physical Laboratories, Manchester University, as controls. Both batches of plates were exposed for 20 days and then developed together. The method of "Temperature Development" was used, the developer being Azol. Great care was taken in treatment of the emulsions, especially in the drying stages, to avoid distortion. The plates were processed in a horizontal position.

(B) *Pic du Midi.*

These plates were exposed, also in a vertical position, in the field of the Blackett magnet which has recently been transported to the Pic du Midi (2800 m.). The pole pieces were 7½ cm. diameter, made of soft iron with permendur tips and gap about 1 cm. With a power consumption of 12 kilowatts the field was 34,000 gauss. Ilford G.5 plates, 200, 400 and 600 microns thick and 5 inches square were used.

The large area was taken to make the maximum use of the field and also to reduce distortion due to edge effects. The plates were dried horizontally at Ilford Ltd., to avoid stresses being introduced into the emulsion, which can later give rise to distortion. They were brought to Pic du Midi in a horizontal position to reduce the number of long no-field tracks, exposed for three weeks, and then brought back for development, again horizontally, and at low temperature to reduce fading.

Development was by Temperature Development, using amidol at low pH (Dulworth *et al* 1950). Great care was taken to avoid sudden changes of temperature, and of pH. Fixing was carried out at low temperature

(10 to 14° C.), with as little agitation as possible consistent with efficient fixing. The plates were washed in a slow non-turbulent stream of water. During the drying the plates were surrounded with a "guard ring" of wet gelatine plates; the whole placed on the glass bottom of an enclosed box, in which the humidity was regulated by the use of a "chimney". The plates were gently warmed by an infra-red lamp placed at some distance below the box. In this way the plates were maintained as far as possible with equal conditions of humidity all over the surface.

(2) *Measurements on the Tracks.*

(i) *Scanning.*

Sea level plates.—The plates were carefully scanned on a Cooke M4000 binocular microscope fitted with a Cooke 45× fluorite oil immersion objective and a pair of 8× compensating eyepieces. Many long straight tracks, mostly due to cosmic-ray mesons, were found. Some 30 tracks of approximately 1 cm. in length were found within the area covered by the high magnetic field, and a similar number of long tracks were found in the control plates.

There were fewer low-energy tracks on the no-field than on the field plates, probably because the former were kept inside a building with thick walls and floors.

Pic du Midi plates.—These plates were scanned on both Cooke M4000 and Baker 4BQ microscopes, using either Cooke 20× dry objective or Cooke 45× fluorite oil objective, and a pair of either 10× or 8× compensating eyepieces. Among the events noted those were chosen for measurement which possessed tracks of sufficient length. In 30 cm.^{2} of one 600 μ plate 40 tracks were found suitable for measurement. This does not include tracks of electron pairs, which are only found consistently with more careful scanning.

(ii) *Measurements.*

The method of measurement of scattering and of deflection has been mentioned in § III., and is described elsewhere (Y. Goldschmidt-Clermont 1950).

To define the direction of the track accurately we require a very fine straight line. Following the procedure of Braddick (1950) we have produced graticules consisting of one line, or of two parallel lines about 1 mm. apart, by ruling with a fine point on a photographic plate. Each line is of width about 0·01 mm. These have proved very suitable for this work. The grains are set symmetrically along the single line or down the space between the two lines. Different cell lengths are obtained by using eyepiece stops, and changing the magnification.

On each plate the distortion has been measured by the method of Cosyns and Vanderhaeghe, using measurements on steeply dipping tracks, and corrections applied to each track according to its dip and its orientation with respect to the distortion vector. As an additional check in the case of the sea level plates no-field control plates have been examined.

On these plates 16 tracks are deflected by less than 0·1° over distances of the order of 1 cm. One track in this group ran for 5 cm., and disregarding the 0·5 cm. near each end where it is in the danger zone near the edge of the plate, the deflection was 0·05°. Corresponding figures for the high energy particles in the field plates are that eleven such tracks were deflected by less than 0·1°.

Direct measurements have been made on the Pic du Midi plates. The distortion is, of course, least on long tracks, corresponding to their small dip. As examples of the total distortion over a whole track length ~1 cm., we found 2′ in one case and 25′ in another.

In many cases it has been possible to identify a particle by comparison of observations on the grain density and scattering. (Camerini *et al.* 1949, Cosyns 1949, Fowler 1950, Goldschmidt-Clermont 1950, Occhialini 1949).

§V. EXPERIMENTAL RESULTS.

(1) *Determination of the Curvature.*

Eleven tracks on the field plates and eight tracks on the no-field control plates have been examined and analysed by Moyal's method. The results for these tracks are presented in Tables I. and II. respectively. In figs. 9 and 10 are presented detailed plots of the tracks.

The values of the ratio

$$\gamma=\phi/\bar{\theta}_s\sqrt{t}$$

have been calculated for both types of track. For no-field tracks these should be distributed normally about zero mean. The standard deviation of the distribution is given by

$$\epsilon(\gamma)\doteqdot\sqrt{\frac{\pi}{2t}}\left\{1+\frac{2}{\pi}\gamma_0^2 t\,\frac{\epsilon^2(\bar{\theta}_s)}{\bar{\theta}_s^2}\right\}^{\frac{1}{2}},$$

the second term in the bracket is frequently small.

For field tracks it should have mean value γ_0 and the same standard deviation.

The weighted mean value of $|\gamma|$ obtained from the no-field tracks is

$$|\bar{\gamma}|=0{\cdot}49\pm0{\cdot}39.$$

For the field tracks the value $|\gamma|$ is found to be

$$|\bar{\gamma}|=1{\cdot}96\pm0{\cdot}44.$$

The difference is 1·47±0·59.

It seems that the presence of a significant effect from the magnetic field is established. To show clearly the effect we have plotted in fig. 11 the value of $g=\gamma\sqrt{t}$ which is subject to a standard error approximately $\pm\sqrt{(\pi/2)}$ against the square root of track length $\sqrt{t}$, field and no field tracks being plotted on the same diagram.

The mean value of $|\bar{\gamma}|$ for the field tracks is consistent with the calculated theoretical value $\gamma_0=1{\cdot}46$ within the rather wide errors. Many more tracks will have to be examined before it will be possible to give an experimental calibration of the scattering by this method.

TABLE I.

Field Tracks on Sea-Level Plates.

Track	Length t cm.	Cell length h microns	Estimated optimum cell h microns	Total devn. ϕ°	Mean scattering angle $\bar{\theta}_s^\circ$	Momentum eV/c		$\gamma=\phi/\bar{\theta}_s\sqrt{t}$	Sign probability %
						Scattering estimate	Magnetic defn. estimate		
1.	0·83	26	11	45·5	$19\cdot4\pm1\cdot2$	$(1\cdot8\pm0\cdot1)\times10^7$	$(1\cdot1\pm0\cdot5)\times10^7$	$2\cdot53\pm1\cdot4$	98
2.	0·80	104	50	5·3	$4\cdot1\pm0\cdot5$	$(8\cdot4\pm0\cdot5)\times10^7$	$(8\cdot7\pm8\cdot6)\times10^7$	$1\cdot45\pm1\cdot43$	89
3.	0·44	104	110	0·75	$0\cdot64\pm0\cdot2$	$(3\cdot6\pm0\cdot9)\times10^8$	$(3\cdot4\pm3\cdot6)\times10^8$	$1\cdot8\pm2\cdot0$	82
4.	0·29	104	110	0·84	$0\cdot45\pm0\cdot12$	$(2\cdot8\pm0\cdot9)\times10^8$	$(0\cdot8\pm0\cdot3)\times10^8$	$5\cdot8\pm2\cdot0$	96
5.	1·79	240	160	2·44	$0\cdot88\pm0\cdot15$	$(5\cdot8\pm1\cdot0)\times10^8$	$(4\cdot3\pm2\cdot6)\times10^8$	$1\cdot87\pm1\cdot0$	99
6.	1·24	185	180	0·33	$0\cdot74\pm0\cdot12$	$(5\cdot7\pm1\cdot4)\times10^8$	$(22\pm44)\times10^8$	$0\cdot40\pm1\cdot1$	60
7.	1·25	240	220	0·84	$0\cdot49\pm0\cdot10$	$(8\cdot3\pm1\cdot7)\times10^8$	$(7\cdot9\pm5\cdot8)\times10^8$	$1\cdot58\pm1\cdot2$	96
8.	0·72	240	300	0·68	$0\cdot29\pm0\cdot08$	$(1\cdot1\pm0\cdot3)\times10^9$	$(0\cdot62\pm0\cdot31)\times10^9$	$2\cdot6\pm1\cdot7$	97
9.	1·30	240	350	1·53	$0\cdot34\pm0\cdot14$	$(1\cdot5\pm0\cdot6)\times10^9$	$(0\cdot4\pm0\cdot4)\times10^9$	$3\cdot4\pm2\cdot1$	94
10.	1·66	240	380	0·51	$0\cdot29\pm0\cdot11$	$(1\cdot7\pm0\cdot6)\times10^9$	$(1\cdot9\pm1\cdot2)\times10^9$	$1\cdot6\pm1\cdot2$	97
11.	2·35	240	560	1·04	$0\cdot21\pm0\cdot17$	$(2\cdot7\pm1\cdot1)\times10^9$	$(1\cdot3\pm0\cdot7)\times10^9$	$3\cdot0\pm2\cdot6$	80

TABLE II.

No-Field Tracks on Sea-Level Plates.

Track	Length t cm.	Cell length h microns	Estimated optimum cell h microns	Total deviation ϕ°	Scattering deviation $\bar{\theta}_s^\circ$	Momentum eV/c scattering estimate	$\gamma=\phi/\bar{\theta}_s\sqrt{t}$
1.	1·89	104	100	1·56	1·6 ± 0·2	$(3{\cdot}3 \pm 0{\cdot}4) \times 10^8$	0·73 ± 1·15
2.	2·25	240	170	0·83	0·85 ± 0·11	$(6{\cdot}7 \pm 0{\cdot}9) \times 10^8$	0·63 ± 0·84
3.	1·08	180	190	0·56	0·52 ± 0·08	$(7{\cdot}8 \pm 1{\cdot}2) \times 10^8$	1·05 ± 1·25
4.	0·79	240	290	0·16	0·26 ± 0·13	$(1{\cdot}3 \pm 0{\cdot}3) \times 10^9$	0·67 ± 1·68
5.	1·30	240	320	0·03	0·31 ± 0·13	$(1{\cdot}4 \pm 0{\cdot}3) \times 10^9$	0·09 ± 1·1
6.	1·68	240	350	0·15	0·30 ± 0·06	$(1{\cdot}7 \pm 0{\cdot}4) \times 10^9$	0·40 ± ·94
7.	1·07	180	390	0·04	0·22 ± 0·12	$(1{\cdot}9 \pm 1{\cdot}0) \times 10^9$	0·17 ± 1·3
8.	2·50	240	500	0·07	0·19 ± 0·25	$(3{\cdot}0 \pm 4{\cdot}4) \times 10^9$	0·24 ± 0·84

The correct sign probability has been calculated for each track from equation (4), and is also presented in Table I. It will be noticed that owing to the generally high values of γ observed, leading to the mean somewhat above $\gamma_0=1{\cdot}46$, these probabilities are quite high.

Fig. 9.

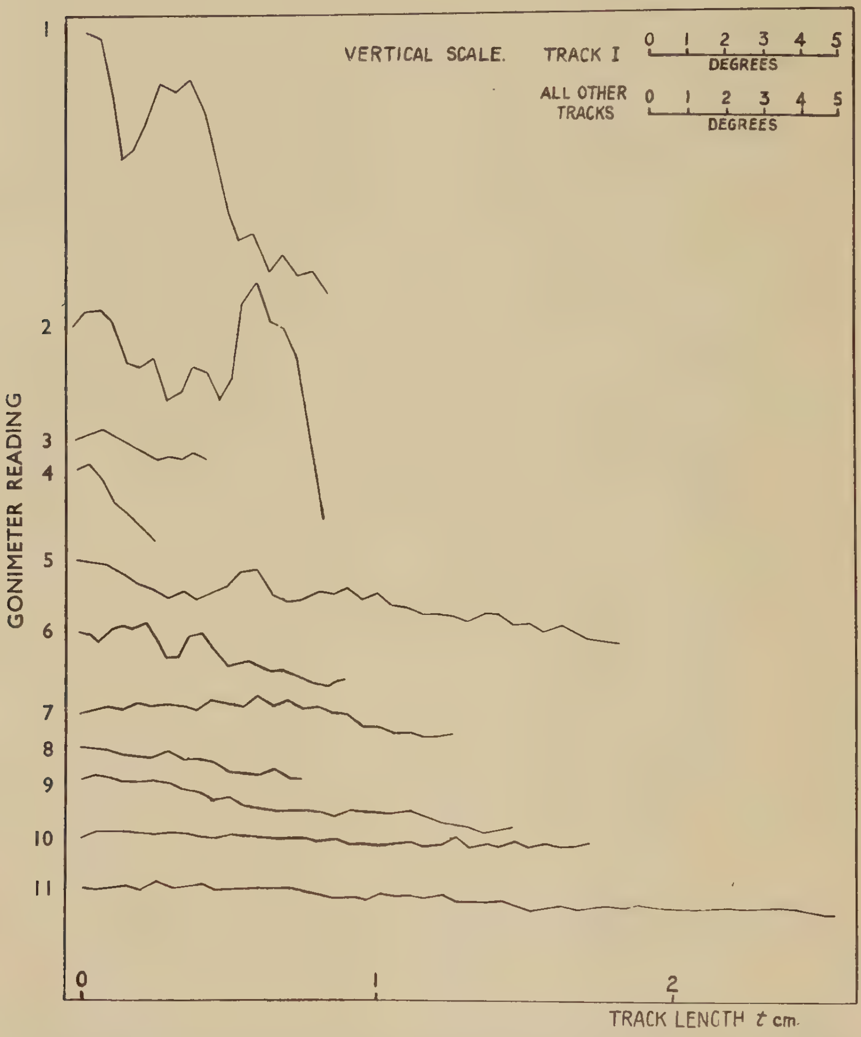

Detailed plot of eleven field tracks arranged in order of their momenta, and corresponding to the eleven tracks in Table I. Tracks 3 and 4 are two halves of the same track. For clarity negative deflections have been inverted to prevent crossing of the lines.

A discussion of the actual significance of the observed deviation is a little difficult, for clearly both the deflected and the undeflected tracks have mean deflection zero if we disregard the possible positive (or negative) excess. On the other hand, a presentation in terms of the modulus of the values of γ does not give an average which has any real meaning since the distribution about the mean is a function of track length. One way of presenting the data which seems reasonable is to calculate for each track the quantity $\{\gamma/\epsilon(\gamma)\}$. For the no-field tracks this should be distributed about zero with unit standard deviation. It follows that the sum of squares of terms such as $\Sigma\{\gamma/\epsilon(\gamma)\}^2$ should be

Fig. 10.

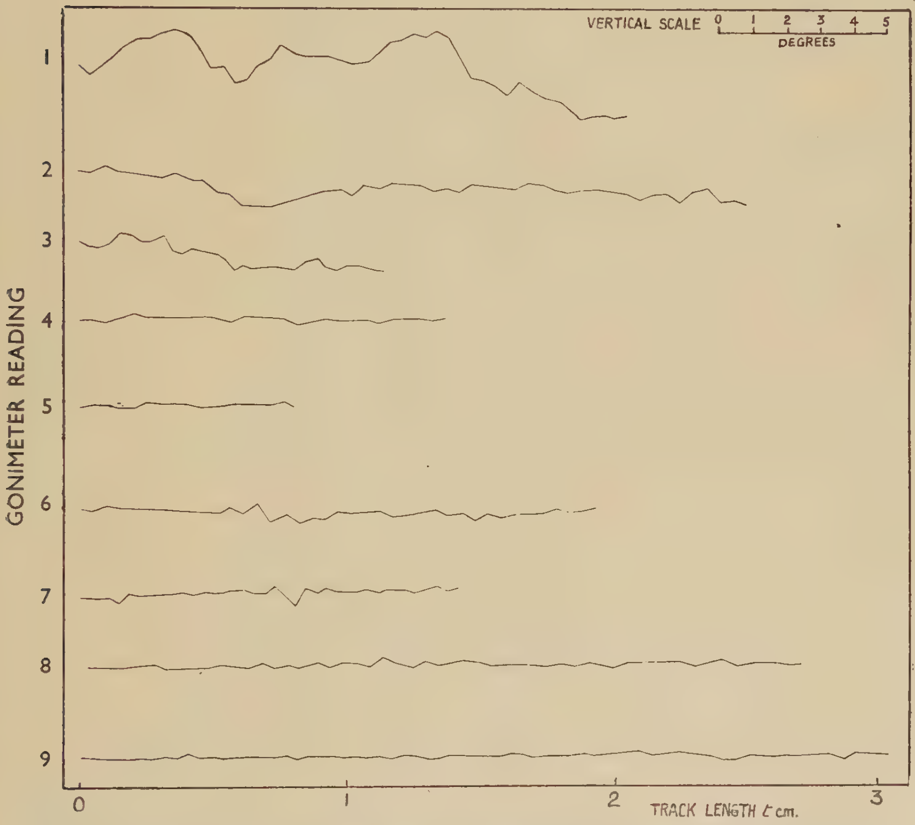

Detailed plot of nine no-field tracks. The first eight are those listed in Table II., the remaining one being a very high energy track, which is included to show the low level of distortion.

distributed according to the so-called χ^2 distribution, and the probability of the observed value being exceeded is easily found from tables of this distribution. The same analysis applied to the field tracks will then show whether the observed set of values of γ are consistent with the hypothesis that they belong to an undeflected (no-field) distribution. For the eleven field tracks the value was

$$\Sigma\{\gamma/\epsilon(\gamma)\}^2=22{\cdot}5$$

and reference to tables shows that this value is exceeded with a probability of only 3 per cent in a random sample from a normal distribution with zero mean. It follows that the observed deviations are not consistent with the hypothesis that they represent merely a fluctuation from a set of undeflected tracks.

Moyal's statistic can give a negative value for the true scattering where the total relative error is large. This happened for some of the no-field tracks since most of them were of rather high energy, and these were discarded. Tracks of similar energy for which the calculation gave a positive true scattering would be accepted. This introduces a bias tending to underestimate the average energy of the tracks. When the test is applied we are, therefore, not surprised to find that the values of γ observed are significantly small. The value obtained for the eight no-field tracks was $\chi^2=2{\cdot}16$. For a random sample there is a probability of 7 per cent that χ^2 should be smaller than this. Operation of a similar bias in the case of field tracks could only have reduced the calculated significance, so that our evaluation of it is a lower limit.

Fig 11.

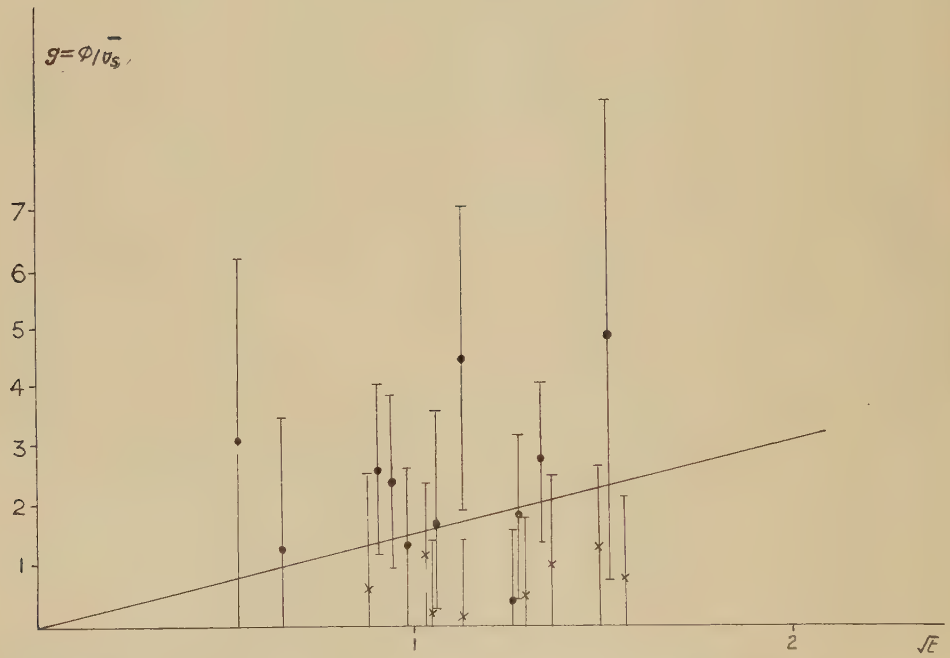

The observed ratio $g=\phi/\overline{\theta}_s$, of the total deviation ϕ to the mean scattering deviation $\overline{\theta}_s$, for eleven field tracks ● and eight no-field tracks × as a function of $\sqrt{t}$. The straight line is the line $g=\gamma_0\sqrt{t}$ for $\gamma_0=1{\cdot}46$.

TABLE III. Cosmic-ray Events.

Event	Track length t cm.	Scattering angle°/cm. $\bar{\theta}_3/\sqrt{t}$	$\phi°$ Total deviation	Energy MeV.	Grain density grains/100 μ	Nature of particle	β	γ	Sign	Probability %	
1. Track linking double star	2	1·0	2·28	185±17	57±3	Proton	0·6	2·0	+	95	
2. Track giving rise to knock-on electron	1·3	0·75	1·32	255±85	61±3	Proton	0·6	2·2	+	93	
3. Track leaving star	1·5	1·34	4·36	140±10	70±4*	Proton	0·5	4·4	+	95	* These tracks are from a different plate with a different grain-density—ionization curve.
4. Primary of star ..	1·5	1·1	0·75	170±17	60±2	Proton	0·5	0·84	+	69	
5. π-μ-e decay electron	0·23	11	6·5	27±3	—	Electron	~ 1	2·5	+	62	
6. γ-ray pair .. (a)	0·7	4·25	4·38	70±7	36±2	Electron	~ 1	1·48	−	86	
(b)	0·9	1·49	2·76	220±18	36±2	Electron	~ 1	2·06	+	95	
7. γ-ray pair .. (a)	1·1	1·48	4·67	220±17	—	Electron	~ 1	2·77	−	96	
(b)	0·9	10·03	1·73	29±3	—	Electron	~ 1	1·86	+	58	
8. γ-ray pair .. (a)	0·6	5·9	1·85	50±7	36±2	Electron	~ 1	0·52	−	79	
(b)	0·5	4·0	5·32	75±10	36±2	Electron	~ 1	2·68	+	92	
9. γ-ray pair .. (a)	0·94	10·6	21·7	28±3	—	Electron	~ 1	2·18	−	99	
(b)	0·4	15·3	3·9	18±2	—	Electron	~ 1	0·64	+	62	
10. Giraffe primary (a)	1·0	0·11	0·07	3, 400±500†	—	?		0·84	+	83	† These tracks are of an unknown nature. The calculations have been done assuming they are electrons. If they are protons the probabilities are somewhat lower since then $\beta < 1$.
Secondaries (b)	1·5	0·21	0·133	1, 700±250†	—	?		0·52	+	78	
(c)	1·6	0·54	2·07	600±120	—	Electron	~ 1	1·24	−	96	
(d)	1·5	0·14	0·56	230±30	—	Electron	~ 1	0·86	+	70	
11. Proton–proton (a)	0·5	1·2	0·44	150±15	60±3*	Proton	0·5	1·46	+	59	
collision.... (b)	0·9	2·2	1·00	90±9	90±4	Proton	0·42	1·20	+	67	
(c)	0·9	4·5	2·46	40±4	120±4	Proton	0·31	2·03	+	61	
12. Meson approaching end	2·1	10·9	13·7	20±2	Increasing	Meson	0·5	1·15	−	88	
13. Track leaving star	1·2	3·4	3·76	50±5	48±3	Meson	0·7	1·61	−	81	
14. Track leaving star	0·6	3·3	2·23	50±8	42±2	Meson	0·7	1·61	+	73	
15. Track leaving star	0·76	0·5	0·2	400±20	47±2	Proton	0·7	0·75	+	70	
16. Primary of star ..	0·55	0·41	0·1	500±100	33±2	Meson	~ 1	0·44	−	62	
17. Primary of star ..	1·2	0·77	3·12	300±25	65±3	Proton	0·7	5·8	+	97	

(2) *The Determination of the Sign of some Particles in Cosmic Ray Events.*

In the plates exposed at high altitude measurements have been made on several tracks of which in some cases the sign and the direction of motion can be deduced from the nature of the event. In others, such as electron pairs, conservation of charge must be maintained. These two groups can eventually be used as a verification of the efficiency of the method when sufficient statistics are available. When either or both the sign and the direction of motion of the particle are unknown a priori, the measurement of the sense of the deflection can be used in the analysis of the event.

Fig. 12

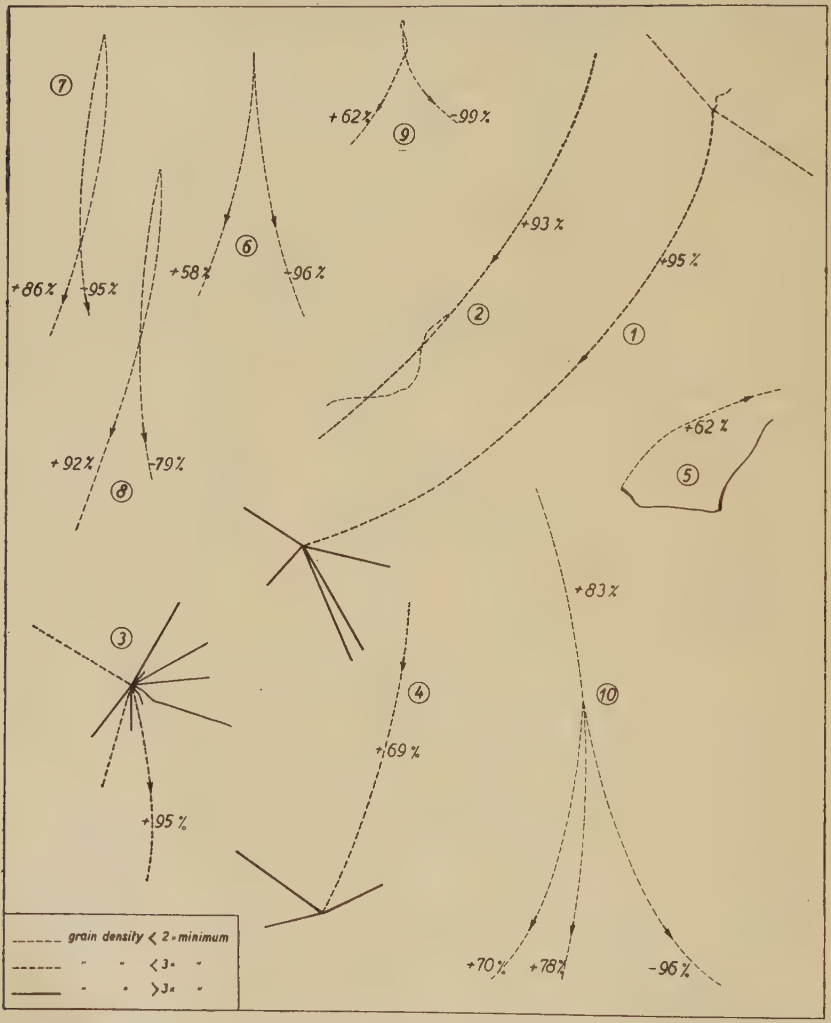

Diagramatic representation of the results presented in detail in Table III.

These tracks are listed in Table III. and sketched diagrammatically in figs. 12 and 13.

Track 1, identified as a proton, links two stars, one of which is evidently of higher energy and is therefore assumed to be the primary. This gives the direction of motion of the particle. Its sign is found to be positive with a probability of 95 per cent. This event is shown in the mosaic of Pl. XXXIV.

Fig. 13

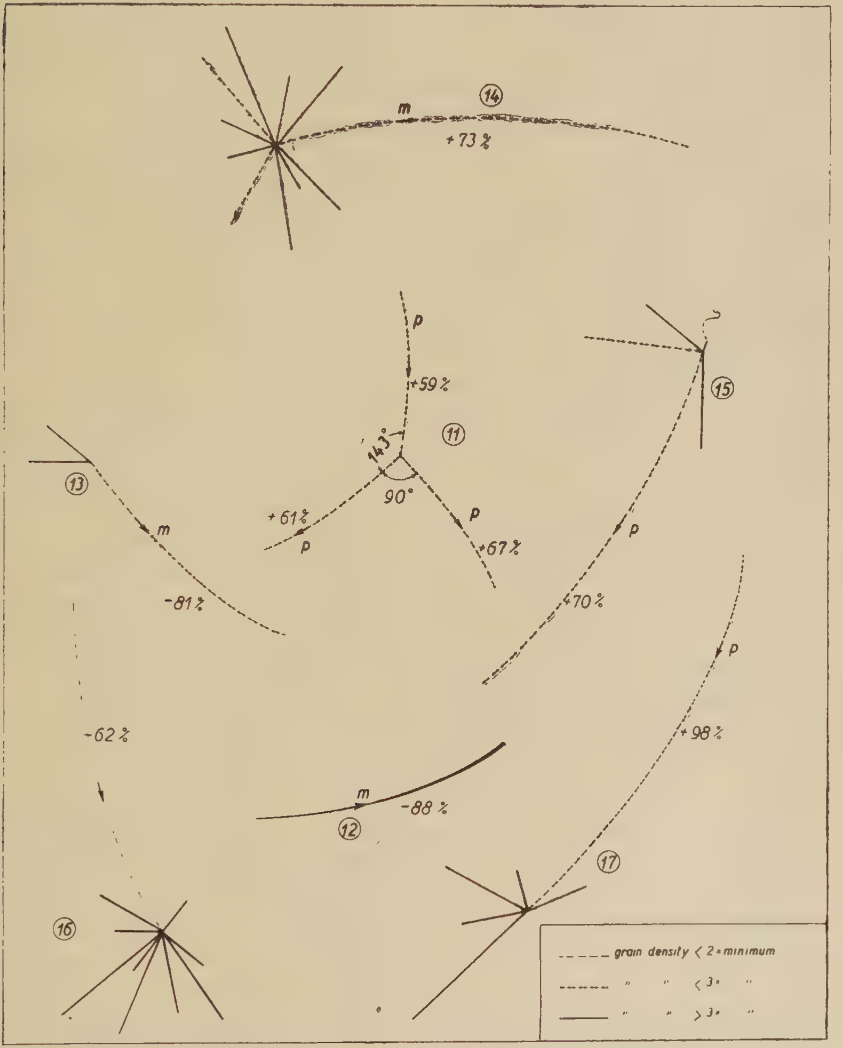

Diagramatic representation of the results presented in detail in Table III.

Track 2, also a proton, gives rise to a knock-on electron, from which we can deduce the direction of motion. There is a probability of 93 per cent that the sign of this proton should be positive.

A branch of a star, track 3, is identified as a proton, its orientation and energy indicate that it comes from the star. It is found to be positive with a probability of 95 per cent.

Another proton, track 4, is the only high energy branch of a 4-branch star and the only one near the vertical. If it is the primary of the star it is positive, with a probability of 69 per cent.

Event 5 is the electron of a π–μ–e decay, it is found to be positive with a probability of 62 per cent. It was found in a corner of the plate, where the field was only 25,000 gauss.

Next there is a group of γ-ray pairs, of which the particles have energies ranging from 29 to 220 MeV. In each case one track of the pair is found to be positive, and the other negative, as should be expected.

Event 10 is a " giraffe " (G. Occhialini 1949). Since this is the direct production of a positron–electron pair by a charged primary, we expect to find the charge of the primary conserved among the three secondary particles. In fact, we find the primary to be positive with 83 per cent probability ; the secondaries to be two positive, one with 78 per cent probability, the other with 70 per cent probability ; and the third negative with 96 per cent probability. There is also a rough energy balance, within the errors of measurement.

Event 11 seems to be a proton–proton collision at high energy. If this is so, the track coming from the vertical, a proton of 150 MeV. energy, is positive with a probability of 59 per cent ; the continuation and recoil tracks are positive, one with 67 per cent and the other with 61 per cent probability. The angle of collision is 90°, the energy of the primary is divided between the two secondary tracks in a ratio in agreement with the angles of deflection.

Track 12 is of a meson which, by the increase of its grain density and scattering, can be seen to be approaching the end of its range. Its average energy is 20 MeV., its sign negative with a probability of 88 per cent.

The orientation of track no. 13, a meson by its grain density and scattering, is such as to make it likely that it comes out of the star ; if this is so it is negative, the probability of the deflection being 81 per cent.

Track 14, also a meson, is moving nearly horizontally, but its energy is so low that it seems unlikely to be the primary of so large a star. Taking it to be a secondary, it is positive with 73 per cent probability.

In event 15 it is difficult to tell whether the track is a primary or secondary from either its orientation or energy. Since, however, it can be identified as a proton, and the deflection is such as to make it 70 per cent positive if it leaves the star, we accept it as a secondary.

Track 16 seems, by orientation and energy, to be the primary of a star of 10 low energy branches ; it is a meson and has 62 per cent probability of being negative.

Event 17 is a star of many low energy branches, with one higher energy track coming from the vertical. Its energy and grain density indicate that it is a proton. It is positive with a probability of 98 per cent.

The average value of γ deduced from these measurements is $1{\cdot}56 \pm {\cdot}33$.

§VI. DISCUSSION.

The results obtained seem to show that the use of a magnetic field to deflect tracks in the photographic plate can already contribute substantially to the information available about the cosmic ray events recorded. We discuss here the improvements which might be made to the technique in order to exploit to the full its possibilities.

Favourable conditions for the determination of the sign and momentum are a large value of the product $\gamma_0\beta\sqrt{t}$ and a low level of distortion in the emulsion. γ_0 can be increased by reducing the scattering constant of the emulsion. Already, as announced by Dr. Berriman of Kodak Ltd., and by Mr. Dodd and Mr. Waller of Ilford Ltd., at the Bristol Photographic Conference (May 1950), it has been possible to produce diluted emulsions containing a smaller proportion of silver bromide. An increase of 16 per cent in the theoretical value of γ_0 is obtained without loss of sensitivity.

While such plates present new problems in processing, the advantage of increasing γ_0 in this way is such as to warrant efforts to overcome the difficulties and to find emulsions with still smaller proportions of heavy elements.

The constant γ_0 may also be increased by increasing the field H, the mean track length by increasing the emulsion thickness, d. It can be shown that the number of tracks per unit area of plate for which $\gamma_0\sqrt{t}$ has a certain minimum value is proportional to H^2 and to d^2. In this sense, therefore, an increase in the thickness is as valuable as an increase in field. Moreover, while it is often of interest to examine single measurable tracks which emerge from a star, it is generally desirable to measure several tracks from the same event. If the directions of the tracks are independent, it can be shown that the number of events per unit area from which n tracks are all measurable is proportional to H^{2n} and to d^{n+1}.

For these reasons, throughout the experiments we have advanced cautiously towards thicker emulsions, and we are now scanning a batch of plates 1200 microns in thickness which show very little distortion. The table includes events taken from one of these plates. Further advances towards thicker emulsions are still possible.

The main difficulty in increasing the field is the high cost. Fields of 100,000 gauss or more are, in principle, quite possible, and the design of such a magnet is being investigated. Thick emulsions are more economical since they reduce the proportion of the field volume which is occupied by glass.

At the very highest momenta even the little information available about momentum from the magnetic deflection may be of value. The relative error of the momentum estimate by the magnetic deflection remains independent of momentum until the distortion becomes important. The distortion over a 1 cm. track in a 600μ plate has been shown in many cases to be as low as 1′, and a correction may be applied even for this. We regard the upper limit of detectable momentum with this length of track as fixed by this angle, corresponding, in a field of 34,000 gauss, to a momentum of $3{\cdot}5\times10^{10}$ eV./*c*. This maximum is roughly proportional to track length and to the field. It is conceivable that measurements in the region above $10''$ eV./*c* may be possible if fields of the order of 100,000 gauss or more become available.

Fields of this magnitude will also make possible a determination of the mass of particles of velocity appreciably less than that of light, by comparison between scattering and magnetic deflection, which yields a value of β. Determination of mass by this method has recently been described for very low energy light particles in the cloud chamber (Groetzinger *et al.* 1950).

ACKNOWLEDGMENTS.

This paper describes part of the work being carried out in collaboration between the Photographic Emulsion groups of the Brussels Centre de Physique Nucléaire and the Manchester University Department of Physics on the magnetic deflection of cosmic-ray particles in the photographic emulsion. We wish to thank Professor P. M. S. Blackett for his constant interest in the work, and for the use of the magnet at the Pic-du-Midi. We are deeply indebted to Professors M. G. E. Cosyns and G. P. S. Occhialini and to Dr. G. D. Rochester for continual help and guidance during the work. Mr. J. E. Moyal has at all times been most helpful in discussion of theoretical problems. We wish to thank him also for communicating to us many of his results before publication. We wish to express our gratitude to our colleagues, Dr. G. Cortini, Dr. N. Page and Mr. G. Vanderhaeghe for their valuable assistance in the processing of the plates and in part of the measurements.

We wish to thank Professor Mailvaganam of the University of Colombo, for the use of their magnet and the research staff of Metropolitan Vickers Ltd., for operating the magnet during the exposure of the Kodak plates; we are especially grateful to Mr. P. P. Sterling and Mr. A. M. Armour. Mr. J. A. Newth kindly helped us in the design of the pole pieces. Dr. J. G. Wilson also gave us helpful advice in the early stages of the work.

The photographic plates were supplied by Dr. Berriman, of Messrs. Kodak Ltd., and Mr. Waller, of Messrs. Ilford Ltd., to whom we express our thanks. The problems connected with the adhesion and elimination of stress in the production of large plates of great thickness were not easy to overcome. We wish to express our gratitude to Mr. Waller and the staff of Ilford Ltd., who made possible this extension of the technique.

Through the friendly cooperation of Professor J. Svedberg and his staff a parallel sea-level exposure was made on the big magnet at the University of Upsala. The plates from this exposure were, unfortunately, subsequently found to have severe distortion and were therefore not used.

The exposures with the Ilford plates were made on the Blackett electromagnet at the Pic du Midi, France. We are deeply indebted to Dr. Rösch and his staff at the Pic du Midi for their help in the transport

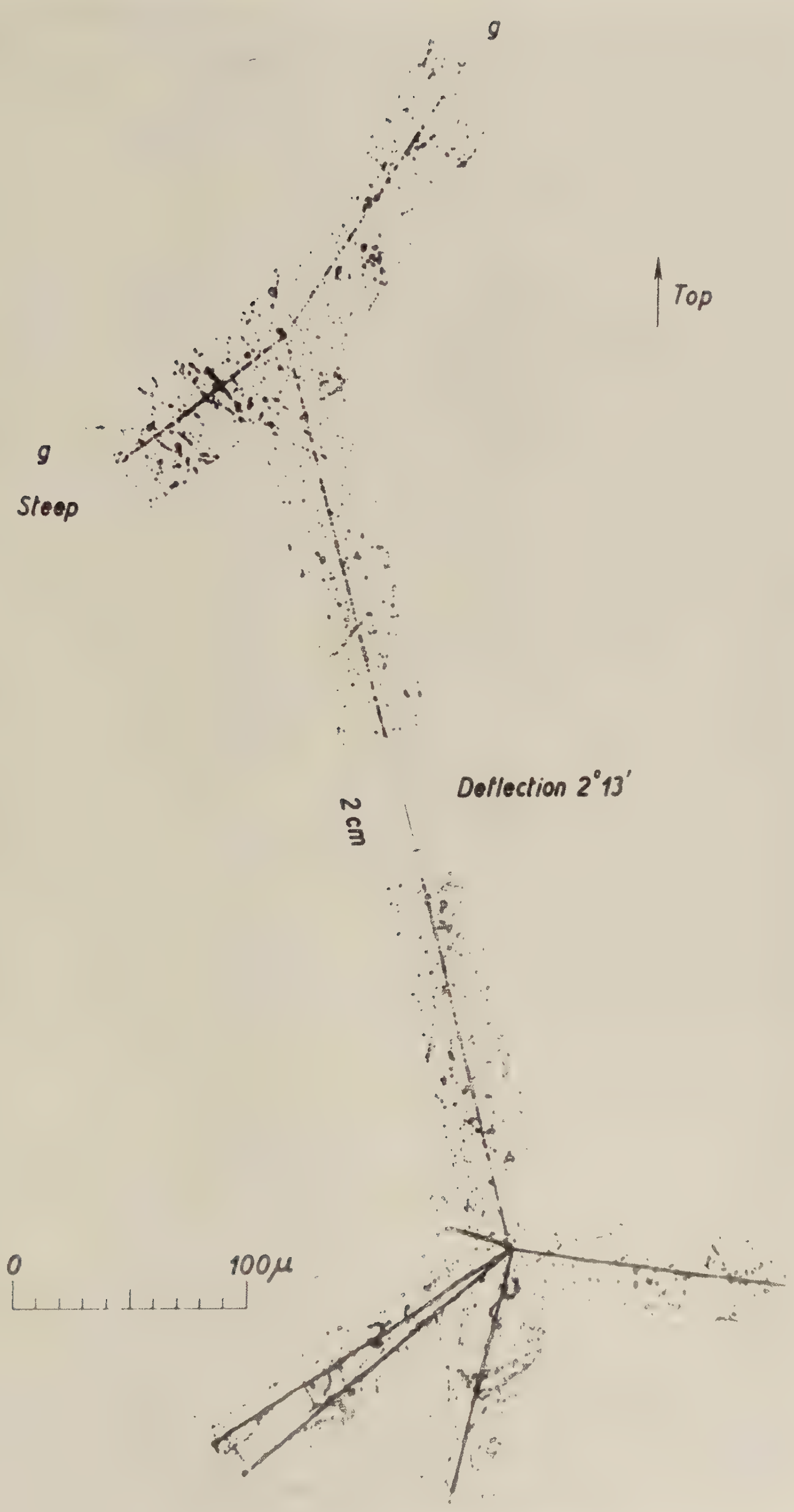

Mosaic of event 1 of Table III. The track linking the two stars is shown to be positive with a probability 95 per cent. the particle being a proton. The direction of motion of the particle is determined from considerations of the

and erection of the magnet and for their unfailing kindness and courtesy. We wish also to express our thanks to Dr. Butler and to Mr. K. H. Barker and the late Mr. C. O. Green for the transportation and erection of the magnet at the Pic du Midi.

REFERENCES.

BLACKETT, 1936, *Proc. Roy. Soc.*, Ser. A, **154,** 564.
BRADDICK, 1950, *J. Sci. I.* To be published.
CAMERINI, COOR, DAVIES, FOWLER, LOCK, MUIRHEAD and TOBIN, 1949, *Phil. Mag.*, **40,** 1073.
COSYNS and VADERHAEGHE, 1950, Note No. 15, *Bull. Cen. de Phys. Nuc., de l'Université Libre de Bruxelles ;* Bristol Congress on the Photographic process.
COSYNS, 1949, Paper read at Como Congress.
DILWORTH, OCCHIALINI and PAYNE, 1948, *Nature,* **162,** 102.
DILWORTH, OCCHIALINI and VERMAESEN, 1950, Note no. 13, *Bull. du Cen. de Phys. Nuc. de l'Université Libre de Bruxelles.*
FOWLER, 1950, *Phil Mag.*, **41,** 169.
GOLDSCHMIDT-CLERMONT, KING, MUIRHEAD and RITSON, 1948, *Proc. Phys. Soc.*, **61,** 183.
GOLDSCHMIDT-CLERMONT, 1950, Note No. 14, *Bull. du Cen. de Phys. Nuc. de l'Université Libre de Bruxelles ;* Nuovo Cimento, **7,** 331.
GROETZINGER, BERGER and LIBE, *Phys. Rev.*, **77,** 584.
MOYAL, 1950, *Phil. Mag.*, **41,** 1058.
OCCHIALINI, 1949, Paper read at Como Congress.
SCOTT, 1949, *Phys. Rev.*, **76,** 213.

XCV. *The Momentum and Sign of Fast Cosmic Ray Particles.*

By J. E. Moyal,
Department of Mathematics, The University, Manchester *.

Summary.

In order to study the statistical estimation of momentum and sign of fast cosmic ray particles from their magnetically deflected and multiply scattered tracks in the photographic emulsion, the probability distribution of the observed angular deviations along the track is derived, taking into account errors of observations. With the help of this distribution, approximate expressions are obtained for the maximum likelihood estimates of the magnetic deviation and the mean-square scattering deviation. The standard errors of these estimates are found, and their efficiency is discussed.

After showing how the observations of magnetic and scattering deviations in a large number of tracks can be combined to verify theoretical mean-square scattering formulæ, the estimation of the momentum p of particles from these deviations is discussed. An expression is derived for the value of the optimum cell-length, at which the error of the scattering determination of p is minimized. The relative errors of the magnetic and scattering determinations of p are compared at this optimum cell-length : it is found that there is a critical value of p, depending on the field, below which the scattering determination is more accurate.

An expression is given for the probability that, given the signed total deviation of a track in the magnetic field, the particle should be positively or negatively charged. A method is given of estimating the ratio of positively to negatively charged particles in terms of the observed signed deviations in a number of tracks.

§1. Introduction.

Fast charged particles passing through the emulsion of photographic plates suffer multiple scattering due to elastic collisions with the nuclei in the emulsion. If a uniform magnetic field is applied normal to the plate, a constant angular deviation per unit track length is superimposed on this random scattering. Estimates of the momentum of a particle may be obtained either from the mean-square angle of scattering (*cf.* Goldschmidt-Clermont *et al.* 1948), or from the mean curvature due to magnetic forces ; estimates of its *sign*, however, are only possible from the magnetic deviation, provided, of course, we know the direction of travel of the particle when it enters the field.

As the expected mean values of magnetic deviation due to fields of 20,000 to 250,000 gauss is of the same order of magnitude as the scattering angle and the spurious apparent deviations due to finite grain size in the emulsion, errors of observation, etc., the statistical problem of estimation from photographic plate data becomes important. The purpose of the present paper is to develop the theory of multiple scattering with a superimposed magnetic deviation in a form suitable for the study of estimates of the signs and momenta of particles from data contained in their tracks, and to evaluate the relative merits of such estimates and the errors affecting them.

---

* Communicated by Professor P. M. S. Blackett, F.R.S.

§ 2. MOTION OF MULTIPLY SCATTERED PARTICLES IN A UNIFORM MAGNETIC FIELD.

In this section the theory of multiple scattering is expressed in a form convenient for the solution of statistical estimation problems. We shall be concerned with the "true" motion only: the effects of errors of observation will be considered in the next section. We limit ourselves to particles fast enough for the loss of energy to be negligible in any given track, so that the velocity $\boldsymbol{\beta}$ has very approximately a constant magnitude β; the letter t will therefore be used to denote both time divided by β and distance along the track. We shall use the units common in cosmic ray work: velocity will be measured in multiples of the velocity of light c, charge in multiples of the electron charge, energy in electron-volts, momentum in eV./c., length in cm.; magnetic fields, however, will be in gauss (a unit consistent with the previous ones would be V/cm.c.).

The quantum mechanical treatment of scattering by nuclei of relativistic charged particles, such that nuclear interactions and the recoil of nuclei can be neglected, gives the following results (Williams 1939; *cf.* also Molière 1947):

(1) The cross-section for single scattering is very approximately the Coulomb cross-section modified to account for screening and finite size of the nucleus. Roughly speaking, the effect of screening is to introduce a lower limit to the scattering angle, while the finite size of the nucleus introduces an upper limit.

(2) Successive collisions may be treated as independent events; in a dense scatterer, the distribution of the total angle through which a particle scatters in an interval δt long enough for a large number N of collisions to occur is, therefore, the resultant of the composition of N independent modified Coulomb scattering distributions. The mean-square of the angular deviation $\delta\phi$ projected on a plane is then shown to be proportional to δt:

$$\overline{\delta\phi^2}=s^2\delta t=\left(\frac{\nu}{p}\right)^2\delta t \quad . \quad . \quad . \quad . \quad . \quad . \quad . \quad . \quad (1)$$

(the bar over a symbol denotes its expectation value); the mean-square deviation per unit track s^2 is shown to be inversely proportional to the square of the momentum p, the coefficient ν *depending only on the properties of the scatterer.* For either Ilford G5 or Kodak NT4 electron sensitive plates the calculation of ν on the basis of Williams' approximate formulæ gives $\nu=8{\cdot}48\times10^6$ (with $\delta\phi$ in radians). As δt increases, the distribution of $\delta\phi$ tends rapidly to the Gaussian in its central part, but maintains a longer "tail" to begin with, due to an appreciable probability of occasional close collisions with large scattering (*cf.* Williams, *loc. cit.*; see also Goudsmit and Saunderson (1940), Molière (1948), Snyder and Scott (1949), and Lewis (1950) for a more complete treatment; the application to photographic plates is considered by Goldschmidt-Clermont (1950). In particular, for the order of intervals and range of momenta of interest in this paper, one may assume (as we shall do henceforth) a Gaussian distribution for $\delta\phi$, provided one excludes these occasional large-angle single scatterings from the observations, *e. g.* by "cutting" the observed distribution at its mean ± 3 times its standard deviation*.

What we shall require for later work is the joint distribution of angular deviations and coordinates of particles for tracks selected to lie approximately in a plane (the emulsion plane). This may be obtained by solving the appropriate "diffusion" equation which this distribution function obeys (*cf.* Fermi, as quoted by Rossi and Greisen (1941)); it is convenient, however, when dealing with the estimation problem, to treat directly the equations of motion for the angles and coordinates themselves †. Let then θ, ϕ be the polar angles defining the direction of the particle velocity $\boldsymbol{\beta}$, with the emulsion in the equatorial or (x, y) plane. The relativistic equations of motion for a multiply scattered particle in the presence of a uniform magnetic field H normal to the emulsion plane lead to the following expressions for the increments $\delta\theta$, $\delta\phi$ of the polar angles in a small interval δt:

$$\delta\theta=\delta\Theta; \quad \sin\theta\,\delta\phi=\omega\sin\theta+\delta\Phi, \qquad (2)$$

where

$$\omega=\frac{300\,eH}{p} \qquad (3)$$

is the magnetic deviation per unit track (e being the charge, p the momentum of the particle), and $\delta\Theta$, $\delta\Phi$ are the projections of the scattering angular deviations in δt on two orthogonal planes containing $\boldsymbol{\beta}$, the first containing the z-axis as well. Owing to the symmetry of the scattering distribution about the velocity at the beginning of the interval, $\delta\Theta$ and $\delta\Phi$ must be independent with zero means and equal mean squares, so that

$$\overline{\delta\Theta^2}=\overline{\delta\Phi^2}=s^2\delta t. \qquad (4)$$

The formal integration of (2) from time 0 to t gives

$$\phi(t)=\phi_0+\omega t+\int_0^t\frac{d\Phi(\tau)}{\sin\theta(\tau)},$$

---

* See Dilworth *et. al.* (1950) for further discussion of effect of cut-off.

† These correspond to the Langevin equations for the Brownian motion, while the diffusion equation corresponds to the Fokker-Planck equation (see, *e. g.* Moyal 1949).

where ϕ_0 is the azimuth at $t=0$. Since we are selecting tracks lying approximately in the (x, y) plane, $\theta=\left(\frac{\pi}{2}\pm\epsilon\right)$, where $\epsilon<5^0$ say. Neglecting, then, terms of order ϵ^2, we have

$$\phi(t)=\phi_0+\omega t+\int_0^t d\Phi(\tau)=\phi_0+\omega t+\Phi(t). \quad . \quad . \quad . \quad . \quad (5)$$

The velocity components along the x- and y-axes respectively are

$$\left.\begin{aligned}\beta_x(t)/\beta&=\cos\phi=\cos(\phi_0+\omega t+\Phi)\simeq\cos\phi_0-(\omega t+\Phi)\sin\phi_0,\\ \beta_y(t)/\beta&=\sin\phi=\sin(\phi_0+\omega t+\Phi)\simeq\sin\phi_0+(\omega t+\Phi)\cos\phi_0,\end{aligned}\right\} \quad . \quad (6)$$

where the last approximate expressions in the right-hand sides of equations (6) are valid as long as both magnetic and scattering deviations remain small (both $s\sqrt{t}$ and $\omega t<5^0$ say). Integrating, we obtain for the coordinates of the particle

$$\left.\begin{aligned}x(t)&=x_0+t\cos\phi_0-\tfrac{1}{2}\omega t^2\sin\phi_0-\sin\phi_0\int_0^t(t-\tau)d\Phi(\tau),\\ y(t)&=y_0+t\sin\phi_0+\tfrac{1}{2}\omega t^2\cos\phi_0+\cos\phi_0\int_0^t(t-\tau)d\Phi(\tau),\end{aligned}\right\} \quad . \quad (7)$$

where x_0, y_0 are the coordinates at $t=0$.

Equations (5) and (7) are valid in the small angle approximation, whatever the distribution of $\delta\Phi$. If the latter is Gaussian, then it can be shown (see *e. g.* Moyal 1949) that the joint distribution of ϕ, x and y will be of the *multivariate Gaussian* type, whose general expression for n variables $z_1, \ldots, z_n$ (which we shall require again later) may be written succinctly as follows (*cf.* Kendall 1946 or Cramèr 1946): let the vector $\mathbf{z}$ stand for the n variables, $\mathbf{m}$ for their means, $\mathbf{\Lambda}$ for their *covariance matrix*, whose elements are

$$\lambda_{ij}=\overline{(z_i-m_i)(z_j-m_j)},$$

$\mathbf{\Lambda}^{-1}$ for the inverse of $\mathbf{\Lambda}$ and Λ_n for its determinant; the probability that $\mathbf{z}$ should lie in the n-dimensional volume element $dz_1 \ldots dz_n$ is then

$$\mathrm{P}(\mathbf{z})dz_1\ldots dz_n=(2\pi)^{-\frac{1}{2}n}\Lambda_n^{-\frac{1}{2}}\exp\{-\tfrac{1}{2}(\mathbf{z}'-\mathbf{m}')\mathbf{\Lambda}^{-1}(\mathbf{z}-\mathbf{m})\}dz_1\ldots dz_n. \quad (8)$$

$\mathrm{P}(\mathbf{z})$ is completely determined by the means and covariances of the variables. In the present case the means are obviously (since $\overline{\delta\Phi}=0$)

$$\left.\begin{aligned}m_\varphi&=\overline{\phi}=\omega t,\\ m_x&=\overline{x}=x_0+t\cos\phi_0-\tfrac{1}{2}\omega t^2\sin\phi_0,\\ m_y&=\overline{y}=y_0+t\sin\phi_0+\tfrac{1}{2}\omega t^2\cos\phi_0.\end{aligned}\right\} \quad . \quad . \quad . \quad (9)$$

The calculation of the variances and covariances is simplified by the fact that the scattering deviations over non-overlapping intervals are independent, so that formally

$$\overline{d\Phi(\tau)d\Phi(\tau')}=s^2\delta(\tau-\tau')d\tau d\tau',$$

where $\delta(\tau)$ is Dirac's delta-function. Hence, *e. g.*

$$\int_0^t\int_0^t (t-\tau)(t-\tau')\overline{d\Phi(\tau)d\Phi(\tau')}=s^2\int_0^t (t-\tau)^2 d\tau=\tfrac{1}{3}s^2t^3,$$

and similarly for other terms involving the expectation values of products of such integrals. Finally, we find

$$\left.\begin{aligned}
\lambda_{\varphi\varphi}&=\overline{\phi'^2}=s^2t,\\
\lambda_{xx}&=\overline{x'^2}=\tfrac{1}{3}s^2t^3\sin^2\phi_0,\\
\lambda_{yy}&=\overline{y'^2}=\tfrac{1}{3}s^2t^3\cos^2\phi_0,\\
\lambda_{\varphi x}&=\overline{\phi'x'}=\tfrac{1}{2}s^2t^2\sin\phi_0,\\
\lambda_{\varphi y}&=\overline{\phi'y'}=\tfrac{1}{2}s^2t^2\cos\phi_0,\\
\lambda_{xy}&=\overline{x'y'}=\tfrac{1}{3}s^2t^3\sin\phi_0\cos\phi_0,
\end{aligned}\right\}\quad . \; . \; . \; . \; . \quad (10)$$

where we have written $\phi'=\phi-\bar{\phi}$, etc. With the origin of coordinates at x_0, y_0, and the x-axis along the initial direction of the particle ($\phi_0=0$) so that in the small angle approximation $\lambda_{xx}=0$ and $x=t$, the distribution reduces to that of ϕ and y only :

$$\mathrm{P}(\phi, y, t)$$
$$=\frac{\sqrt{3}}{\pi s^2t^2}\exp\left\{-\frac{2}{s^2t^3}\left[t^2(\phi-\omega t)^2-3t(\phi-\omega t)(y-\tfrac{1}{2}\omega t^2)+3(y-\tfrac{1}{2}\omega t^2)^2\right]\right\}.$$
$$. \; . \; . \quad (11)$$

Fermi's solution of the diffusion equation (Rossi and Greisen, *loc. cit.*) is obtained from (11) by making $\omega=0$.

§ 3. THE DISTRIBUTION OF OBSERVED ANGULAR DEVIATIONS.

The fundamental quantities that we have to estimate from the data in the tracks are : (*a*) the magnetic deflection, and (*b*) the mean-square scattering deviation, *i.e.* in the notation of § 2, the parameters ω and s^2. Two experimental methods have been used for this purpose : in the first, which we may call the *angular difference method* (Goldschmidt-Clermont *et. al.* 1948), the eyepiece goniometer of a microscope is rotated until a straight line graticule is in line with the track, and its angle with a fixed reference line is noted. The operation is repeated along the whole length of the track, advancing each time the plate (which is mounted on a stage movement with micrometer adjustment) by a fixed distance, called the *cell-length*. The estimations are made from the angular differences between successive cells. In the second method, which may be called the *coordinate method* (Fowler 1950), the track is aligned approximately parallel to one of the directions of motion of the stage, say the x-axis and the y-coordinate at which the track intersects a graticule in the eyepiece is determined by means of an eyepiece scale. These measurements are repeated at every cell-length along the whole track, as in the first method. Clearly, this method could be extended to measure the coordinates of every blackened grain : this would yield all the information contained in the track. Cell-lengths would then cease to be constant, but would be equal to the distances between successive grains : apart from this last added complication, the estimation problem would remain unchanged. Methods based on the same principles may, of course, be used in conjunction with a projection microscope.

The first step in formulating the problem of statistical estimation is to derive the probability distribution of the actual observation, taking into account not only scattering, but also errors of various kinds. This requires a closer analysis of the actual methods of observation : we consider first the angular difference method. When aligning the eyepiece graticule along the track, the observer has to use his judgment to determine the best straight line through the grains in each cell (for a particle at minimum ionization, the grain density is of the order of 33 in a 100-micron cell). The line taken may be expected to lie somewhere between the tangent at midpoint and the chord in each cell (smoothing effect). There will, of course, be a random error due (*a*) to observer and instrumental error, and (*b*) to finite grain size and to the asymmetry of grain distribution along the trajectory : the centres of developed grains may be slightly displaced from the actual trajectory. In addition, there is the possibility of systematic errors due to distortion of the emulsion. Special precautions are taken to eliminate this last effect : we shall therefore ignore it in our analysis. Here we shall assume that at each measurement the observer aligns the graticule along a line which divides the angle between chord and tangent in a fixed ratio q, with a total random error ϵ, due to various causes enumerated above. (We shall call ϵ the *spurious deviation* and q the *smoothing factor*.) We also assume that ϵ has a Gaussian distribution, with zero mean and the same standard deviation s_0 in every cell. These assumptions seem to be well-founded on the basis of the careful study of sources of error made by Goldschmidt-Clermont *et. al* (1948 and 1950).

We proceed now to derive the required probability distribution of the observed angular deviations. In a track of total length t, let h be the length of each cell, $n+1$ the number of cells, so that $(n+1)h=t$: we shall assume throughout in what follows that n is large, *e. g.* >25. We take the track to be initially aligned along the x-axis, and define all angles relative to this axis. Let then ψ_r be the *observed* angle so defined of the rth cell, ϕ_r the angle of the tangent to the *true* trajectory at the midpoint of this cell, α_r the angle of the corresponding chord :

$$\alpha_r \simeq (y_{r+1}-y_r)/h,$$

where y_r, y_{r+1} are the end coordinates of the cell ; ϵ_r is the error of observation in the setting of ψ_r. According to the foregoing assumptions

$$\left.\begin{aligned}\psi_r&=\alpha_r+q(\phi_r-\alpha_r)+\epsilon_r,\\ \delta\psi_r&=\psi_{r+1}-\psi_r=q\delta\phi_r+(1-q)\delta\alpha_r+\epsilon_{r+1}-\epsilon_r.\end{aligned}\right\} \quad . \quad . \quad . \quad (1)$$

Each angular deviation $\delta\psi_r$ is thus a sum of Gaussian variables, and is therefore itself Gaussian. Hence the joint distribution of the observations (known as the *likelihood function*) will be the Gaussian multivariate distribution, as defined by equation (8) of § 2, the vector $\mathbf{z}$ standing now for the n deviations $\delta\psi_1, \ldots, \delta\psi_n$; all we have to do in order to find the explicit expression of this distribution in terms of the parameters we wish to estimate, *i. e.* of ω, s and s_0, is to express the means, variances, and covariances of the deviations in these terms. This is easily achieved by the methods of § 2, with the following results: the means are

$$m_r = \overline{\delta\psi_r} = \omega h, \quad (r=1, 2, \ldots, n); \quad . \quad . \quad . \quad . \quad . \quad (2)$$

the covariances are (writing $\delta\psi'_r = \delta\psi_r - \overline{\delta\psi_r}$)

$$\left.\begin{aligned} \lambda_{r,r} &= \overline{\delta\psi_r'^2} &&= \tfrac{2}{3}(1-\tfrac{1}{2}q+q^2)s^2h+2s_0^2, \\ \lambda_{r,r+1} &= \overline{\delta\psi_r'^2\delta\psi'_{r+1}} &&= \tfrac{1}{6}(1+q-2q^2)s^2h-s_0^2, \\ \lambda_{r,r+k} &= \overline{\delta\psi'_r\delta\psi'_{r+k}} &&= 0, \quad (k>1;\ r=1, 2, \ldots, n). \end{aligned}\right\} \quad . \quad . \quad (3)$$

Note that the sum

$$\lambda_{r,r} + 2\lambda_{r,r+1} = s^2h \quad . \quad . \quad . \quad . \quad . \quad . \quad . \quad . \quad . \quad . \quad (4)$$

is independent of the " smoothing factor " q. If $q=1$, then

$$\lambda_{r,r} = s^2h+2s_0^2 \quad \text{and} \quad \lambda_{r,r+1} = -s_0^2, \quad (r=1, 2, \ldots, n). \quad . \quad . \quad . \quad (5)$$

In the coordinate method we may expect the random error affecting each coordinate measurement to arise, as in the angular difference method, (*a*) from observer and instrumental errors, and (*b*) from finite grain size and asymmetry of grain distribution about the track; there will, however, be no equivalent to the " smoothing effect". It is reasonable, therefore, to regard the rth measured coordinate as the sum of the " true " coordinate y_r and of a total random error ϵ_r, and to assume that the ϵ_r all have the same Gaussian distribution with zero mean and standard deviation s_0. Since this method can be applied to the measurement of coordinates of every developed grain, we shall develop the theory *ab initio* for unequal cell-lengths.

Let h_r be the rth cell-length and $n+1$ the number of cells in a track of total length t, so that $\sum\limits_1^{n+1} h_r = t$. It is convenient to form the estimates in terms of second-differences of the *observed* coordinates, corresponding to the angular differences of the previous method: we write, therefore,

$$\delta\psi_r = \frac{y_{r+2}-y_{r+1}}{h_{r+1}} - \frac{y_{r+1}-y_r}{h_r} + \frac{\epsilon_{r+2}-\epsilon_{r+1}}{h_{r+1}} - \frac{\epsilon_{r+1}-\epsilon_r}{h_r}. \quad . \quad . \quad (6)$$

Once again these deviations are sums of Gaussian variables, and, therefore, Gaussian themselves : their joint distribution is hence again of the form (8), *cf.* § 2. Calculation of the means, variances and covariances gives the following results :

$$\left.\begin{aligned} m_r&=\overline{\delta\psi_r}=\tfrac{1}{2}\omega(h_{r+1}+h_r),\\ \lambda_{rr}&=\overline{\delta\psi_r'^2}=\tfrac{1}{3}s^2(h_{r+1}+h_r)+2s_0^2\left(\frac{1}{h_{r+1}^2}+\frac{1}{h_{r+1}h_r}+\frac{1}{h_r^2}\right),\\ \lambda_{r,r+1}&=\overline{\delta\psi_r'\delta\psi_{r+1}'}=\tfrac{1}{6}s^2h_{r+1}-s_0^2\left(\frac{1}{h_{r+2}h_{r+1}}+\frac{1}{h_{r+1}^2}+\frac{1}{h_{r+1}h_r}\right),\\ \lambda_{r,r+2}&=\overline{\delta\psi_r'\delta\psi_{r+2}'}=s_0^2\left(\frac{1}{h_{r+2}h_{r+1}}\right),\\ \lambda_{r,r+k}&=\overline{\delta\psi_r'\delta\psi_{r+k}'}=0, \qquad (k>2\ ;\ r=1, 2, \ldots, n). \end{aligned}\right\} \quad . \quad (7)$$

Note that in consequence

$$\lambda_{r,r}+\lambda_{r,r-1}+\lambda_{r,r+1}+\lambda_{r,r-2}+\lambda_{r,r+2}=\tfrac{1}{2}s^2(h_r+h_{r+1}). \quad . \quad . \quad (8)$$

§ 4. MAXIMUM LIKELIHOOD ESTIMATES OF THE PARAMETERS.

What we must do now is to establish suitable statistics giving s and ω in terms of the observed deviations ; it will be necessary, incidentally, to estimate s_0 as well. We use for this purpose the *maximum likelihood method* (*cf.* Kendall 1946, Cramer 1946), *i. e.* we maximize the probability of the whole set of observations, obtained in the last section, with respect to the parameters, ω, s and s_0 considered as unknowns. In this section we shall give a formal solution of the problem, which covers the angular difference and the coordinate methods.

Let $\mathbf{h}$ stand for the cell lengths $h_1, \ldots, h_n$; the means vector is then

$$\mathbf{m}=\omega\mathbf{h}.$$

The logarithm of the likelihood function is (*cf.* equation (8) of § 2)

$$\mathrm{L}=\log \mathrm{P}=-\frac{n}{2}\log 2\pi-\tfrac{1}{2}\log \mathit{\Lambda}_n-\tfrac{1}{2}(\mathbf{z}'-\omega\mathbf{h}')\,\mathbf{\Lambda}^{-1}(\mathbf{z}-\omega\mathbf{h}). \quad . \quad . \quad (1)$$

The covariance matrix $\mathbf{\Lambda}$ is a function of s and s_0 only (*cf.* equations (3) and (7) of § 3). It is convenient to express it in the form

$$\mathbf{\Lambda}(s, s_0)=\eta\mathbf{A}(\chi), \quad . \quad . \quad . \quad . \quad . \quad . \quad . \quad . \quad (2)$$

where η is a linear combination of s^2 and s_0^2, χ some function of s^2 and s_0^2, the elements of the matrix $\mathbf{A}$ are functions of χ only, and to maximize the likelihood function

$$\mathrm{L}=-\frac{n}{2}\log(2\pi\eta)-\tfrac{1}{2}\log \mathrm{A}_n-\frac{1}{2\eta}(\mathbf{z}'-\omega\mathbf{h}')\mathbf{A}^{-1}(\mathbf{z}-\omega\mathbf{h}) \quad . \quad . \quad (3)$$

(A_n being the determinant of $\mathbf{A}$) in terms of these new variables. Solving $\partial L/\partial\omega=0$, one obtains for the estimate $\hat{\omega}$ of the magnetic deviations per unit track

$$\omega=\frac{\mathbf{h}'\mathbf{A}^{-1}\mathbf{z}}{\mathbf{h}'\mathbf{A}^{-1}\mathbf{h}}. \qquad (4)$$

Similarly, the estimate $\hat{\eta}$ is obtained by solving $\partial L/\partial\eta=0$:

$$n\hat{\eta}=\boldsymbol{\xi}'\mathbf{A}^{-1}\boldsymbol{\xi}, \qquad (5)$$

where $\boldsymbol{\xi}=\mathbf{z}-\omega\mathbf{h}$. In order to estimate χ we write

$$\frac{\partial L}{\partial\chi}=-\frac{1}{2}\frac{\partial\log A_n}{\partial\chi}-\frac{1}{2\eta}\frac{\partial}{\partial\chi}(\boldsymbol{\xi}'\mathbf{A}^{-1}\boldsymbol{\xi})=0,$$

or, substituting for η from (5),

$$\frac{\partial}{\partial\chi}\{A_n^{1/n}\boldsymbol{\xi}'\mathbf{A}^{-1}\boldsymbol{\xi}\}=0. \qquad (6)$$

Substituting for ω from (4), (6) becomes a transcendental equation in χ only. The substitution of its solution $\hat{\chi}$ in (4) and (5) gives the estimates $\hat{\omega}$ and $\hat{\eta}$; finally s^2 and s_0^2 are obtained from $\hat{\eta}$ and $\hat{\chi}$. Formally, this completes the solution of the problem. In practice (6) has to be solved by some approximation method : *e. g.* by choosing χ such that $|\chi|<1$, one can expand A_n and $\mathbf{A}^{-1}$ in powers of χ, and approximate to the left-hand side of (6) by a polynomial in χ (*cf.* the calculations in the next paragraph).

It has been shown in the case of independent observations (*cf.* Kendall, Cramér, *loc. cit.*) that the variances of the maximum likelihood estimates are asymptotically the smallest, in the sense that no other estimate can have a smaller variance in the limit when the number of observations $n\to\infty$. Though this proposition is not proved in general for correlated observations, we may yet expect it to hold in the present case, because the correlations extend only to first, or first and second, nearest neighbour. It is often found that these variances have comparatively simple expressions, even when the maximum likelihood estimates themselves are complicated. In such cases, their knowledge allows one to assess the *efficiency* of any simple (or approximate) estimate, defined formally as the limit when $n\to\infty$ of the inverse ratio of the variance of the latter to that of the corresponding maximum likelihood estimate.

The expression for the variances of the maximum likelihood estimates may be obtained as follows (*cf.* Kendall, *loc. cit.*) : let θ_1, θ_2, . . . be the parameters we wish to estimate. The covariance matrix $\mathbf{V}$ of the estimates $\hat{\theta}_1, \hat{\theta}_2, \ldots$ is then the inverse of a matrix $\mathbf{V}^{-1}$, whose elements are

$$V_{ij}=-E\left\{\frac{\partial^2 L}{\partial\theta_i\partial\theta_j}\right\}=-\int\frac{\partial^2 L}{\partial\theta_i\partial\theta_j}P(\mathbf{z})d\mathbf{z} \qquad (7)$$

(E denoting expectation value). We are interested only in the variances of $\hat{\omega}$ and $\hat{s}^2$: we may start again from expression (3) for the likelihood function but with different parameters, substituting $\mathbf{B}$ for $\mathbf{A}$, s^2h for η, ξ for χ, and taking ξ such that the elements of $\mathbf{B}$ are linear in ξ. Write $\theta_1=\omega$, $\theta_2=s^2h$ and $\theta_3=\xi$. The following expressions are found for the elements of $\mathbf{V}^{-1}$:

$$\mathrm{V}_{11}=\frac{\mathbf{h}'\mathbf{B}^{-1}\mathbf{h}}{s^2h}\,;\ \mathrm{V}_{22}=\frac{n_4}{2s^4h^2}\,;\ \mathrm{V}_{33}=-\,\tfrac{1}{2}\frac{d^2\log \mathrm{B}_n}{d\xi^2}\,;$$

$$\mathrm{V}_{23}=\frac{1}{2s^2h}\,\frac{d\log \mathrm{B}_h}{d\xi}\,;\ \mathrm{V}_{12}=\mathrm{V}_{13}=0. \qquad \ldots \quad (8)$$

Finally, writing $\log \mathrm{B}_n=n\log b$, we obtain

$$\left.\begin{aligned}\text{var. }(\hat{\omega})&=\frac{1}{\mathrm{V}_{11}}=\frac{s^2h}{\mathbf{h}'\mathbf{B}^{-1}\mathbf{h}},\\ \text{var. }(\hat{s}^2h)&=\frac{\mathrm{V}_{33}}{\mathrm{V}_{22}\mathrm{V}_{33}-\mathrm{V}_{23}^2}=\frac{2s^4h^2}{n}\left\{1-\frac{(db/d\xi)^2}{b(d^2b/d\xi^2)}\right\}.\end{aligned}\right\} \quad \ldots \quad (9)$$

§ 5. STATISTICAL ESTIMATES IN THE ANGULAR DIFFERENCE METHOD.

We proceed now to apply the results of the last paragraph to the estimation problem in the angular difference method ; it is hoped to consider the coordinate method in a later paper. Write

$$\lambda_{r,\,r}=v, \qquad \lambda_{r,\,r+1}=-w, \qquad (r=1,2,\ldots,n)$$

for the elements of the covariance matrix (equations (2) and (3) of § 3), and $\mathbf{\Lambda}=v\mathbf{A}$ (*i. e.*, we take $\eta=v$ in expression (2) of § 4), so that

$$\mathbf{A}=\begin{bmatrix} 1 & -\alpha & 0 & 0\,\ldots\ldots\,0 & 0 \\ -\alpha & 1 & -\alpha & 0\,\ldots\ldots\,0 & 0 \\ \ldots & \ldots & \ldots & \ldots & \ldots \\ \ldots & \ldots & \ldots & \ldots & \ldots \\ 0 & 0 & 0 & 0 \qquad -\alpha & 1 \end{bmatrix} \quad \ldots \quad (1)$$

where $\alpha=w/v$. It is easily seen that the determinant A_n of $\mathbf{A}$ satisfies the following difference equation (*cf.* Koopmans 1942) :

$$\mathrm{A}_n=\mathrm{A}_{n-1}-\alpha^2\mathrm{A}_{n-2}, \quad \ldots\ldots\ldots \quad (2)$$

which is satisfied by a solution proportional to β^n, provided that

$$\beta^2-\beta+\alpha^2=0. \quad \ldots\ldots\ldots \quad (3)$$

Finally, introducing as " initial " conditions the values of $\mathrm{A}_1=1$ and $\mathrm{A}_2=1-\alpha^2$, we find

$$\mathrm{A}_n=\frac{\beta_1^{n+1}-\beta_2^{n+1}}{\beta_1-\beta_2}, \quad \ldots\ldots\ldots \quad (4)$$

where β_1, β_2 are the two solutions of (3) :

$$\beta_1=\tfrac{1}{2}(1+\sqrt{(1-4\alpha^2)})\,; \qquad \beta_2=\tfrac{1}{2}(1-\sqrt{(1-4\alpha^2)}). \quad . \quad . \quad . \quad (5)$$

It is easily shown that the elements A_{rs} of $\mathbf{A}^{-1}$ can be written

$$A_{rs}=\alpha^{s-r}\left(\frac{A_{r-s}A_{r-1}}{A_n}\right), \qquad (s\geqslant r). \quad . \quad . \quad . \quad . \quad . \quad (6)$$

Write now $\lambda^2=\beta_2/\beta_1$; after a few simple transformations one finds

$$\left.\begin{aligned} \alpha&=\frac{\lambda}{1+\lambda^2}, \\ A_n&=(1-\lambda^2)^{-1}(1+\lambda^2)^{-n}(1-\lambda^{2(n+1)}), \\ A_{r,\,r+k}&=\frac{1+\lambda^2}{1-\lambda^2}\,\lambda^k(1-\lambda^{2r})(1-\lambda^{2(n-r-k+1)})(1-\lambda^{2(n+1)})^{-1}\,; \end{aligned}\right\} \quad . \quad (7)$$

A_n and $\mathbf{A}^{-1}$ have thus comparatively simple expressions as functions of λ only, and it will be convenient to maximize the likelihood function with respect to v and λ ; *i. e.* to take $\eta=v$ and $\chi=\lambda$ in (2) of § 4.

From their definition, one can see that $-\tfrac{1}{2}\leqslant w/v\leqslant\tfrac{1}{2}$, and hence $\alpha^2\leqslant\tfrac{1}{4}$, $\lambda^2\leqslant 1$. It is shown in the next section that optimum conditions are realized when $s_0/s\sim\tfrac{1}{2}$, and hence $\alpha\sim\tfrac{1}{6}$ and $\lambda^2\sim 0{\cdot}03$, so that near optimum $\lambda^k\ll 1$ for $k>2$: in what follows we shall therefore neglect $1/n$ and λ^k as compared to unity for $k>2p$, where $p\ll n/2$.

With these approximations, a straightforward calculation, using (7), gives

$$\sum_{r,\,s} A_{rs}=n\,\frac{1+\lambda^2}{(1-\lambda)^2}, \quad . \quad . \quad . \quad . \quad . \quad . \quad . \quad . \quad (8)$$

so that the estimate (4) of § 4 for the magnetic deviation becomes

$$\hat{\omega}t=n\frac{\sum\limits_{r,\,s} A_{rs}\delta\psi_s}{\sum\limits_{r,\,s} A_{rs}}=\psi-\frac{1}{1+\lambda}\sum_{k=1}^{2p}\lambda^k(\delta\psi_k+\delta\psi_{n-k+1}), \quad . \quad . \quad . \quad (9)$$

where $\psi=\sum\limits_{1}^{n}\delta\psi_k$ is simply the total observed deviation of the track ; the last term in the right-hand side of (9), representing what we may term an "end-effect" of the extreme observations, will generally be $\ll\psi$. Hence the first approximation to $\hat{\omega}$ will be just

$$\hat{\omega}_1 t=\psi. \quad . \quad . \quad . \quad . \quad . \quad . \quad . \quad . \quad . \quad . \quad (9\,a)$$

Similarly, (6) of § 4 gives for $\hat{v}$ (writing $\xi_k=\delta\psi_k-\omega h$)

$$n\hat{v}=\boldsymbol{\xi}'\mathbf{A}^{-1}\boldsymbol{\xi}=\frac{1+\lambda^2}{1-\lambda^2}\left\{\sum_{1}^{n}\xi_r^2+2\sum_{k=1}^{2p}\lambda^k\sum_{r=1}^{n-k}\xi_r\xi_{r+k}-\left(\sum_{k=1}^{p}\lambda^k\xi_k\right)^2\right.$$
$$\left.-\left(\sum_{k=1}^{p}\lambda^k\xi_{n-k+1}\right)^2\right\}, \quad . \quad . \quad . \quad (10)$$

where "end effects" are again apparent in the last two terms in the right-hand side of (10). Let us now write

$$\boldsymbol{\xi}'\mathbf{A}^{-1}\boldsymbol{\xi}=\frac{1+\lambda^2}{1-\lambda^2}[\mathrm{S}+\mathrm{U}(\lambda)],\ \text{where } \mathrm{S}=\sum_1^n \xi_r^2\ ;\ \text{and also } \mathrm{S}_k=\sum_1^{n-k}\xi_r\xi_{r+k}.$$

Equation (6) of § 4, which determines $\hat{\lambda}$, may then be written

$$\frac{d}{d\lambda}\left\{\frac{\mathrm{S}+2\mathrm{U}(\lambda)}{1-\lambda^2}\right\}=0,$$

whence

$$\hat{\lambda}=-\frac{1}{\mathrm{S}}\{(1-\hat{\lambda}^2)\mathrm{U}'(\hat{\lambda})+2\hat{\lambda}\mathrm{U}(\hat{\lambda})\}. \quad . \quad . \quad . \quad . \quad . \quad . \qquad (11)$$

where $\mathrm{U}'=d\mathrm{U}/d\lambda$. Note the expectation value of S_k is zero for $k>1$; the first approximation to the solution of (11) is obtained by neglecting such terms, as well as those having λ^k as factor, with $k>2$:

$$\frac{\hat{\lambda}_1}{1+\hat{\lambda}_1^2}=-\frac{\mathrm{S}_1}{\mathrm{S}}=\alpha_1. \quad . \quad . \quad . \quad . \quad . \quad . \quad . \quad . \qquad (11\,a)$$

Substitution in (10) gives the first approximation to $\hat{v}$:

$$n\hat{v}_1=\mathrm{S}\left(\frac{1+\hat{\lambda}_1^2}{1-\hat{\lambda}_1^2}\right)\left(1+2\hat{\lambda}_1\frac{\mathrm{S}_1}{\mathrm{S}}\right)=\mathrm{S}=\sum_{r=1}^{n}\delta\psi_r^2-\psi^2/n. \quad . \quad . \quad . \qquad (12)$$

Using the relation $\alpha=w/v$, we obtain

$$n\hat{w}_1=-\sum_{r=1}^{n-1}\delta\psi_r\delta\psi_{r+1}+\psi^2/n. \quad . \quad . \quad . \quad . \quad . \quad . \quad . \qquad (13)$$

Finally, since $s^2t=n(v-2w)$, the first approximation to the maximum likelihood estimate of the mean-square scattering deviation is

$$\hat{s}_1^2t=\sum_{r=1}^{n}\delta\psi_r^2+2\sum_{r=1}^{n-1}\delta\psi_r\delta\psi_{r+1}-3\psi^2/n=\theta_s^2 \quad . \quad . \quad . \quad . \qquad (14)$$

(we shall use θ_s to denote the observed r.m.s. scattering deviation in the whole track). Note that this estimate of s^2 *is independent of the smoothing factor* q: this is a desirable feature in practice, since the value of q will depend to a certain extent on the idiosyncrasies of individual observers.

Equation (11) is in the right form for obtaining higher order approximations to $\hat{\lambda}$ by iteration: the kth iterate would be

$$\lambda_k=-\frac{1}{\mathrm{S}}\{(1-\hat{\lambda}_{k-1}^2)\mathrm{U}'(\hat{\lambda}_{k-1})+2\hat{\lambda}_{k-1}\mathrm{U}(\hat{\lambda}_{k-1})\}. \quad . \quad . \quad . \qquad (15)$$

We can find out whether higher order approximations are worth obtaining by calculating the efficiencies of the first order approximations above, as defined at the end of the last paragraph. Their variances (standard errors squared) may be calculated by the methods of § 2 and § 3 : the algebra is somewhat tedious and need not be reproduced; neglecting some terms whose ratios to the main terms is of order $1/n$,

$$\left.\begin{aligned} \epsilon^2(\hat{\omega}_1 t) &= E(\psi-\overline{\psi})^2 = s^2t+2w, \\ \epsilon^2(\hat{s}_1^2 t) &= E(\theta_s^2-\overline{\theta_s^2})^2 = \frac{2}{n}\{(s^2t+2nw)^2+2(s^2t)^2\}. \end{aligned}\right\} \quad . \quad . \quad (16)$$

The determinants B_n in (8), (9) of § 4 and A_n in (1) of this paragraph are related by

$$\log \mathrm{B}_n = n \log (v/s^2h) + \log \mathrm{A}_n = n \log b, \quad . \quad . \quad . \quad . \quad (17)$$

so that, neglecting terms of order $1/n$ and λ^n compared to unity,

$$b=\tfrac{1}{2}\{a+2s_0^2/s^2h+(2a-1+4s_0^2/s^2h)^{\frac{1}{2}}\}, \quad . \quad . \quad . \quad . \quad (17\,a)$$

where $a=\frac{2}{3}(1-\frac{1}{2}q+q^2)$. We therefore obtain the variances of the (exact) maximum likelihood estimates by substituting from (17) in their expression (9) of § 4, taking $\xi=s_0^2/s^2h$: thus

$$\left.\begin{aligned} \epsilon^2(\hat{\omega} t) &= \frac{s^2h}{\mathbf{h}'\mathbf{B}^{-1}\mathbf{h}}\,t^2 = \frac{n^2v}{\sum\limits_{r,s} \mathrm{A}_{rs}} = nv\left(1-\frac{2w}{v}\right) = s^2t, \\ \epsilon^2(\hat{s}^2 t) &= \frac{2(s^2t)^2}{n}\left\{1-\frac{(db/d\xi)^2}{bd^2b/d\xi^2}\right\} = \frac{2(s^2t)^2}{n}\{1+2(2a-1+4s_0^2/s^2h)^{\frac{1}{2}}\}. \end{aligned}\right\} \quad . \quad (18)$$

The required efficiencies of the approximate estimates are therefore

$$\left.\begin{aligned} \text{Eff. }(\hat{\omega}_1 t) &= \lim_{t\to\infty}\left\{\frac{s^2t}{s^2t+2w}\right\} = 1, \\ \text{Eff. }(\hat{s}_1^2 t) &= \frac{1+2(2a-1+4s_0^2/s^2h)^{\frac{1}{2}}}{2+(a+2s_0^2/s^2h)^2}\,. \end{aligned}\right\} \quad . \quad . \quad . \quad (19)$$

The efficiency of $\hat{s}_1^2 t$, taking $a=1$, has been plotted in fig. 1 against the ratio $\rho=s_0/s\sqrt{h}$: it is $\sim$90 per cent near optimum conditions, where $\rho\sim\frac{1}{2}$*. We conclude therefore that *one can be content as a rule with the first approximation to the maximum likelihood estimates of ω and s^2*, as given in equations (9 *a*) and (14) of this paragraph ; in what follows we shall no longer distinguish between the approximate and the exact estimates.

The fact that the estimate of the magnetic deviation is simply the total deviation in the track may seem surprising at first sight, but a moment's reflection will show that it must be so. It is clearly the best estimate when $s_0=0$ and $q=1$, since the observed deviations are then all independent, and its variance is then s^2t. It follows that no improved estimate could possibly reduce the error, as given in equation (16), by a factor greater than $1+2w/s^2t$, which is of order $1+1/2n$ at optimum cell-length.

---

* Fig. 1 can still be used for $a\neq 1$ if we take $[\rho^2-\frac{1}{2}(1-a)]^{\frac{1}{2}}$ as abscissæ ; *e. g.* with $a=5/8$ (which is its minimum value) and $\rho=\frac{1}{2}$ the efficiency is >99 per cent.

§ 6. ESTIMATES OF MOMENTUM. OPTIMUM CELL-LENGTH.

It is proposed in this section to compare estimates of momentum obtained from magnetic and scattering deviations under optimum conditions, using the angular difference method. Before doing so, however, we may note the following application for joint measurements of the two deviations : the ratio

$$\gamma_0=\left|\frac{\omega}{s}\right|=\left|\frac{300eH}{\nu}\right| \qquad . \quad . \quad . \quad . \quad . \quad . \quad . \quad . \quad (1)$$

Fig. 1.

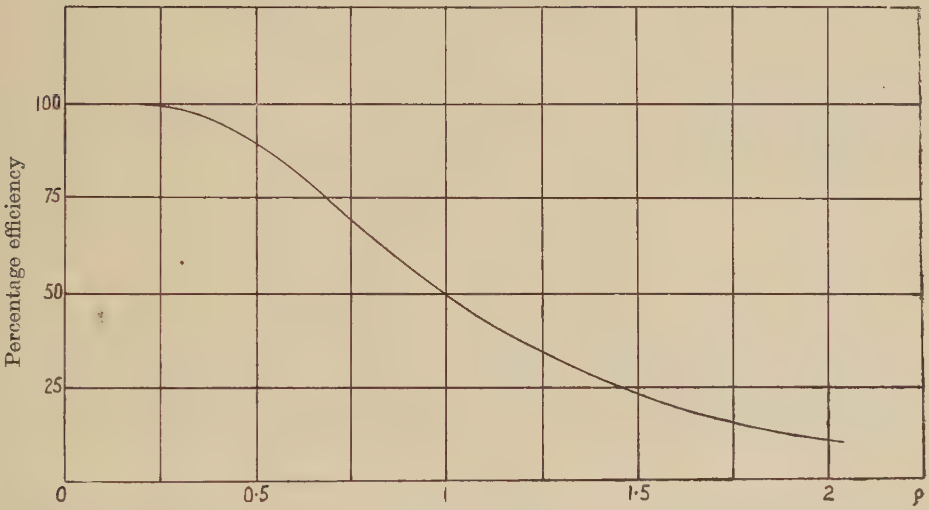

The ordinates represent the percentage efficiency of the approximate estimates of mean-square scattering deviations, plotted against the ratio $\rho=s_0/s\sqrt{h}$ of the r.m.s. spurious to scattering deviations.

of the magnitudes of the magnetic to the r.m.s. scattering deviations per unit track, ω and s, is *independent of momentum and length of track* (equations (1) and (3) of § 2). Since e and H are known, *it will therefore be possible to combine measurements from a large number of tracks in estimating γ_0, and hence verify the theoretical value for the scattering constant ν, or alternatively determine it experimentally.* For e=charge of the electron, $\nu=8{\cdot}48\times10^6$ and $H=34{,}000$ gauss, $\gamma_0=1{\cdot}20$ cm.$^{-\frac{1}{2}}$. An estimate γ of γ_0 from the data in a single track is clearly, from the results of § 5,

$$\gamma=\frac{|\hat{\omega}|}{\hat{s}}=\frac{|\psi|}{\theta_s\sqrt{(t)}} . \qquad . \quad . \quad . \quad . \quad . \quad . \quad . \quad (1\,a)$$

An approximate expression for the standard error of this estimate in terms of the standard errors of $\hat{\omega}$ and $\hat{s}$ (known from equations (16) of § 5) is easily obtained by well-known methods :

$$\epsilon^2(\gamma)\simeq\frac{\gamma_0^2}{t}\left\{\frac{\epsilon^2(\hat{\omega}t)}{(\omega t)^2}+\frac{\epsilon^2(\hat{s}^2t)}{4(s^2t)^2}\right\}=\frac{1}{t}+\frac{\gamma_0^2}{2n}\left\{2+\left(1+\frac{2n\omega}{s^2t}\right)^2+\frac{4n\omega}{(\omega t)^2}\right\}. \quad . \quad . \quad (2)$$

When n is large and the spurious scattering small, $\epsilon(\gamma)\simeq 1/\sqrt{(t)}$. An improved estimate γ_{N} of γ_0 may be obtained in the usual manner from the data in N tracks (with same e, H and ν) by taking a weighted average of the estimates γ_k from each track :

$$\gamma_{\mathrm{N}}=\sum_{k=1}^{\mathrm{N}}\frac{\gamma_k}{\epsilon^2(\gamma_k)}\Bigg/\sum_{k=1}^{\mathrm{N}}\frac{1}{\epsilon^2(\gamma_k)}. \quad . \quad . \quad . \quad . \quad . \quad . \quad . \quad (3)$$

The standard error of γ_{N} is approximately

$$\epsilon^2(\gamma_{\mathrm{N}})=\mathrm{N}\Bigg/\sum_{k=1}^{\mathrm{N}}\frac{1}{\epsilon^2(\gamma_k)}. \quad . \quad . \quad . \quad . \quad . \quad . \quad . \quad . \quad (4)$$

It is equally possible, of course, to combine the data from tracks with different e_k and H_k by weighting each γ_k inversely as $e_k\mathrm{H}_k$.

We now come to the estimation of momentum. An estimate from the magnetic deviation, denoted by p_m, is clearly

$$p_m=\frac{300e\mathrm{H}}{\hat{\omega}}=\frac{300e\mathrm{H}t}{\psi}. \quad . \quad . \quad . \quad . \quad . \quad . \quad . \quad . \quad (5)$$

Its relative error is approximately

$$\frac{\epsilon(p_m)}{p}\simeq\frac{\epsilon(\hat{\omega}t)}{\hat{\omega}t}\simeq\frac{1}{\gamma_0\sqrt{(t)}}\left(1+\frac{2\omega}{s^2t}\right)^{\frac{1}{2}}. \quad . \quad . \quad . \quad . \quad . \quad (6)$$

Provided that t is large enough and the spurious scattering small enough for $2\omega/s^2t$ to be $\ll 1$, the product of this relative error by $\sqrt{(t)}$,

$$\eta(p_m)=\sqrt{(t)}\epsilon(p_m)/p\simeq 1/\gamma_0 \quad . \quad . \quad . \quad . \quad . \quad . \quad . \quad . \quad (7)$$

is approximately equal to $1/\gamma_0$, and hence independent of momentum and length of track and inversely proportional to H.

The scattering estimate of momentum may be written

$$p_s=\frac{\nu}{\hat{s}}=\frac{\nu\sqrt{(t)}}{\theta_s}; \quad . \quad . \quad . \quad . \quad . \quad . \quad . \quad . \quad . \quad (8)$$

its relative error is approximately

$$\frac{\epsilon(p_s)}{p}\simeq\frac{\epsilon(s^2t)}{2s^2t}\simeq\frac{1}{\sqrt{(2n)}}\left[\left(1+\frac{2n\omega}{s^2t}\right)^2+2\right]^{\frac{1}{2}}. \quad . \quad . \quad . \quad . \quad . \quad (9)$$

In order to compare these two estimates, we shall have to find out how changes in cell-length affect the error on p_s. The standard error of $\hat{s}^2t$ (equation (16) of § 5) may be written as follows :

$$\epsilon^2(\hat{s}^2t)=2ht\left\{\left(as^2+\frac{2s_0^2}{h}\right)^2+2s^4\right\}, \quad . \quad . \quad . \quad . \quad . \quad (10)$$

where $a=\frac{2}{3}(1-\frac{1}{2}q+q^2)$. A decrease in the magnitude of h must, on the one hand, tend to decrease this error, because it increases the number $n=t/h$ of observations ; on the other hand, we may expect it to increase the spurious deviation s_0, and hence increase the error. There must, therefore, be an *optimum value*, say h_0, of h, dependent on the way s_0 varies with h, which will minimize $\epsilon(\hat{s}^2t)$. A stationary value is obtained by solving $d\epsilon^2/dh=0$; this leads to

$$\frac{s_0^2}{h_0}-\frac{d(s_0^2)}{dh_0}=\left(\frac{d(s_0^2)}{dh_0}\right)^2+as^2\frac{d(s_0^2)}{dh_0}+\frac{2+a}{4}s^4. \quad . \quad . \quad . \quad (11)$$

It is easily shown that this gives a minimum, provided that

$$\frac{d^2(s_0^2)}{dh_0^2}>-\frac{2}{h_0}\left(\frac{d(s_0^2)}{dh_0}-\frac{s_0^2}{h_0}\right)\Big/\left(s^2-\frac{2s_0^2}{h_0}\right).$$

There is experimental evidence that the dependence of s_0 on h is in the form of a power law (*cf.* Dilworth, *et. al.* 1950),

$$s_0^2=\alpha^2h^{-\mathrm{K}}, \quad . \quad . \quad . \quad . \quad . \quad . \quad . \quad . \quad . \quad . \quad (12)$$

with α roughly independent of momentum, and $\mathrm{K}\simeq 3/2$. Substituting in (11), we find that the ratio ρ of spurious to scattering deviations at optimum cell-length,

$$\rho^2=\frac{s_0^2}{s^2h_0}=\frac{a\mathrm{K}}{2(1+2\mathrm{K})}\left\{\left[1+\frac{(2+a)(1+2\mathrm{K})}{a^2\mathrm{K}^2}\right]^{\frac{1}{2}}-1\right\}, \quad . \quad . \quad (13)$$

is determined by the values of K and a (a can range from $\frac{5}{8}$ to 1 ; *cf.* § 3). Table 1 shows that ρ is not very sensitive to variations of either a or K. The explicit expression for the optimum cell-length in terms of momemtum is

$$h_0=\left(\frac{\alpha}{\rho\nu}p\right)^{\frac{2}{1+\mathrm{K}}}. \quad . \quad . \quad . \quad . \quad . \quad . \quad . \quad . \quad (14)$$

TABLE I.

K	1	1	3/2	3/2	3	3
a	1	5/8	1	5/8	1	5/8
ρ	0·60	0·61	0·53	0·55	0·42	0·45

Substituting this in (10) and (9), one finds for $\sqrt{(t)}$ times the relative error on p_s *at optimum cell-length*

$$\eta(p_s)=\frac{\sqrt{(t)}\epsilon(p_s)}{p}=[1+\tfrac{1}{2}(a+2\rho^2)]^{\frac{1}{2}}\left(\frac{\alpha}{\rho\nu}p\right)^{\frac{1}{1+\mathrm{K}}}. \quad . \quad . \quad . \quad (15)$$

Both h_0 and $\eta(p_s)$ increase with p. Since there are practical limits to the cell-length when one uses a microscope, there will be a range of values of p outside which one will have to use respectively the maximum and minimum practicable values of h. For such values of p, h is fixed and $\eta(p_s)$ becomes

$$\eta(p_s)=h^{\frac{1}{2}}\left[1+\tfrac{1}{2}\left(1+2h^{-(\mathrm{K}+1)}\left(\frac{\alpha}{\nu}p\right)^2\right)^2\right]^{\frac{1}{2}} \quad . \; . \; . \; . \; . \quad (16)$$

With $\alpha=4{\cdot}25\times10^5$, $\mathrm{K}=3/2$*, $\nu=8{\cdot}48\times10^6$ and $a=1$

$$h_0\,(\text{microns})=(p\ \text{MeV/c.})^{4/5},$$

$$\eta(p_s)\ \text{cm.}^{\frac{1}{2}}=1{\cdot}5\times10^{-2}\ (p\ \text{MeV/c.})^{2/5}, \quad (h=h_0),$$

and the optimum cell-length range with 25 microns $\leqslant h \leqslant 400$ microns, is 60 MeV/c.$\leqslant p \leqslant$2000 MeV/c.

We saw before that $\eta(p_m)$ for the magnetic estimate of p is very approximately independent of p : hence for every value of H there will be a critical value of the momentum below which the scattering determination of p is better than the magnetic one. In the optimum cell-length range, and with the values of α, ν, K and a above, this critical value is

$$p\ \text{MeV/c.}=(1{\cdot}76\times10^6/\text{H gauss})^{5/2}.$$

§ 7. Determination of the Signs of Particles. Estimation of the Ratio of Positive to Negative Particles.

It was seen in the last section that scattering determinations of momentum are more accurate than magnetic ones for all momenta smaller than a critical value. There is, however, one important item of information which can be inferred only from the magnetic deviation, and that is information regarding the *sign* of the particle ; such information is available provided we know the direction of travel of the particle.

The magnetic deflection is estimated, as seen in § 5, by the total deviation ψ of the track. What we require, therefore, is the probability, given this deviation, and assuming the direction of travel is known, that the particle should be positive or negative. Let us introduce a charge variable τ, with $\tau=1$ for positive, $=-1$ for negative, particles. Let $p(\tau)$ be the *prior* sign probability of the particle ; we shall also write $q=p(1)/p(-1)$ for the ratio of positive to negative particles (not to be confused with the "smoothing" factor of § 3). We shall assume at first that q is known, either for primaries or for star secondaries ; we shall see later how q can be *estimated* from the statistics of particles. The probability of a deviation ψ *given* the sign of the particle may be written, if we take ω to mean the *magnitude* of the magnetic deviation per unit track,

$$\mathrm{P}(\psi|\tau)=\frac{1}{(2\pi s^2t)^{\frac{1}{2}}}\,e^{-(\psi-\tau\omega t)^2/2s^2t} \quad . \; . \; . \; . \; . \; . \; . \quad (1)$$

---

* Based on preliminary results ; see Dilworth *et. al.* 1950, for improved results and discussion.

Hence the joint probability of ψ and τ is

$$\mathrm{P}(\psi, \tau)=\mathrm{P}(\psi \mid \tau)p(\tau), \quad . \quad . \quad . \quad . \quad . \quad . \quad . \quad . \quad (2)$$

the probability of ψ irrespective of the sign of the particle is

$$\mathrm{P}(\psi)=p(1)\mathrm{P}(\psi \mid 1)+p(-1)\mathrm{P}(\psi \mid -1). \quad . \quad . \quad . \quad . \quad (3)$$

Finally, the probability of τ given ψ is

$$\mathrm{P}(\tau \mid \psi)=\frac{\mathrm{P}(\psi, \tau)}{\mathrm{P}(\psi)}=\left[1+\frac{p(-\tau)}{p(\tau)}\, e^{-2\tau\omega\psi/s^2}\right]^{-1}. \quad . \quad . \quad . \quad . \quad (4)$$

(We may note at this point that (4) is essentially an application of Bayes' theorem, which is indubitably valid here since the prior probabilities $p(\tau)$ can be observed.) Equation (4) expresses the maximum information a track can yield regarding sign : this can be shown in the following way. All the information obtained from the track is contained in the set of observed deviations $\delta\psi_r$ $(r=1, 2, \ldots, n)$. Let $\mathbf{z}$ stand as before (§ 3) for this set of observations. The considerations above may be repeated word for word in terms of the probabilities of $\mathbf{z}$ and τ instead of ψ and τ, yielding

$$\mathrm{P}(\tau \mid \mathbf{z})=\frac{\mathrm{P}(\mathbf{z}, \tau)}{\mathrm{P}(\mathbf{z})}=\left[\frac{p(1)}{p(\tau)}\,\frac{\mathrm{P}(\mathbf{z} \mid 1)}{\mathrm{P}(\mathbf{z} \mid \tau)}+\frac{p(-1)}{p(\tau)}\,\frac{\mathrm{P}(\mathbf{z} \mid -1)}{\mathrm{P}(\mathbf{z} \mid \tau)}\right]^{-1} \quad . \quad . \quad (4\,a)$$

Substituting expression (8) of § 2 for $\mathrm{P}(\mathbf{z} \mid \tau)$ in $(4\,a)$, we get

$$\mathrm{P}(\tau \mid \mathbf{z})=\left[1+\frac{p(-\tau)}{p(\tau)}\exp.\,(-2\tau\omega\mathbf{h}'\mathbf{\Lambda}^{-1}\mathbf{z})\right]^{-1},$$

or, in terms of the maximum likelihood estimates of ω and its variance (expressions (4) and (5) of § 4),

$$\mathrm{P}(\tau \mid \mathbf{z})=\left[1+\frac{p(-\tau)}{p(\tau)}\exp\,(-2\tau\omega\hat{\omega}/\epsilon^2(\hat{\omega}))\right]^{-1}, \quad . \quad . \quad (4\,b)$$

which reduces to (4) if one substitutes expressions $(9\,a)$ and (18) of § 5 for $\hat{\omega}$ and $\epsilon^2(\hat{\omega})$.

Expression (4) is exact if we know s and ω (*i. e.* if we know the momentum of the particle). If not, then $\omega/s=\gamma_0$, which is a constant depending only on the field and the composition of the emulsion (*cf.* § 6), and

$$\frac{\psi}{s}=\frac{\psi\sqrt{(t)}}{\theta_s}=\gamma t$$

can be estimated from the track, where γ is now taken as *signed*. Hence, an estimate of (4) is

$$\mathrm{P}(\tau \mid \psi)=\left[1+\frac{p(-\tau)}{p(\tau)}\, e^{-2\tau\gamma\gamma_0 t}\right]^{-1}. \quad . \quad . \quad . \quad . \quad . \quad (5)$$

This estimate becomes dubious for high energy particles, such that the error on the estimate $\hat{s}$ is large. In this case we may consider the problem from a different angle. If the number of cells n is large, the distribution of the observed γ given τ is approximately Gaussian, with mean $\tau\gamma_0$.

The probability $P(\tau|\gamma)$ of sign *given* γ may then be obtained by substituting $1/\epsilon^2(\gamma)$ (*cf.* equation (2) of § 6) for t in (5). In fig. 2, $P(1|\gamma)$ is plotted against γt for $\gamma_0=1{\cdot}20$ and $q=1$.

Another problem arising in connection with sign determination is the estimation of the ratio q of positive to negative particles from a set of n tracks of a certain type : *e. g.* primaries in a certain range of momenta, or secondaries from certain types of stars. The probability of a total deviation ψ_r in the rth track, irrespective of sign, may be written

$$P_r(\psi_r)=(2\pi s_r^2t_r)^{-\frac{1}{2}}e^{-(\psi_r^2+\omega_r^2t_r^2)/2s_r^2t_r}[p_+e^{\omega_r\psi_r/s_r^2}+(1-p_+)e^{-\omega_r\psi_r/s_r^2}],$$
$$(r=1, 2, \ldots, n) \quad . \quad . \quad . \quad . \quad (6)$$

Fig. 2.

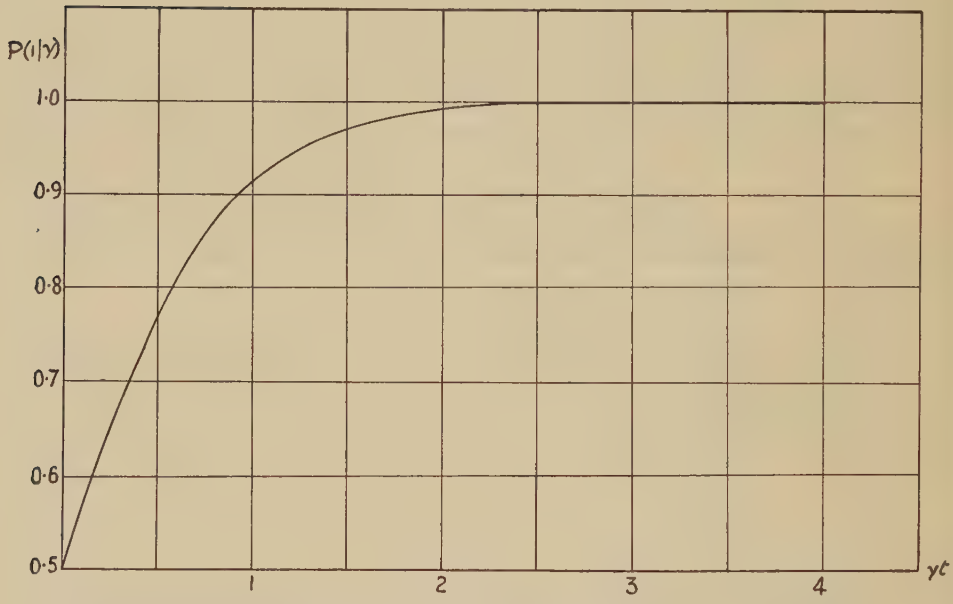

A plot of the probability $P(1|\gamma)$ of the particle being positive as a function of $\gamma t=\psi\sqrt{(t)}/\theta_s$ for $\gamma_0=1{\cdot}20$.

where $p_+=p(+1)$, t_r, s_r are respectively the length and r.m.s. scattering deviation per unit track for the rth track. Since the deviations in the n tracks are independent, the maximum likelihood estimate of p_+ is obtained by maximizing

$$L=\sum_{r=1}^{n}\log P_r(\psi_r),$$

i. e. by solving

$$\frac{\partial L}{\partial p_+}=\sum_{r=1}^{n}\frac{e^{\omega_r\psi_r/s_r^2}-e^{-\omega_r\psi_r/s_r^2}}{p_+e^{\omega_r\psi_r/s_r^2}+(1-p_+)e^{-\omega_r\psi_r/s_r^2}}=0.$$

Hence the maximum likelihood estimate of $q=p_+/(1-p_+)$ in terms of the n observed deviations is

$$\hat{q}=\frac{\sum_1^n\left[1+\frac{1}{\hat{q}}e^{-2\omega_r\psi_r/s_r^2}\right]^{-1}}{\sum_1^n[1+\hat{q}e^{2\omega_r\psi_r/s_r^2}]^{-1}}\simeq\frac{\sum_1^n \mathrm{P}(1\,|\,\gamma_r;\,\hat{q})}{\sum_1^n \mathrm{P}(-1\,|\,\gamma_r;\,\hat{q})}, \quad . \quad . \quad . \quad . \quad (7)$$

where γ_r is the value of γ observed for the rth track. Equation (7) involves $\hat{q}$ on both sides and must be solved by a method of successive approximation. The following iteration method may be used: take $q_0=1$ as the zero order approximation; then the kth order approximation q_k is obtained from the $(k-1)$th by

$$q_k=\frac{\sum_1^n \mathrm{P}(1\,|\,\gamma_r;\,q_{k-1})}{\sum_1^n \mathrm{P}(-1\,|\,\gamma_r;\,q_{k-1})} \quad . \quad . \quad . \quad . \quad . \quad . \quad . \quad . \quad (8)$$

If the exact solution $\hat{q}>1$ then it is easily seen that (*a*) the sequence q_k is an increasing one, and (*b*) that, for every k, $q_k\leqslant\hat{q}$; conversely, if $\hat{q}<1$, then the sequence q_k is a decreasing one, and $q_k\geqslant\hat{q}$ for every k. Hence, in both cases q_k converges to $\hat{q}$ as k increases.

ACKNOWLEDGMENTS.

It is a pleasure to acknowledge my indebtedness to Dr. G. D. Rochester and his group, and in particular Mme F. Lévy and Mr. S. J. Goldsack, for suggesting this problem and keeping me informed about their experimental work; to Professor M. S. Bartlett for his valuable suggestions; to M. Yves Goldschmidt-Clermont for stimulating discussion and correspondence. Mr. Goldsack suggested some of the results in § 7.

REFERENCES.

CRAMÉR, 1946, *Mathematical Methods of Statistics*, pp. 498–506.
DILWORTH, GOLDSACK, GOLDSCHMIDT-CLERMONT and LÉVY, 1950, *Phil. Mag.*, **41**, 1032.
FOWLER, 1950, *Phil. Mag.*, **41**, 169.
GOLDSCHMIDT-CLERMONT, KING, MUIRHEAD and RITSON, 1948, *Proc. Phys. Soc.*, **61**, 183.
GOLDSCHMIDT-CLERMONT, 1950, *Bulletin du Centre de Physique Nucléaire de l'Université de Libre Bruxelles*, No. 14.
GOUDSMIT and SAUNDERSON, 1940, *Phys. Rev.*, **57**, 24, 552.
KENDALL, 1946, *The Advanced Theory of Statistics*, Vol. 2, pp. 12–42.
KOOPMANS, 1942, *Ann. Math. Stats.*, **13**, 27.
LEWIS, 1950, *Phys. Rev.*, **78**, 526.
MOLIÈRE, 1947, *Z. für Naturforschung*, **2a**, 133; 1948, *Ibid.*, **3a**, 78.
MOYAL, 1949, *J. Roy. Statist. Soc. Suppl.*, **11**, 150.
ROSSI and GREISEN, 1941, *Rev. Mod. Phys.*, **13**, 240.
SNYDER and SCOTT, 1949, *Phys. Rev.*, **76**, 220.
WILLIAMS, 1939, *Proc. Roy. Soc.* A, **169**, 531.

XCVI. CORRESPONDENCE

The Velocity of Second Sound Below 1° *K.*

By K. R. Atkins and D. V. Osborne,
Royal Society Mond Lab., Cambridge *.

[Received August 15, 1950.]

Peshkov (1948), Maurer and Herlin (1949) and Pellam and Scott (1949) have shown that, as predicted by Landau (1941), the velocity of second sound in liquid helium II increases as the temperature is decreased below 1° K. We have extended these measurements to lower temperatures and have found that the velocity rises to 152 ± 5 metres/sec. at 0·1° K. Subject to the uncertainties which will be discussed below, this agrees with Landau's further prediction that, at 0° K., the velocity of second sound should be equal to the velocity of first sound divided by $\sqrt{3}$.

The low temperatures were produced by demagnetizing a mixture of 2 g. of liquid helium and 30 g. of ferric alum from a field of 10,000 gauss. The mixture was contained in a small metal Dewar vessel and was pumped by a diffusion pump of speed 7 litres/sec. through a constriction of diameter 0·1 mm. Owing to certain technical difficulties, this cryostat has not yet behaved ideally, and the warming times were only of the order of 60 sec. However, this was sufficient to enable the velocity measurements to be made and the preliminary results described below establish the main characteristics of the variation of velocity with temperature. Temperatures after demagnetization were deduced from the magnetic susceptibility of the ferric alum, measured by means of a mutual inductance and a ballistic galvanometer. The primary current of the mutual inductance was automatically reversed every three sec. and the throws of the ballistic galvanometer were photographically recorded.

The second sound measurements used a pulse technique, in which a D.C. pulse of duration 100 μ sec. was fed into a constantan wire heater. The resulting second sound pulse was propagated along a glass tube of length 3·40 cm. and internal diameter 0·5 cm. embedded in the ferric alum, and was received by a phosphor-bronze resistance thermometer. The time of flight was measured by displaying the received signals on a cathode-ray tube, which was photographed with a cine camera during the 60 sec. immediately following the demagnetization. Fig. 1 has been built up from tracings of actual photographs. In agreement with the observations of Pellam and Scott (1949), the received pulse is seen to be considerably distorted and lengthened at these low temperatures. This distortion can be explained in terms of dissipative losses during propagation, and a full analysis will be published shortly. No detectable change in velocity was caused by altering the pulse amplitude, so that the shock-wave effects discovered by one of us (Osborne, to be published shortly) do not seem to be relevant to the present results.

---

* Communicated by the Authors.

Fig. 2 presents our results for the variation of velocity with temperature, together with previous results at higher temperatures. Owing to the large heat influx, it is uncertain how closely the temperature of the liquid followed that of the ferric alum, and so the temperatures must be considered as only approximate, especially above 0·3° K. when the warming up was particularly rapid. Landau (1941) predicts that the velocity of second sound (u_2) at 0° K. should be $1/\sqrt{3}$ times the velocity of ordinary sound (u_1). The existing measurements of u_1 (Findlay *et al.*, 1938, Pellam and Squire, 1947) do not extend below 1·5° K. and the extrapolation to 0° K. is rather uncertain. A linear extrapolation gives, at 0° K, $u_1 = 272$ metres/sec. and $u_1/\sqrt{3} = 157$ metres/sec. Therefore, apart from the uncertainty of this extrapolation and the possibility that u_2 changes appreciably between 0·1° K and 0° K., the relation $u_2 = u_1/\sqrt{3}$ is well borne out by fig. 2. In Landau's theory the falling away of u_2 from this initial value is due to rotons, and fig. 2 therefore suggests that rotons are becoming important at about 0·1° K. and are predominant above 0·5° K. For this reason it seems unlikely that the specific heat of liquid helium will obey a T^3 law above 0·1° K.

Fig. 1.

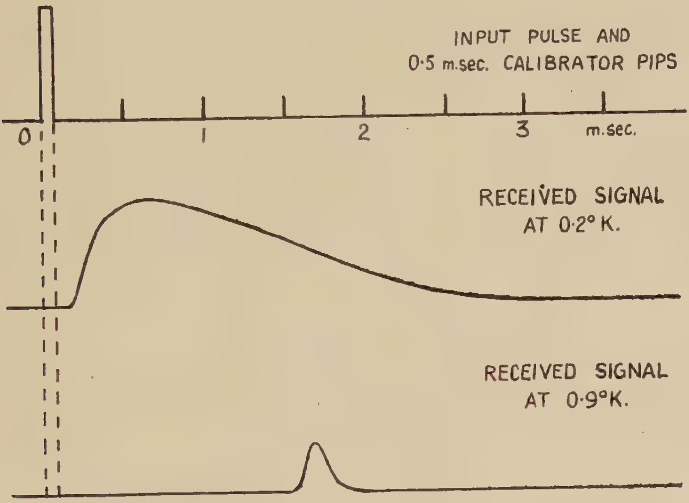

Tracings taken from photographs of the oscilloscope screen.

The two aspects of Landau's theory which are mainly responsible for the particular result $u_2 = u_1/\sqrt{3}$ are (1) his method of calculating the density of the normal component, ρ_n, and (2) his fundamental assumption that the liquid can be treated as a continuum, in much the same way as a solid is treated in the Debye theory of specific heats, and that the thermal motion can therefore be built up from phonons and rotons. Near 0° K. only phonons are important and, since these are just ordinary sound waves, it is easy to see how u_1 becomes involved in the formula for u_2. The alternative theory developed by London (1938) and Tisza (1947), attaching less importance to the interatomic forces, builds up the wave function of the liquid as a whole from the wave functions of individual atoms, and then makes use of those special properties of Bose–Einstein statistics which lead to a condensation of atoms into the lowest state. Temperley (to be published shortly) has shown that if ρ_n/ρ is equated to the proportion of

Fig. 2.

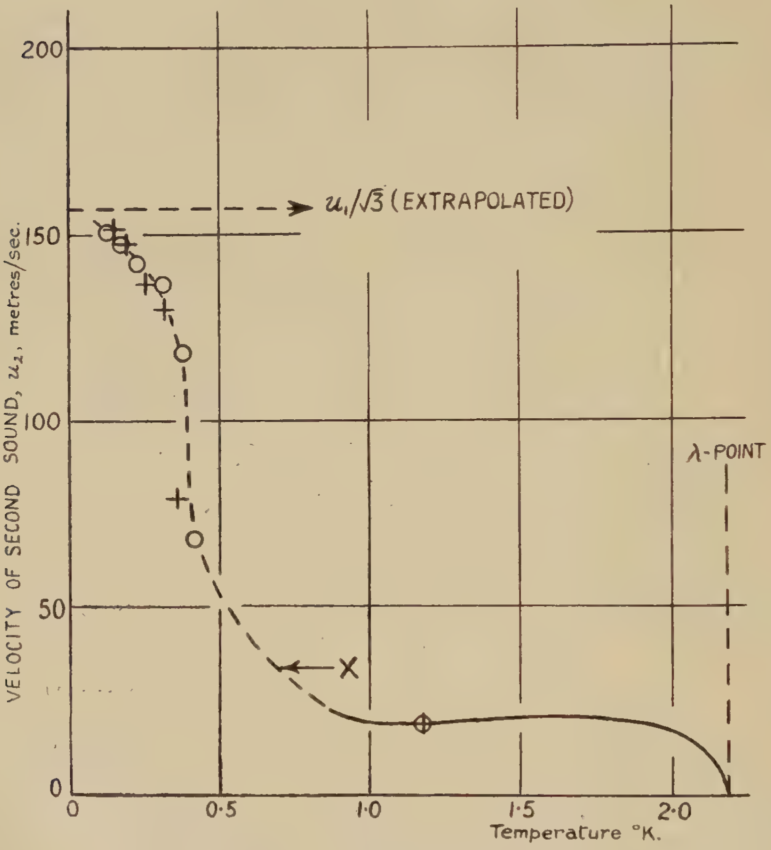

Variation of velocity with temperature.

○ + The present results. Two separate demagnetisations.

—— Results of Peshkov and of Maurer and Herlin at higher temperatures.

× Highest velocity reached by Pellam and Scott. Temperature unspecified.

atoms not in the lowest state, then this type of theory always leads to $u_2=0$ at 0° K. If, however, ρ_n/ρ is evaluated by a method similar to Landau's, this conclusion remains true for the Bose–Einstein gas, but probably does not hold when interactions between atoms are taken into account. It is conceivable, therefore, that a Bose–Einstein type of theory making due allowance for interatomic forces would give a value of u_2 tending at 0° K. to a finite value related, presumably, to the average velocity of zero-point motion, which has the same order of magnitude as u_1. Nevertheless, until such a theory has been developed and has satisfied the exacting requirement that $u_2=u_1/\sqrt{3}$ at 0° K., the present experimental results must be considered strongly in favour of Landau's method of approach.

We should like to express our indebtedness to Dr. D. Shoenberg for encouraging this research, to Dr. J. Ashmead for technical advice, and to Mr. H. N. V. Temperley for showing us his results before publication.

References.

Findlay, J. C., Pitt, A., Grayson Smith, H. and Wilhelm, J. O., 1938, *Phys. Rev.*, **54**, 506.
Herlin, M. A., and Maurer, R. D., 1949, *Phys. Rev.*, **76**, 948.
Landau, L., 1941, *J. Phys., U.S.S.R.*, **5**, 71.
London, F., 1938, *Phys. Rev.*, **54**, 947.
Pellam, J. R., and Scott, R. B., 1949, *Phys. Rev.*, **76**, 869.
Pellam, J. R., and Squire, C. F., 1947, *Phys. Rev.*, **72**, 1245.
Peshkov, V., 1948, *J. Phys., U.S.S.R.*, **18**, 951.
Tisza, L., 1947, *Phys. Rev.*, **72**, 838.

The Velocity of Flow of Helium II in the Creeping Film.

By L. C. Jackson and D. G. Henshaw *,
H. H. Wills Physical Laboratory, University of Bristol.

[Received August 30, 1950.]

In their paper on the measurement of creep rates and the thickness of the helium II film Daunt and Mendelssohn (1939) combined the two results to calculate the average velocity of flow of the helium in the film. Their value (about 20 cm./sec. at 1·5° K.) can, however, only have an order of magnitude significance as the thickness determination was made on a stationary film and was an average value over a considerable range of heights above the liquid level and the determinations of the volume of helium transported per sec. were of necessity made on the moving film.

We have, therefore, undertaken the simultaneous measurement with the same apparatus of the rate of creep and the thickness of the creeping film, using for the latter the optical method of Jackson and Burge (1949).

---

* On leave of absence from the National Research Council of Canada.

In addition to providing the mean velocity of flow of the helium II at various temperatures, this work has brought to light an interesting feature of the flow itself which, in our opinion, warrants a preliminary report at this time.

The beaker A (fig. 1) is of stainless steel, 4 mm. internal diameter, 1 mm. wall thickness. A polished 2 mm. wide flat on the outer surface of the beaker is used for the optical measurements of the thickness of the helium film, while a glass capillary B, attached to the beaker by means of a copper-nickel tube and a kovar-glass seal is used for the liquid level measurements. The beaker is mounted in a brass radiation shield C and is supported at the bottom by means of the copper-nickel capillary tube. A disc D is attached to the capillary tube to maintain the beaker central in the dewar. The assembly is then suspended from a glass and tungsten support to which is attached a glass beaker E, which holds liquid helium during the experiment and which provides additional thermal protection to the stainless steel beaker. The apparatus is mounted in the dewar F which contains the liquid helium, the latter being protected by liquid hydrogen and liquid nitrogen in the outer dewars.

Fig. 1.

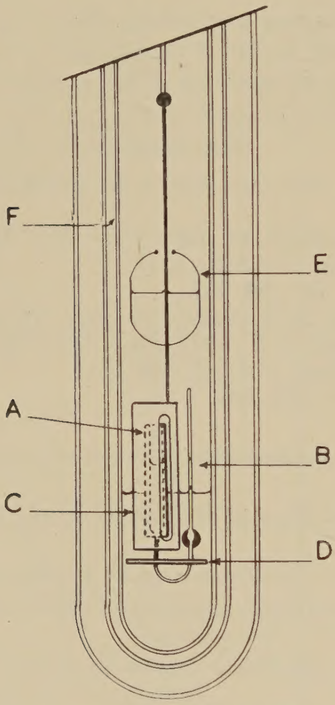

Apparatus for simultaneous measurement of film thickness and creep rate. A, stainless steel beaker ; B, glass capillary tube ; C, radiation shield ; D, centering disc ; E, glass beaker on support ; F, helium dewar.

The creep rates observed are of the same order of magnitude as those reported by Mendelssohn and White (1950) for cleaned platinum and considerably in excess of those for glass beakers. Although the stainless steel beaker has mono-layers of barium stearate on the outside, it apparently behaves as a " clean beaker " in the sense of Bowers and Mendelssohn (1949), since the creep rate is practically independent of the height of the inner liquid level except for the first few millimeters, where, as usual, the creep rate is considerably greater (see fig. 2). The accompanying table gives the measured values of the creep rates and the thickness and the deduced value of $\bar{v}$, the helium velocity averaged over the film thickness. The recorded thicknesses are those obtained when the point of observation of the thickness is 1 cm. above the main liquid helium level. The variation of the thickness of the moving film with height will be dealt with in a more detailed communication.

Fig. 2.

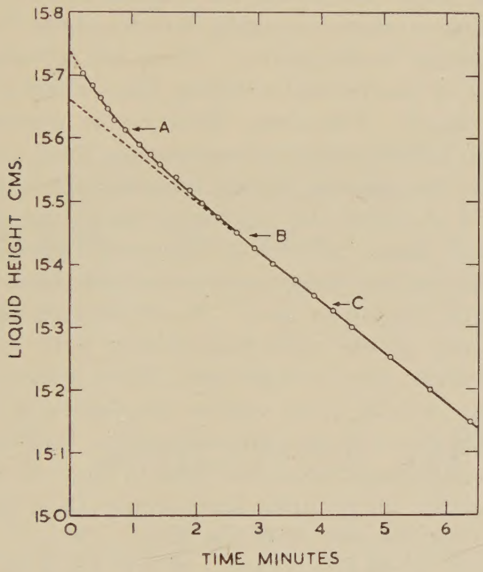

Creep curve at 1·89° K. Height of liquid helium II inside beaker v. time. A, drops decreasing in number ; B, very few drops visible ; C, no drops visible.

T° K.	Creep rate cm.^{3}/cm./sec.	Thickness cm.	Velocity $\bar{v}$ cm./sec.
1·1	$16{\cdot}9 \times 10^{-5}$	$1{\cdot}63 \times 10^{-6}$	72
1·3	$16{\cdot}9 \times 10^{-5}$	$1{\cdot}63 \times 10^{-6}$	72
1·5	$16{\cdot}8 \times 10^{-5}$	$1{\cdot}66 \times 10^{-6}$	68
1·7	$16{\cdot}1 \times 10^{-5}$	$1{\cdot}82 \times 10^{-6}$	60
1·9	$12{\cdot}8 \times 10^{-5}$	$1{\cdot}94 \times 10^{-6}$	29

A very striking phenomenon is observed when the full beaker is withdrawn from the main body of the liquid helium II at the commencement of measurements. The mirror is seen to be covered with a large number of bright specks of light moving down and disappearing into the liquid helium below. Fifty or more may be visible at once immediately after the beaker has been raised. As the level of the liquid in the beaker falls the number of specks decreases steadily, the last ones disappearing in the present case when the liquid is some 3 mm. from the rim of the beaker. The bright specks, which are obviously "drops" of liquid helium, are somewhat elongated in the direction of motion, are 1/10 to 1/3 mm. long and move downwards at a speed of about 1 cm. per sec. It is not yet possible to state anything definite about the dimensions of the drops perpendicular to the mirror. They are certainly much greater than the thickness of the normal creeping film, which is observed when the drops have ceased. The drop thickness is greater than can be measured with the existing mica compensating plate and the drops are too small for it to be possible to say whether they show interference contours. In fig. 2, A marks the position at which the observer reported that the number of drops visible had decreased appreciably, B that at which only a few individual drops were visible on the mirror, and C that for which drops were no longer seen. It will be seen that the region in which the drops are present coincides closely with that in which an anomalously high creep rate is observed. There seems little doubt that the straight part of the creep curve represents a flow of helium characteristic of the continuous film and that in the initial curved part the excess helium is transported in the form of discrete drops. It will be noted that these drops move much more slowly than the film itself and presumably slide over the surface of the film.

REFERENCES.

BOWERS, R., and MENDELSSOHN, K., 1949, *Nature*, **163**, 870.
DAUNT, J. G., and MENDELSSOHN, K., 1939, *Proc. Roy. Soc.* A, **170**, 423.
JACKSON, L. C., and BURGE, E. J., 1949, *Nature*, **164**, 660.
MENDELSSOHN, K., and WHITE, G., 1950, *Nature*, **166**, 127.

BOOKS RECEIVED

A new scientific publication has been received—'Journal of Atmospheric and Terrestrial Physics', edited by Sir Edward Appleton with the assistance of an eminent Advisory Board. Published by Butterworth-Springer Ltd. (London). Price per vol. (approx. 300 pp.) £3 10*s*. 0*d*.

[*The Editors do not hold themselves responsible for the views expressed by their correspondents.*]